

**PYROLYSIS OF PALM OIL SOLID WASTE USING HELICAL SCREW
FLUIDIZED BED REACTOR**

KHAN MUHAMMAD QURESHI

**FACULTY OF ENGINEERING
UNIVERSITI MALAYA
KUALA LUMPUR**

2021

**PYROLYSIS OF PALM OIL SOLID WASTE USING
HELICAL SCREW FLUIDIZED BED REACTOR**

KHAN MUHAMMAD QURESHI

**THESIS SUBMITTED IN FULFILMENT
OF THE REQUIREMENTS FOR THE DEGREE
OF DOCTOR OF PHILOSOPHY**

**FACULTY OF ENGINEERING
UNIVERSITY OF MALAYA
KUALA LUMPUR**

2021

UNIVERSITY OF MALAYA
ORIGINAL LITERARY WORK DECLARATION

Name of Candidate: Khan Muhammad Qureshi

Registration/ Matric No: Old KHA 140117 / New KHA17005628

Name of Degree: Doctor of Philosophy

Title of Project Paper/Research Report/Dissertation/Thesis (“this Work”):

**PYROLYSIS OF PALM OIL SOLID WASTE USING
HELICAL SCREW FLUIDIZED BED REACTOR**

Field of Study: Chemical Engineering (Pyrolysis Technology)

I do solemnly and sincerely declare that:

- (1) I am the sole author/writer of this Work;
- (2) This Work is original;
- (3) Any use of any work in which copyright exists was done by way of fair dealing and for permitted purposes and any excerpt or extract from, or reference to or reproduction of any copyright work has been disclosed expressly and sufficiently and the title of the Work and its authorship have been acknowledged in this Work;
- (4) I do not have any actual knowledge nor do I ought reasonably to know that the making of this work constitutes an infringement of any copyright work;
- (5) I hereby assign all and every rights in the copyright to this Work to the University of Malaya (“UM”), who henceforth shall be owner of the copyright in this Work and that any reproduction or use in any form or by any means whatsoever is prohibited without the written consent of UM having been first had and obtained;
- (6) I am fully aware that if in the course of making this Work, I have infringed any copyright whether intentionally or otherwise, I may be subject to legal action or any other action as may be determined by UM.

Candidate’s Signature

Date: 30 / 7/ 2021

ABSTRACT

Biomass pyrolysis processes for bio-oil production were commonly done using batch, semi-continuous or continuous process. However, past studies have shown many concerning issues in regard to the use of batch process such as high residence time, product inconsistencies across batches, high labor cost and difficulty in industrial scale up. Therefore, a quantitative study was performed using slow and fast pyrolysis mode over novel Helical Screw Fluidized Bed Reactor (HSFBR) stainless-steel (CS309) with an internal diameter of 228 mm and total length of 1,524 mm using palm shell (PS) for bio-oil production. The stainless-steel (CS309) helical screw has a total length of 1,550 mm including 6 flights a pitch distance of 95.25 mm and an external diameter of 203.2 mm. Accordingly, this research aims to investigate the performance of novel HSFBR with some desired outcomes: high particle dynamics, heat transfer rate, feed rate, effect of temperature, pyrolysis time and vapor residence time with high liquid and low biochar yield with improved properties. The torque was optimized to 50 rpm with slow heating rate of 10°C/min to achieve 500°C without involving any inert gas. The maximum quantity of organic phase with lower oxygen content and biochar products were obtained with 51.6 wt.% and 26.6 wt.%, respectively. The further experiments were performed with low, medium and high heating rates from 75 to 275°C/min at 50 rpm torque to achieve the reaction temperature of 500°C without involving any inert gas. Present study showed the major improvement in formation of organic yield was basically linked with increasing heating rate. The maximum bio-oil yield of 72.84 wt.% with HHV of about 44.41 MJ/kg was achieved at heating rate of 275°C/min, which is compatible with the diesel fuel HHV (45 MJ/kg). The parametric results also showed that the temperature and the feed rate had significant effects on pyrolytic products. When pyrolysis temperature was increased from 400 to 650°C the yields of bio-oil and biochar were decreased while

gas yield was increased. In addition, on increasing feed rate from 3 to 25 g/min the bio-oil and gas yield were increased, while biochar yield was decreased. The effect of particle size, pyrolysis time and vapor residence time showed the optimum bio-oil yield obtained at 2 mm particle size, 30 min pyrolysis time and 0.25s vapor residence time with (72.11 wt.%), (72.40 wt.%) and (73.86 wt.%), respectively at 500°C. In addition, 10 mm particle size also showed an acceptable bio-oil yield of 71.23 wt.% which saved the costs of biomass grinding and size reduction time. The optimum value of HHV for fuel properties of bio-oil (organic phase) at 0.25 mm particle size, 30 min pyrolysis time and 0.25 vapor residence time were found 42.80, 43.02 and 43.14, respectively. The qualitative and quantitative evaluation of pyrolytic products (organic phase and by-product biochar) strongly suggests their significance in liquid and solid fuel applications. These findings of novel HSFBR reactor technology ranked well for biomass material and have provided a good understanding when it was used in pyrolysis modes slow medium and high heating rate.

ABSTRAK

Pirolisis biojisim untuk pengeluaran bio-minyak biasanya dilakukan dengan menggunakan proses kelompok, separa-lanjar atau berterusana. Walau bagaimanapun, kajian terdahulu telah menunjukkan banyak perkara berkaitan dengan penggunaan proses kelompok seperti masa mastautin yang tinggi, ketidakkonsistenan produk di seluruh kelompok, kos buruh yang tinggi dan kesukaran dalam skala industri. Oleh itu, satu kajian kuantitatif dilakukan menggunakan reaktor Lapisan Terbendalir Skru Heliks (RLTSH) novel dengan (CS309) diameter dalaman 228 mm dan panjang 1,524 mm menggunakan kelapasawit (KS) untuk pengeluaran bio-minyak. Skru heliks keluli tahan karat (CS309) mempunyai panjang keseluruhan 1,550 mm termasuk 6 penerbangan jarak jauh 95.25 mm dan diameter luaran 203.2 mm. Oleh itu, penyelidikan ini bertujuan untuk menyiasat prestasi RLTSH baru dengan beberapa hasil yang diingini: dinamik zarah tinggi, kadar pemindahan haba, kadar suapan, kesan suhu, masa pirolisis dan masa pemendapan wap dengan hasil bio-arang rendah dan bio-arang rendah dengan sifat yang lebih baik. Tork dioptimumkan kepada 50 rpm dengan kadar pemanasan perlahan 10°C/min untuk mencapai 500°C tanpa melibatkan sebarang gas lengai. Kuantiti maksimum fasa vrganic dengan kandungan oksigen yang rendah dan produk bio-arang diperoleh dengan 51.6 wt.% dan 26.6 wt.%. Eksperimen selanjutnya dilakukan dengan kadar pemanasan yang rendah, sederhana dan tinggi dari 75 hingga 275°C/min pada tork 50 rpm untuk mencapai suhu reaksi 500°C tanpa melibatkan sebarang gas lengai. Kajian semasa menunjukkan peningkatan utama pembentukan hasil organik pada dasarnya dikaitkan dengan peningkatan kadar pemanasan. Hasil bio-minyak maksimum 72.84 wt.% dengan HHV kira-kira 44.41 MJ / kg dicapai pada kadar pemanasan 275°C / min, yang serasi dengan HHV bahan api diesel (45 MJ / kg). Keputusan parametrik juga menunjukkan bahawa suhu dan kadar suapan mempunyai kesan yang ketara terhadap produk pirolisis. Apabila suhu pirolisis meningkat dari 400 ke 650°C, hasil bio-minyak dan bio-arang telah

menurun manakala hasil gas meningkat. Di samping itu, untuk meningkatkan kadar suapan dari 3 hingga 25 g / min, hasil bio-minyak dan gas meningkat, sementara hasil bioarang telah menurun. Kesan saiz zarah, masa pirolisis dan masa pemendapan wap menunjukkan hasil bio-minyak optimum yang diperolehi pada saiz zarah 2 mm, masa pirolisis 30 min dan masa mastautin wap 0.25s (72.11%), (72.40 wt.%) dan (73.86 wt.%), masing-masing pada 500°C. Di samping itu, saiz zarah 10 mm juga menunjukkan hasil bio-minyak yang boleh diterima sebanyak 71.23 wt.% yang menyelamatkan kos pengisaran biojisim dan masa pengurangan saiz. Nilai optimum HHV bagi bahan bakar bio-minyak (fasa organik) pada saiz zarah 0.25 mm, masa pirolisis 30 minit dan masa kediaman wap 0.25 didapati 42.80, 43.02 dan 43.14. Penilaian kualitatif dan kuantitatif produk pirolisis (fasa organik dan produk bio-arang) sangat mencadangkan kepentingan mereka dalam aplikasi bahan api cecair dan pepejal. Penemuan teknologi reaktor RLTSH novel ini berada di kedudukan yang baik untuk bahan biojisim dan telah memberikan pemahaman yang baik apabila ia digunakan dalam mod pirolisis yang sederhana dan kadar pemanasan yang tinggi.

ACKNOWLEDGEMENT

First of all, and foremost, I thank to my almighty ALLAH for giving me the strength, willpower, patience against many odds and fulfilling my prayers, Alhamdulillah. All of my best wishes are always given to the Holy Prophet Muhammad S. A. W, his families, and all of us as their followers until the end of time.

I would like to sincerely pay thanks and express my gratitude to Prof. Dr. Wan Mohd Ashri Wan Daud for serving as both my advisor and mentor of his encouragement and financial support during the research work through GSP-MOHE, University of Malaya for fully funding this study through the project number MO008-2015.

I also appreciate Dr. Faisal Abnisa for the patience, guidance and criticism to improve this work. I would like to thank all the supporting staff and technicians in the Department of Chemical Engineering: Mr. Hadi, Mr. Jalaluddin, Mr. Ishak, Mr. Kamaruddin, Mr. Rustam, Mr. Osman, Mr. Azaruddin, Mr. Exram, Mr. Ismail, Mr. Kamalrul, Mrs. Fazizah, and Mrs. Azira, for their assistance and support throughout my Ph.D. study.

My gratitude goes to my vice chancellor Prof. Dr. Mohammad Aslam Uqaili and Mr. Saifullah Hassan deputy director planning and development of Mehran University of Engineering and Technology Jamshoro Pakistan for providing me study leave. I am also great full to Prof. Dr. Iqbal Ahmed and Prof. Dr. Abrar Inayat who motivated me to pursue for PhD at UM. I am also grateful to Miss. Thaneissha Marimuthu she helped me in sample analysis and thesis submission during COVID-19. I would like to pay thanks my wife Saima Khan for her unconditional love and continued support, without her moral support during whole period of my studies and research work, it would not have been possible to come that far in my career. She boosted my confidence in my hard times and advised me to stay humble in my happy times.

TABLE OF CONTENT

Title page.....	i
Original Literary Work Declaration Form.....	ii
Abstract.....	iii
Abstrak.....	v
Acknowledgement.....	vii
TABLE OF CONTENT.....	viii
LIST OF FIGURES.....	xiii
LIST OF TABLES.....	xv
LIST OF SYMBOLS AND ABBREVIATIONS.....	xix
CHAPTER 1: INTRODUCTION.....	1
1.1 Research Background.....	1
1.2 Problem statement.....	5
1.3 Aim and Objectives.....	6
1.4 Research Scope.....	7
1.5 Significance of the Research.....	7
1.6 Outline and Structure.....	8
CHAPTER 2: LITERATURE REVIEW.....	11
2.1 Introduction.....	11
2.2 Feed Treatment.....	15
2.3 Thermal Treatment.....	15
2.4 Physical treatment.....	18
2.5 Feeding role and equipment.....	19
2.6 Discussion on Current Status of Pyrolysis Reactor Technology.....	24
2.6.1 Bubbling fluidized bed reactor.....	24
2.6.2 Circulating fluidized bed reactor.....	28
2.6.3 Conical spouted bed reactor.....	33
2.6.4 Rotary cone reactor.....	37

2.6.5	Ablative reactor	41
2.6.6	Auger/screw reactor.....	45
2.7	Overview of pyrolysis reactor technologies	49
2.7.1	Effect of operating parameters	52
2.7.2	Effect of particle size.....	52
2.7.3	Effect of feed rate	53
2.7.4	Effect of heating rate	54
2.7.5	Effect of temperature.....	56
2.7.6	Effect of vapor residence time.....	58
2.8	Condensation	58
2.9	Additional particulate separation devices.....	60
2.9.1	Cyclone separator	60
2.9.2	Electrostatic precipitators (ESPs).....	61
2.9.3	Filters.....	64
2.10	Outlooks on pyrolysis reactor technologies.....	65
CHAPTER 3: METHODOLOGY		67
3.1	Introduction.....	67
3.2	Material.....	67
3.3	Part 1: Designing of fluidized bed reactor for oil palm solid waste pyrolysis and experimental procedure using helical screw as a new concept for fluidization for improved oil production.	68
3.4	Characterization.....	71
CHAPTER 4: RESULTS AND DISCUSSION		74
4.1	Part 2: Novel helical screw-fluidized bed reactor for bio-oil production in slow pyrolysis mode: A Preliminary study	74
4.1.1	Introduction	74

4.1.2	Product yields	76
4.1.3	Effect of helical screw rotation	78
4.1.4	Effect of reactor design on slow pyrolysis performance	79
4.1.4.1	Effect of helical design on pyrolysis time	79
4.1.4.2	Effect of helical design on pyrolysis pressure.....	80
4.1.4.3	Distribution of liquid product based on the type of phase	81
4.1.5	Characterization.....	83
4.1.5.1	Characterization of liquid product.....	83
4.1.5.2	FTIR analysis of liquid product	85
4.1.5.3	GC/MS analysis of liquid product.....	87
4.1.5.4	Characterization of bio-oil (organic phase) for fuel properties.	89
4.1.5.5	Characterization of the by-products	90
4.1.5.6	FTIR analysis of by-product char.....	91
4.1.5.7	TGA/DTG analysis of by-product char.....	93
4.2	Part 3: Pyrolysis of Palm Shell using Helical Screw-Fluidized Bed Reactor: Effect of Heating Rate.....	96
4.2.1	Phase separation	96
4.2.2	Influence of heating rate on product yields.	98
4.2.3	Characterization of bio-oil.....	99
4.2.3.1	Physico-chemical properties of bio-oil at different heating rates.....	99
4.2.3.2	Ultimate analysis of bio-oil at selected heating rates.....	102
4.2.3.3	FTIR analysis of bio-oil at different heating rates	104
4.2.3.4	GC-MS analysis of bio-oil	106
4.2.3.5	Characterization of bio-oil for fuel properties.....	108
4.2.4	Characterization of by-products	109

4.2.4.1	Ultimate and proximate analysis of biochar.....	109
4.2.4.2	FTIR analysis of biochar	110
4.2.4.3	TGA/DTG analysis of biochar	112
4.2.4.4	Analysis of gas product	114
4.3	Part 4: Effect of temperature and feed rate on pyrolysis oil produced by novel helical screw fluidized bed reactor	115
4.3.1	Phase separation	115
4.3.2	Product yields	116
4.3.2.1	Effect of Temperature	116
4.3.2.2	Effect of feed rate	117
4.3.3	Characterization of bio-oil.....	118
4.3.3.1	Effect of temperature on physicochemical properties of bio-oil.....	118
4.3.3.2	Effect of feed rate on physicochemical properties of bio-oil. .	120
4.3.3.3	Ultimate analysis of bio-oil at different temperatures.....	121
4.3.3.4	Ultimate analysis of bio-oil at different feed rates.....	122
4.3.3.5	FTIR analysis of bio-oil attained at different temperatures and feed rates	123
4.3.3.6	GC-MS analysis of bio-oil obtained at different temperatures	125
4.3.3.7	GC-MS analysis of bio-oil at different feed rates	128
4.3.4	Characterization of by-product biochar.....	130
4.3.4.1	Effect of temperature on physicochemical properties of by-product biochar.....	130
4.3.4.2	Effect of feed rate on physicochemical properties of by-product biochar	133

4.4	Part 5: Palm shell pyrolysis in a novel helical screw fluidized bed reactor: Effect of particle size, pyrolysis time and vapor residence time on bio-oil yield and characteristic.....	136
4.4.1	Effect of PS particle size	136
4.4.2	Effect of pyrolysis time	144
4.4.3	Effect of vapor residence time.....	148
4.4.4	Optimized conditions of HSFBR	153
CHAPTER 5: CONCLUSION AND RECOMMENBATIONS FOR FUTURE WORK.....		154
5.1	Conclusions	154
5.1.1	Part 1: A technical review on semi-continuous and continuous pyrolysis process of biomass to bio-oil.....	154
5.1.2	Part 2: Novel helical screw-fluidized bed reactor for bio-oil production in slow pyrolysis mode: A preliminary study.....	155
5.1.3	Part 3: Pyrolysis of Palm Shell using Helical Screw-Fluidized Bed Reactor: Effect of Heating Rate.....	156
5.1.4	Part 4: Effect of temperature and feed rate on pyrolysis oil produced via helical screw fluidized bed reactor	157
5.1.5	Part 5: Palm shell pyrolysis in a novel helical screw fluidized bed reactor: Effect of particle size, pyrolysis time and vapor residence time on bio-oil yield and characteristics	158
5.2	Recommendations for future work	159
REFERENCES.....		160
APPENDIX A: FTIR spectra of palm shell biomass sample.....		184
APPENDIX B: Experimental setup of novel (HSFBR).....		185
APPENDIX C: LIST of Publications and conferences.....		186

LIST OF FIGURES

Figure 1. 1: Schematic work flow diagram.....	10
Figure 2. 1: Bubbling fluidized bed reactor with particulate separation facility. Redrawn based on	27
Figure 2. 2: Schematic diagram of a circulating fluidized bed reactor. Redrawn based on	29
Figure 2. 3: Schematic diagram of a conical spouted bed reactor.	33
Figure 2. 4: Schematic diagram of rotary cone reactor. Redrawn based on	38
Figure 2. 5: Schematic diagram of an ablative reactor. Redrawn based on	41
Figure 2. 6: Schematic diagram of an auger/screw reactor pyrolysis.	45
Figure 2. 7: Effect of feeding rate on pyrolytic products yield at 450°C. Redrawn based on	54
Figure 2. 8: Types of different condensers used in pyrolysis. Redrawn based on [169].	59
Figure 2. 9: Cyclone separator. Redrawn based on	61
Figure 2. 10: Electrostatic Precipitator. Redrawn based on	62
Figure 2. 11: Combination of devices for particulate separation. Redrawn based on	63
Figure 2. 12: Type of filters used in vapor purification during pyrolysis.	64
Figure 3. 1: Schematic diagram of novel helical screw fluidized bed pyrolysis reactor:	69
Figure 4. 1: Effect of helical screw rpm on pyrolysis time.	79
Figure 4. 2: Effect of helical design on pyrolysis pressure.	80
Figure 4. 3: Separation of bio-oil phases obtained with 0 and 50 rpm conditions.....	81
Figure 4. 4: FTIR spectra of the bio oil (organic phase) attained at 0 and 50 rpm torque.	85
Figure 4. 5: FTIR spectra of by-product char obtained at 0 and 50 rpm condition.	92
Figure 4. 6: Thermogravimetric analysis of by-product char obtained at 0 and 50 rpm.	93
Figure 4. 7: DTG analysis of by-product char obtained at 0 and 50 rpm.	94

Figure 4. 8: Phase separation of bio-oil under the influence of polar affinity and gravity.	96
Figure 4. 9: FTIR spectra of the bio oil (organic phase) attained at different heating rates.	104
Figure 4. 10: FTIR spectra of the by-product biochar attained at different heating rates.	110
Figure 4. 11: (a) TGA analysis and (b) DTG analysis of by-product char attained at 50, 150 and 275°C/min heating rate.	112
Figure 4. 12: Phase separation of bio-oil with various temperatures under the influence of gravity.	115
Figure 4. 13: FTIR spectra of organic phase attained at different (a) Temperatures and (b) Feed rates.	123
Figure 4. 14: FTIR spectra of the by-product biochar attained at different temperatures.	131
Figure 4. 15: (a) TGA analysis and (b) DTG analysis of by-product biochar obtained at 400, 500 and 650°C.	132
Figure 4. 16: FTIR spectra of the by-product biochar attained at different feed rate. ...	134
Figure 4. 17: (a) TGA analysis and (b) DTG analysis of by-product biochar attained with 5 g/min, 15 g/min and 25 g/min.	134
Figure 4. 18: Phase separation of bio-oil under the influence of polar affinity and gravity.	136
Figure 4. 19: FTIR spectra of the bio-oil (organic phase) obtained at selected particle sizes.	140
Figure 4. 20: Phase separation of bio-oil under the influence of polar affinity and gravity.	144
Figure 4. 21: FTIR spectra of bio-oil (organic phase) obtained at selected pyrolysis time.	146
Figure 4. 22: Phase separation of bio-oil under the influence of polar affinity and gravity.	148
Figure 4. 23: FTIR spectra of bio-oil (organic phase) obtained at selected vapor residence time.	150

LIST OF TABLES

Table 2. 1: Status and operation capacity of existing commercialized pyrolysis plant	14
Table 2. 2: Different types of biomass feeding equipment.	23
Table 2. 3: Bubbling fluidized bed reactor.	25
Table 2. 4: Circulating fluidized bed reactor.	31
Table 2. 5: Conical spouted bed reactor.	36
Table 2. 6: Rotary cone reactor.	39
Table 2. 7: Ablative reactor.	43
Table 2. 8: Auger/screw reactor.	47
Table 2. 9: Overview of pyrolysis reactor technology.	51
Table 3.1: Product characterization.	74
Table 4. 1: Comparison of pyrolysis products using different fluidization system with slow and fast pyrolysis mode at a reaction temperature of 500°C.	77
Table 4. 2: Effect of helical screw rotation on the distribution of slow pyrolysis products.	78
Table 4. 3: Distribution of bio-oil yield based on the type of phase.	82
Table 4. 4: Physical and chemical properties of bio-oil (organic phase) produced at 0 and 50 rpm settings.	84
Table 4. 5: Functional group compositions of bio-oil (organic phase) derived from palm shell.	86
Table 4. 6: Main compounds detected by GC/MS analysis of bio-oil (organic phase) attained at 0 and 50 rpm.	88
Table 4. 7: Characterization of bio-oil (organic phase) for fuel properties.	89
Table 4. 8: Ultimate and proximate analysis of by-product char obtained at 0 and 50 rpm.	91
Table 4. 9: Distribution and quantification of the bio-oil yield based on the type of phase.	97

Table 4. 10: Influence of low, medium and high heating rate on pyrolysis yields.	98
Table 4. 11: Physical and chemical properties of bio-oil attained at different heating rates.	100
Table 4. 12: Ultimate analysis of bio-oil (organic phase) with different heating rates.	103
Table 4. 13: Functional group composition of the bio-oil (organic phase) derived from PS.	105
Table 4. 14: GC/MS analysis of bio-oil attained with optimum heating rate of 275°C/min.	107
Table 4. 15: Characterization of bio-oil (organic phase) for fuel properties.	108
Table 4. 16: Ultimate and proximate analysis of by-product biochar with different heating rates.	109
Table 4. 17: Functional group composition of the by-product biochar derived from PS.	111
Table 4. 18: DTG analysis of by-product char at different heating rates.	113
Table 4. 19: Distribution of gas products of PS at different heating rates.	114
Table 4. 20: Influence of temperature on bio-oil yields.	116
Table 4. 21: Effect of feed rates on pyrolytic yields.	117
Table 4. 22: Effect of temperature on physicochemical characteristics of bio-oil organic phase.	119
Table 4. 23: Effect of feed rate on physicochemical characteristics of bio-oil at 500°C.	120
Table 4. 24: Ultimate analysis of bio-oil (organic phase) at different temperatures.	121
Table 4. 25: Ultimate analysis of bio-oil (organic phase) at 500°C with different feed rate.	122
Table 4. 26: Functional group composition of the bio-oil (organic phase) attained at different temperatures and feed rates.	123
Table 4. 27: GC/MS analysis for the identification of compound existing in bio-oil (Organic phase) achieved at 400, 500 and 650°C.	127
Table 4. 28: GC/MS analysis of bio-oil (Organic phase) produced at different feed rates.	129

Table 4. 29: Ultimate and Proximate analysis of by-product biochar with different temperatures.	130
Table 4. 30: Functional group composition of the by-product biochar.....	131
Table 4. 31: Detail of weight loss present of by-product biochar samples obtained at different temperatures.	132
Table 4. 32: DTG analysis of by-product biochar obtained at different temperatures.	132
Table 4. 33: Ultimate and Proximate analysis of by-product biochar with different feed rates.	133
Table 4. 34: Functional group composition of the by-product biochar.....	134
Table 4. 35: TGA analysis of by-product biochar samples obtained with different feed rates.	135
Table 4. 36: DTG analysis of by-product biochar obtained with different feed rates. .	135
Table 4. 37: Effect of particle size on product yields.	138
Table 4. 38: Effect of particle size on physico-chemical characteristics of bio-oil organic and aqueous phase*.....	138
Table 4. 39: Ultimate analysis of bio-oil (organic phase) with selected particle size...	139
Table 4. 40: Functional group composition of the bio-oil (organic phase) 0.25 mm, 4 mm and 10 mm particle size.....	140
Table 4. 41: GC/MS analysis of bio-oil produced at selected particle sizes of 0.25, 4 and 10 mm.	142
Table 4. 42: Characterization of bio-oil (organic phase) for fuel properties at selected particle sizes.....	143
Table 4. 43: Effect of pyrolysis time on product yields.	144
Table 4. 44: Effect of pyrolysis time on physicochemical characteristics of bio-oil....	146
Table 4. 45: CHNS/O analysis of bio-oil (organic phase) at selected pyrolysis time...	146
Table 4. 46: GC/MS analysis of bio-oil achieved at selected pyrolysis time of 20, 30 and 60 min.	147
Table 4. 47: Characterization of bio-oil (organic phase) for fuel properties at selected pyrolysis time of 20, 30 and 60 min.....	148

Table 4. 48: Effect of vapor residence time on product yields.	149
Table 4. 49: Effect of vapor residence time on physicochemical characteristics of bio-oil organic and aqueous phase*.....	149
Table 4. 50: CHNS/O analysis of bio-oil (organic phase) at selected vapor residence time.	150
Table 4. 51: Characterization of bio-oil (organic phase) for fuel properties at selected vapor residence time at 0.25, 10 and 20 s.	151
Table 4. 52: GC/MS analysis of bio-oil achieved at selected vapor residence time of 0.25, 10 and 20 s.	152

Universiti Malaysia

LIST OF SYMBOLS AND ABBREVIATIONS

PS	:	Palm shell
HSFBR	:	Helical Screw Fluidized Bed Reactor
BFBR	:	Bubbling fluidized bed reactor
CSBR	:	Conical spouted bed reactor
RCR	:	Rotary cone reactor
ESPs	:	Electrostatic precipitators
HHV	:	Higher heating value
LHV	:	Lower heating value
TGA	:	Thermogravimetric analysis
DTG	:	Differential thermal gravimetric
FTIR	:	Fourier-transform infrared spectroscopy
GC-MS	:	Gas chromatography–mass spectrometry
kWh/t	:	kilowatts per hour per ton

CHAPTER 1: INTRODUCTION

1.1 Research Background

Biomass resources have long been identified as sustainable source of renewable energy particularly in countries where there are abundant agricultural activities. Malaysia is the second largest producer of crude palm oil in the world. Almost 70% by volume from the processing of fresh fruit bunch is removed as wastes in the form of empty fruit bunches, palm kernel shells, palm oil mill effluent etc. With more than 423 mills in Malaysia, this palm oil industry generating around 80 million dry tones of biomass waste in a year across the country. A survey of the literature indicates that most of the biomass is handled with unsatisfactory practices that negatively impact on the environment. Therefore, intensive use of biomass as renewable energy source in Malaysia can reduce dependency on fossil fuels and significant advantage lies in reduction of net carbon dioxide emissions to atmosphere leading to less greenhouse effect. However, increased competitiveness will require large-scale investment and advances in technologies for converting this biomass to energy efficiently and economically.

There are several methods to utilize the biomass waste for energy utilization such as combustion, gasification and pyrolysis. Direct Combustion is the ancient method of utilizing biomass waste into heat with 10 percent efficiency. The gasification technology transforming the biomass to only syngas. The end byproducts after biomass combustion and gasification are only ash content. While, bio-oil through pyrolysis is achieved by thermal decomposition of biomass when it is subjected to elevated temperature ($> 500^{\circ}\text{C}$) in an inert atmosphere [1], since it can produce liquid yield up to 75 wt. % on a dry-feed basis [2]. The by-products of this process are bio-char, and syngas [3]. The bio-oil obtained from pyrolysis can be used in the production of electricity, mechanical work and

various chemical commodities [4]. In contrary to combustion and gasification processes, which involve entire or partial oxidation of material, pyrolysis bases on heating in the absence of air. This makes it mostly endothermic process that ensure high energy content in the products received. Due to these features, pyrolysis becomes increasingly important process for today industry as it allows to bring far greater value to common materials and waste. Bio-oil production is advantageous because it includes ease of storage, transportation and utilization for fuels and chemical feedstocks. Also, the oil obtained from the pyrolysis of biomass exhibits the properties of fossil fuels such as heating value. The obtained bio-gas as a by-product from pyrolysis can be used as a source of energy [5] and fluidizing medium [6]. Furthermore, bio-char has many potentially attractive applications. For example, it can be used as sorbent for the purification of compounds, soil conditioner to enhance the soil fertility due to its high sorption capacity for water and nutrients [7] and activated carbon for waste water treatment [8]. Since the products obtained from this process are useful, this process has been recommended as an environmentally friendly method [9].

Several pyrolysis processes were based on laboratory-scale reactors and investigations were made using batch, semi-continuous/semi-batch and some continuous processes. According to Lam et al., most studies were conducted using batch process in laboratory scale [10]. Batch process is a closed system process, in which reactants and products remain inside the reactor for a period of time while the reaction is being carried out. Batch process is advantageous in several aspects as it can offer better process simplicity; does not need a high-pressure pump or compressor and it can cater for all types of biomasses feedstock. Besides that, the absence of fluidization medium in batch pyrolysis process also reduces the separation complexity of byproduct char. However, the disadvantages of batch process are: extended reaction time, inconsistency of product from each batch, high labor cost, it requires time to heat up and cool down, and the difficulty

of large scale production [11]. Due to these technical limitations, scientists are moving towards to use of semi-continuous and continuous process. In semi-continuous pyrolysis process, feed is gradually added inside the reactor as reaction proceeds. The production rate in semi-continuous process is better than the batch process because of its partial withdrawal of products over the time. The performance of semi-continuous process is little bit complicated due to the accumulation of feed inside the reactor which leads to unsteady-state operation [12]. However, the feeding of reactants and withdrawal of products or byproducts while the reaction is still progressing can be obtained continuously without any interruption and delay, which makes continuous process more efficient and stable during the bio-oil production [13]. This adjustment is basically called as a continuous pyrolysis process. This process is advantageous over batch and semi-continuous process because of the ease of operation, consistency in product quality, low labor cost, less processing time, saving costs for temporary storage, easy control of the entire course of production and steady state operation.

The first step in both semi-continuous and continuous process basically deals with the feeding mode, where pre-treatment of raw material and feeding method becomes the first priority. Therefore, biomass feedstock is subjected to some form of pretreatment before its pyrolysis. The aim of the pretreatment is to change or even destruct the lignocellulosic structure so that the pyrolysis efficiency can be enhanced [14]. Different biomasses have different physical and chemical properties. Several techniques were available for biomass treatment which were divided into two major categories, including 1) physical treatment (e.g., milling/grinding and extrusion) and 2) Thermal treatment (e.g., torrefaction, steam explosion/liquid hot water pretreatment and ultrasound/microwave irradiation) [14]. In physical treatment, biomass is subjected to size reduction to increase the interfacial surface area [15] of the particle in order to avoid coagulation [15, 16] and to facilitate mass and heat transfer [17, 18] in the reactor during

fluidization [15]. For that purpose, different kinds of equipment were available for milling/grinding and extrusion of biomass. Generally, particle size of 1-2 mm is recommended for effective bio-oil production and to suppress secondary reactions in pyrolysis [14, 19, 20].

Thermal treatment includes the drying process. It is highly recommended as to reduce the moisture contents in biomass in order to minimize instability issue of liquid product [21]. Generally, drying usually requires reduction to moisture content below 10 wt.% [20, 22]. Besides the two major treatments, transportation of feed into the reactor has a remarkable influence on the operational efficiency of the whole process [23]. For this purpose, various feeding equipment were widely available such as: hopper free fall feeding [24], screw/auger feeder [25], conveyor belt [26] and pinch valve [27]. Research on the development of semi-continuous and continuous pyrolysis reactors are at an early stage [28, 29]. Generally several reactors were used in semi-continuous and continuous pyrolysis process on laboratory scale and considered as suitable reactors for commercialization were: Bubbling Fluidized Bed (BFB) reactor [30], Circulating Fluidized Bed (CFB) reactor [30, 31], Circulating Spouted Bed (CSB) reactor [32], Rotary Cone (RC) reactor [33], Ablative reactor [34-36] and Screw/auger reactor [33, 36]. Among these reactors, semi-continuous fluidized bed reactor was found to be the feasible option to carry out the pyrolysis process. Bridgwater reported a stable performance with significant amount of liquid yields: usually 70–75 wt.% from wood on a dry feed basis with semi-continuous bubbling fluidized bed reactor [37, 38]. The use of semi-continuous and continuous pyrolysis has attracted the attention of the industrialists. A number of companies such as Ensyn Technologies, Dynamotive, and Biomass Technology Group (BTG) are working on the commercialization of continuous pyrolysis process with the main aim to produce liquid fuels. The list of existing commercial plants was shown in Table 1 [39, 40]. From Table 1.1, it can be seen that biomass processing

capacity of AE Cote Nord Bioenerg/Ensyn using Fluid bed/riser technology was 9,000 kg/hr and bio-oil yield of 6,400 kg/hr higher than others.

Table 1. 1: Status and operation capacity of existing commercialized pyrolysis plant [41].

Host Organization	Country	Technology	Feeding Capacity (kg/hr)	Bio-oil yield (kg/hr)	Status	Year
BTG-BTL EMPYRO	Netherlands	Rotating cone	5000	3,250	Operational	2014
KiOR	USA	Catalytic fast pyrolysis	21,000	NM	Inactive	2014
Fortum - VALMET	Finland	Fluid bed / riser	10,000	NM	Operational	2013
Genting	Malaysia	Rotating cone	2000	1200	Inactive	2005
AE CoteNord Bioenergy / Ensyn	Canada	Fluid bed / riser	9,000	6,400	Operational	NM
Red Arrows - Ensyn	Canada	Fluid bed / riser	1,667	NM	Operational	1996

NM= Not mentioned.

Many researchers have conducted several studies on process parameters for upgradation of pyrolysis systems from laboratory to industrial scale. Each parameter has its own importance in pyrolysis for a specific mode, i.e. batch, semi-continuous, and continuous process. Various operating parameters such as heating rate, temperature, feed rate, gas flow rate, and reaction/residence time should be considered while performing biomass pyrolysis [42, 43]. Furthermore, these operating parameters considerably effect on the quality [43] and quantity of pyrolytic products [44]. The conversion of biomass to bio-oil through pyrolysis involves both endothermic and exothermic processes, which is sustained by pyrolysis temperature. Therefore, pyrolysis temperature was found to be the most significant parameter in affecting liquid yield [45]. Based on the above explanations, it can be seen that the pyrolysis reactors performance is mainly depending on the operating parameters.

1.2 Problem statement

Formerly, the residues of oil palm are the main contributors to biomass waste in Malaysia. A survey of the literature indicates that most of the biomass is handled with

unsatisfactory practices that negatively impact on the environment. One of the potential techniques is to convert oil palm residues into bio-oil via pyrolysis. Bio-oil production is advantageous because it includes ease of storage, transportation and utilization for fuels and chemical feedstocks. Fast pyrolysis with combined continuous fluidized bed system is recommended to produce high liquid yield. However, there were some problems which occurred during the pyrolysis such as energy intensive issue to achieve average particle size ~1 - 2mm, extended solid residence time, particle agglomeration, pressure drop, difficulty of char removal, high gas fluidization requirement and post-treatment of the liquid product for char removal. In addition, high gas velocity may increase the overall cost of process by installation of cyclone separators and AC power requirement. This study will help to resolve fluidized bed reactor problems through developing a novel cost-effective lab-scale continuous helical screw fluidized bed reactor replacing fluidizing gas with helical screw system.

1.3 Aim and Objectives

This main aim of this thesis is to study the work done on novel helical screw fluidized bed reactor for pyrolysis process to produce bio-oil from biomass. This work is precisely achieved through the following specific objectives:

1. To design the fluidized bed reactor using helical screw as a new concept for oil palm solid waste pyrolysis.
2. To determine whether there was an improvement in the quantity and quality of the oil production by using the helical screw fluidized bed reactor.
3. To explore the performance of helical screw fluidized bed reactor in slow, medium and fast pyrolysis modes.
4. To investigate the effect of operating parameters includes (temperature, feed rate, particle size, pyrolysis time and vapor residence time) for the production of bio-oil from biomass by helical screw fluidized bed reactor.

1.4 Research Scope

The scope of the present research is to develop a new reactor technology with potential use in production of bio-oil at cheaper cost in the future. The major aim of the present study is to manage the biomass waste material to produce good quality and quantity pyrolysis oil. This research will contribute in finding sustainable and renewable energy to substitute the depleting fossil fuels. Interestingly, HSFBR technique have advantage to provide high mass transfer by particle dynamics and good pyrolysis control using several biomass feedstocks with high production rate. Generally, pyrolysis reactors are restricted to use 1-2 mm particle size and operated with gas fluidization systems infecting the liquid product by particulate contamination. Therefore, additional particulate separation devices are required such as cyclones, filters and electrostatic precipitators which increase the final product cost. However, in HSFBR reactor can be operated in slow and fast pyrolysis mode from 1- 10 mm particle size with no fluidizing gas to achieve the high fluidization condition and no additional separation devices making it economically feasible process.

1.5 Significance of the Research

This research is conducted in order to address the several problems related to pyrolysis gas fluidized bed reactor and limitations in term of additional equipment's: such pressure pump for inert gas fluidization, cyclone separators, filters, electrostatic precipitators and fine char separation units. Apart from the ability to obtain high-yielding liquids in the slow-pyrolysis condition, the reactor has also other good features, such as low pyrolysis time, fast vapor production, non-agglomeration of particles, non-occurrence of pressure drop during the continuous operation and production of good-quality of bio-oil and byproduct char. Without using any inert gases for fluidization this feature was attributed to the screw propeller design system in helical screw fluidized bed reactor which provided high mass and heat transfer at large particle size range which is 5

times of the particle size limit as recommended in previous studies. This feature would enable the possibility of helical screw fluidized based pyrolysis to be done in the absence of biomass size reduction processes to reduce process cost and complexity. In addition, the new reactor can be operated in both modes of semi-continuous and continuous pyrolysis mode. In light of important features of HSFBR validates the importance of the work has great impact on the pyrolysis reactor technology. Also, that will contribute to new knowledge by mechanical fluidization for other researcher in the field of pyrolysis reactor technology.

1.6 Outline and Structure

The format of this thesis follows the Conventional Style format as mentioned in the University of Malaya guidelines. All of the work that were described in this thesis have been published in ISI Q1 journals. The overall outlines and organization of the thesis is discussed in this section. The thesis comprises on five chapters, and every chapter is presented as follows.

Chapter 1 Introduction: This chapter describes various biomass resources have been identified as sustainable source of renewable energy particularly in countries where there are abundant agricultural activities. Several methods were highlighted to utilize the biomass waste for energy utilization such as combustion, gasification and pyrolysis. In addition, this chapter also provides the research background, problem statement, objective of the research and scope of study.

Chapter 2 Literature review: This chapter introduces semi-continuous and continuous pyrolysis process through several perspectives: reactor technologies, operating parameters, feed treatment, feeding system and additional product separation devices. Therefore, by considering all types of the reactors, design aspects, facilities, advantages

and disadvantages, the designing of a more efficient pyrolysis reactor would certainly be of great need and advantage in the field of pyrolysis process. A comprehensive outlook on pyrolysis reactor technology is also provided. The expressed contents of this chapter will provide an understanding of the technical aspect of pyrolysis process comprehensively, starting from the material treatment to the end of product collection. This chapter refer to the work for objective 1. The content of this chapter has been published in (ISI, Q1 Journal with impact factor 4) in Journal of Analytical and Applied Pyrolysis (K.M. Qureshi, A.N. Kay Lup, S. Khan, F. Abnisa, W.M.A. Wan Daud). vol. 131, p.p. 52-75, 2018.

Chapter 3 Methodology: This chapter provides the information from raw material to experimental procedure. Moreover, details of the product characterization techniques, procedure and equipment's used are also briefly discussed.

Chapter 4 Results and discussion: This chapter epitomizes all the parametric and characterization results for objective 2, 3 and 4. The main purpose of this chapter was to investigate the effect of heating rate, temperature, feed rate, pyrolysis time and vapor residence time on the pyrolytic yields via novel helical fluidized bed reactor using slow, medium and fast pyrolysis mode. This work has been published in (Q1, ISI Journal with impact factor 4) the Journal of Analytical and Applied Pyrolysis in 2019 and 2020.

Chapter 5 Conclusions and recommendations for future work This chapter includes conclusion and future recommendations based on the finding during the pyrolysis study using novel helical screw fluidized bed reactor.

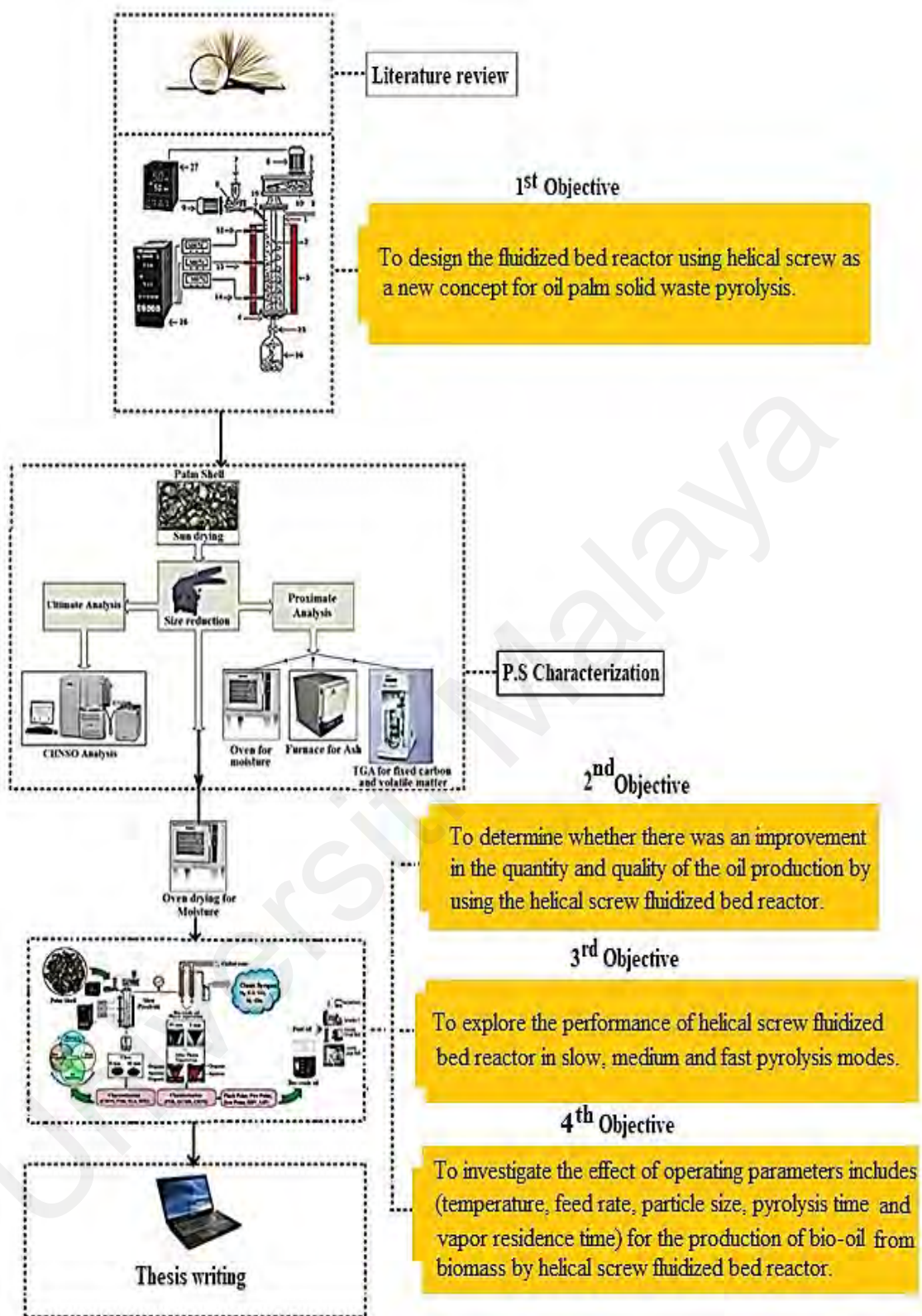


Figure 1. 1: Schematic work flow diagram.

CHAPTER 2: LITERATURE REVIEW

2.1 Introduction

In pyrolysis, thermal decomposition of material occurs when it is subjected to elevated temperature ($> 500^{\circ}\text{C}$) in an inert atmosphere [1]. The products of this process are bio-oil, bio-char, and syngas [3]. Among them, bio-oil was measured to be main products, whereas, bio-gas and bio-char were considered as by-products. The bio-oil obtained from pyrolysis can be used in the production of electricity, mechanical work and various chemical commodities [4]. The conversion of biomass to bio-oil through pyrolysis technique is getting more attention because it can produce liquid yield up to 75 wt. % on a dry-feed basis [2]. Also, the oil obtained from the pyrolysis of biomass exhibits the properties of fossil fuels such as heating value. The obtained bio-gas as a by-product from pyrolysis can be used as a source of energy [5] and fluidizing medium [6]. Furthermore, bio-char has many potentially attractive applications. For example, it can be used as sorbent for the purification of compounds, soil conditioner to enhance the soil fertility due to its high sorption capacity for water and nutrients [7] and activated carbon for waste water treatment [8]. Since the products obtained from this process are useful, this process has been recommended as an environmentally friendly method [9].

Several reported pyrolysis processes were based on laboratory-scale reactor. These investigations were made using batch, semi-continuous/semi-batch and continuous processes. According to Lam et al., most studies were conducted using batch process in laboratory scale [10]. Batch process is a closed system process, in which reactants and products remain inside the reactor for a period of time while the reaction is being carried out. Batch process is advantageous in several aspects as it can offer better process simplicity; does not need a high-pressure pump or compressor and it can cater for all types

of biomasses feedstock. Besides that, the absence of fluidization medium in batch pyrolysis process also reduces the separation complexity of byproduct char. However, the disadvantages of batch process are: extended reaction time, inconsistency of product from each batch, high labor cost, it requires time to heat up and cool down, and the difficulty of large scale production [11]. Due to these technical limitations, scientists are moving towards to use of semi-continuous and continuous process. In semi-continuous pyrolysis process, feed is gradually added inside the reactor as reaction proceeds. The production rate in semi-continuous process is better than the batch process because of its partial withdrawal of products over the time. The performance of semi-continuous process is little bit complicated due to the accumulation of feed inside the reactor which leads to unsteady-state operation [12]. However, the feeding of reactants and withdrawal of products or byproducts while the reaction is still progressing can be obtained continuously without any interruption and delay, which makes continuous process more efficient and stable during the bio-oil production [13]. This adjustment is basically called as a continuous pyrolysis process. This process is advantageous over batch and semi-continuous process because of the ease of operation, consistency in product quality, low labor cost, less processing time, saving costs for temporary storage, easy control of the entire course of production and steady state operation.

The first step in both semi-continuous and continuous process basically deals with the feeding mode, where pre-treatment of raw material and feeding method becomes the first priority. Therefore, biomass feedstock is subjected to some form of pretreatment before its pyrolysis. The aim of the pretreatment is to change or even destruct the lignocellulosic structure so that the pyrolysis efficiency can be enhanced [14]. Different biomasses have different physical and chemical properties. Several techniques were available for biomass treatment which were divided into two major categories, including 1) physical treatment (e.g., milling/grinding and extrusion) and 2) Thermal treatment

(e.g., torrefaction, steam explosion/liquid hot water pretreatment and ultrasound/microwave irradiation) [14]. In physical treatment, biomass is subjected to size reduction to increase the interfacial surface area [15] of the particle in order to avoid coagulation [15, 16] and to facilitate mass and heat transfer [17, 18] in the reactor during fluidization [15]. For that purpose, different kinds of equipment were available for milling/grinding and extrusion of biomass. Generally, particle size of 1-2 mm is recommended for effective bio-oil production and to suppress secondary reactions in pyrolysis [14, 19, 46].

Thermal treatment includes the drying process. It is highly recommended as to reduce the moisture contents in biomass in order to minimize instability issue of liquid product [21]. Generally, drying usually requires reduction to moisture content below 10 wt.% [22, 46]. Besides the two major treatments, transportation of feed into the reactor has a remarkable influence on the operational efficiency of the whole process [23]. For this purpose, various feeding equipment were widely available such as: hopper free fall feeding [24], screw/auger feeder [25], conveyor belt [26] and pinch valve [27]. Research on the development of semi-continuous and continuous pyrolysis reactors are at an early stage [28, 29]. Generally several reactors were used in semi-continuous and continuous pyrolysis process on laboratory scale and considered as suitable reactors for commercialization were: Bubbling Fluidized Bed (BFB) reactor [30], Circulating Fluidized Bed (CFB) reactor [30, 47], Circulating Spouted Bed (CSB) reactor [32], Rotary Cone (RC) reactor [33], Ablative reactor [34-36] and Screw/auger reactor [33, 36].

Among these reactors, semi-continuous fluidized bed reactor was found to be the feasible option to carry out the pyrolysis process. Bridgwater reported a stable performance with significant amount of liquid yields: usually 70–75 wt.% from wood on a dry feed basis with semi-continuous bubbling fluidized bed reactor [37, 38]. The use of

semi-continuous and continuous pyrolysis has attracted the attention of the industrialists. A number of companies such as Ensyn Technologies, Dynamotive, and Biomass Technology Group (BTG) are working on the commercialization of continuous pyrolysis process with the main aim to produce liquid fuels. The list of existing commercial plants was shown in Table 2.1 [39, 40].

Table 2. 1: Status and operation capacity of existing commercialized pyrolysis plant [41].

Host Organization	Country	Technology	Feeding Capacity (kg/hr)	Bio-oil yield (kg/hr)	Status	Year
BTG-BTL EMPYRO	Netherlands	Rotating cone	5000	3,250	Operational	2014
KiOR	USA	Catalytic fast pyrolysis	21,000	NM	Inactive	2014
Fortum - VALMET	Finland	Fluid bed / riser	10,000	NM	Operational	2013
Genting	Malaysia	Rotating cone	2000	1200	Inactive	2005
AE Cote Nord Bioenergy / Ensyn	Canada	Fluid bed / riser	9,000	6,400	Operational	NM
Red Arrows - Ensyn	Canada	Fluid bed / riser	1,667	NM	Operational	1996

From Table 2.1, it can be seen that biomass processing capacity of AE Cote Nord Bioenergy/Ensyn using Fluid bed/riser technology was 9,000 kg/hr and bio-oil yield of 6,400 kg/hr higher than others. Many researchers have conducted several studies on process parameters for upgradation of pyrolysis systems from laboratory to industrial scale. Each parameter has its own importance in pyrolysis for a specific mode, i.e. batch, semi-continuous, and continuous process. Various operating parameters such as heating rate, temperature, feeding rate, gas flow rate, and reaction/residence time should be considered while performing biomass pyrolysis [42, 43]. Furthermore, these operating parameters considerably effect on the quality [43] and quantity of pyrolytic products [44]. The conversion of biomass to bio-oil through pyrolysis involves both endothermic and exothermic processes, which is sustained by pyrolysis temperature [45]. Therefore, pyrolysis temperature was found to be the most significant parameter in affecting liquid

yield [45]. Furthermore, physical parameters: hopper level, large particle size, irregular shape, particle surface roughness, wet biomass and bulk densities also showed notable effects on final yield [48]. Based on the above explanations, it can be seen that the pyrolysis reactors performance is mainly depending on the operating parameters.

This study aims to evaluate the previous work done on semi continuous and continuous pyrolysis systems using biomass as a feedstock. The effect of different operating parameters on product quality [43] and quantity [44] using both semi-continuous and continuous pyrolysis system were also discussed. Furthermore, the use of additional equipment's such as condensation unit, and fine char separation units were also briefly discussed in this paper. In addition, the economic evaluation of semi-continuous and continuous pyrolysis system was also discussed in this study.

2.2 Feed Treatment

For smooth and proficient process, biomass feed treatment is a prerequisite before being used in pyrolysis. The main role of pretreatment is to remove the moisture content, destruct the lignocellulosic structure and get uniform particle size. This would subsequently improve pyrolysis efficiency and bio-oil yield. Biomass pretreatment methods can be divided into two different treatments 1) Thermal treatment (drying) and 2) Physical treatment (crushing and grinding).

2.3 Thermal Treatment

Drying is an important thermal treatment method in which water/moisture content is removed from feedstock before starting pyrolysis. Moisture can effects the physiochemical properties of products such as chemical stability, heating value, viscosity, corrosiveness and pH [1]. They also significantly limit the application of bio-oil particularly as motor fuel [49]. Drying involves the application of heat to vaporize

moisture and some means of removing water vapors from the material [50]. The importance of feed drying is to avoid the sticking of biomass particles, maintain the steady state condition during the biomass feed flow and to avoid the presence of water content in bio-oil product.

Most of the biomass feedstock containing high moisture content such as birch (18.9 wt.%) [51] food waste (74 – 90 wt.%) [52], paper sludge (70 – 80 wt.%) [53], textile sludge (80 wt.%) [54], leather (10.25 wt. %) [55], municipal solid waste (MSW) (52 – 66 wt.%) [56], wood (20 wt.%) [57], barley straw (30 wt.%) [1] and wheat straw (15 – 16 wt.%) [58]. From the literature, it can be seen that food waste contains higher moisture content which would affect the composition of the pyrolysis products and reduces the quality of the bio-oil. Thus, higher moisture content in feedstock is not a feasible option for pyrolysis [50]. Moisture content in feedstock of not more than 10 wt.% is recommended for bio-oil production [21, 59]. The wide range of drying methods were employed to reduce moisture content, which are waste heat drying [60], sun drying [61], solar drying [62] and microwave drying [63]. Biomass drying is an energy-intensive process, so utilizing waste heat energy from flue gases for biomass drying makes pyrolysis process more efficient and reduces the inclusive energy demand.

Hanning et al. used waste heat drying method through hot flue gas stream of temperature ranges 250-450 °C produced from process industry combustor. The moisture content in pine wood chips was reduced from 50-60 wt.% to 10 wt.% at 450°C. In addition, the waste heat drying method is a good option of biomass drying which may decrease the overall capital cost of continuous pyrolysis process [60]. Whereas, sun drying is the most widespread conventional but uncontrolled drying method in which temperature varies in the day round the clock and may decrease the drying rate. It was noted that during conventional drying, wet material was spread in thin layers on the mats, roof tops or cemented floors and left until the completion of drying [64]. Additionally,

sun drying involves simultaneous heat and mass transfer to vaporize the moisture from the exposed material. In this manner, the average moisture content of the coconut biomass was reduced from about 57.4 % to 6.8 % after 22 hours of sun drying [64]. Thus, sun drying is supposed to be an economical method for moisture removal from agricultural biomass, food and many other materials [62]. Nevertheless, external drying parameters such as heat input, moisture content, temperature and air flow rate cannot be controlled, which can result in less drying or extended time [65]. Moreover, solar drying is a controlled aeration method which is achieved in a closed system through sun energy for various commodities.

A box shaped housing unit consisting a transparent cover was used to allow sun rays to enter in the box to dry the material approximately in range of 50 to 60°C [62]. Using this method the moisture content of the oil palm fronds reduced from 60 wt.% to 10 wt.% [66] and from wheat 25 wt.% to 16 wt.% [62]. In terms of fuel/energy cost, it is likely an economical drying method, at present solar drying is not commercialized due to its slow process [66, 67]. Microwave drying is a new drying method in which microwave radiation polarizes water molecules in biomass to generate more vibrational motions which in turn generate heat energy. Hence in the generated heat penetrates inside the material. The liquid start evaporating through the solid pore structure by macro-capillary system, resulting high drying velocity [68]. It was observed that moisture content of pine reduced from 13% to 6% in a microwave dryer with energy consumption of 55 kWh/m³ in a very short residence time.

In contrast to other drying options, waste heat drying methods is reasonably economical and more feasible [60]. Sun drying method is conventional but is also relatively slow and uncontrollable. Moreover, solar drying is not so far commercialized due to its high cost and slow process. In addition, microwave drying is reasonably costly and energy intensive method that is why it is still not used on large scale. To develop

continuous pyrolysis by waste heat drying method, Fagernas et al., suggested the possible heat sources for biomass drying are hot furnace, engine or gas turbine exhaust gases, high-pressure steam from a steam or combined cycle plant, warm air from an air-cooled condenser in a steam or combined cycle plant and steam from dedicated combustion of surplus biomass, or diverted product gas, char or bio-oil [69].

2.4 Physical treatment

This treatment is aimed to change the physical properties of biomass to enhance the continuous fast pyrolysis process [70]. Furthermore, biomass particle size has a key effect on the heating rate which makes it an important parameter in controlling the drying rates [19], mass transfer [64] and heat transfer rates [19] during continuous pyrolysis. In this regard, crushing and grinding techniques can be used to get the desired feed particle size. This feed treatment will increase the surface area of particles, increase the heat transfer rate and pyrolysis efficiency. Manlu et al. reviewed a variety of particle size reduction equipment and technologies available for biomass applications [71]. Different types of crushing and grinding equipment's for biomass feed treatment were used such as hammer mill, ball mill, roller mill and disc mill.

Hammer mill is relatively easy to operate and produces wide range of particle size [72]. In addition, small particle size is ideal for good heat transfer in continuous fast pyrolysis [73]. During the milling process, material is broken into small fragments by the top edge of the "hammers" impact forces [71] as the hammers drive and forcing it to pass through the bottom mounted screen [74]. Tumuluru et al. investigated the energy consumption for grinding of canola straw, barley and oat straw using hammer mill. They found the energy consumptions for grinding to be 2.91 kWh/t for canola straw, 3.15 kWh/t for barley and 8.05 kWh/t for oat straws 8.05 kWh/t. This variation in energy consumption is dependent on the type of material used. [75]. Comparing the process of ball-milling it has been designated as a high-efficiency continuous biomass milling method. This

process depends on the speed of mill rotation, number of balls and its size to get required particle size [76]. In general, ball milling is a low-cost and effective method [77] with less energy consumption of 0.1 kWh/t [78].

In addition, roller mill produces lesser amount of heat energy in contrast ball milling during milling operation [71]. However, roller mills are less energy efficient and consume higher energy (15.240 kWh/t) which makes them not preferentially used [79]. Beside this, disc mill consists of two discs, one disc is fixed and the second one is driven by electric motor through belt system. The material is passed gradually through the adjustable gap between the two discs surfaces which produce grinding by friction to obtain the required particle size. Romuliet et al. investigated the effect of physical change on different size 8, 9, 10 and 12 mm of *J. curcas* seeds on crushing performance using a modified disc mill. They observed that under optimum conditions, the crushing efficiency for the four samples were 81.0, 83.5, 83.7, and 84.6%, respectively. The energy consumption of disc mill was reported to be about 2.032 kWh/t [80].

Within the context of the study, the grinding performances of different size reduction mills were compared in regard to their specific energy consumptions. The main equipment included hammer mill, ball mill, roller mill and disc mill with specific energy consumptions of 8.05, 0.1, 15.240 and 2.032 kWh/t, respectively. Among these milling machines, ball mill was found to be good as it has the least specific energy consumption (0.1 kWh/t) for size reduction operation.

2.5 Feeding role and equipment

For a consistent and proficient feed flow, feeding equipment is a prerequisite for a semi-continuous or continuous pyrolysis process. This can only be managed by using a mechanized feeding system that is customized for the specific type of feed, so it can bring a regular flow of biomass material to the pyrolysis reactor. The accuracy of the feeding

system is an important factor in the operational efficiency of any pyrolysis process [23]. There are several devices used to control feeding system, which can be seen in Table 2.2. Various feeding equipment were used in pyrolysis process such as hopper/lock hopper [81] screw/auger (both single screw and twin-screw) feeder [25, 82] conveyor belt [26] and pinch valve [27].

The most common and primary feeding source is hopper or lock hopper which feeds raw material directly or indirectly into the reactor. Hopper/lock hopper relies on the free-falling principles of mass. It comprises of converging inclined wall or conical shape consisting a lock at the bottom end by which mass flows downwards with the support of gravitational pull. It can be operated by two methods: 1) under atmospheric pressure and 2) gas pressurization. In atmospheric pressure the required size of biomass feed is introduced into hopper/lock hopper and allowed to flow under the action of gravity. The opening of bottom lock can be supported manually or with motor to maintain the constant feed rate.

Moreover, in pressurized feeding system N_2 or syngas were used to avoid the back flow of pyrolytic gases and to ensure smooth feeding. In addition, Dai et al. operated hopper/lock hopper above with pressure of < 3.5 MPa supported by N_2 gas has improved the feed flow rate and restricted the back flow of pyrolytic gases during continuous pyrolysis [81]. Furthermore, screw/auger feeders are also capable to transport bulk solids over a wide range of feed rates [81] for bio-oil production [25, 82]. In screw feeder, feeding system includes rotating helical screw which is typically covered with a tube and operated by motor to move granular particles. Kim et al. and Puy et al. studied the production of bio-oil using screw or auger feeding equipment [25, 82]. It was shown that screw feeder can efficiently transfer the measured quantity of biomass. Currently, recent technology has made the screw feeder one of the most efficient and economical methods of moving bulk material. This feeding system has been applied for many types of

feedstock such as food waste, wood chips, aggregates, cereal grains, animal feed, boiler ash, meat and bone meal, municipal solid waste, and several other materials [83] during semi-continuous and continuous pyrolysis.

Belt conveyor is a commonly used equipment of continuous transport, it has a high efficiency and large conveying capacity, simpler construction, small amount of maintenance. Can be achieved at different distances, different materials transportation. Conveyor belt system is generally used in many industrial applications for continuously feeding the large quantity of raw materials. Specifically, a conveyor belt consists of two or more pulleys, with an endless belt of carrying medium (the conveyor belt) that rotates continuously about them [84]. Milhe et al. used 1.5 m conveyor belt to feed wood chips with 6 kg/h and controlled the feed rate by airlock system and found that continuous feeding through conveyor belt is acceptable when compared the rate of the wood delivery (1 min) with the total residence time of the wood/char in the reactor about 1 h [26].

Pinch valve is made of rubber works based on the principle of pinching or pulsing effect to normally open by pneumatically and close periodically (typically every 10 s), for a short period of time about 4 seconds. The pinch valve and the solenoid valve are controlled by programmable logic controller system. However, pinch valve allows a small amount of biomass material which falls in the injector tube towards the reactor. During each cycle, some feed was accumulated in the injector tube which may cause solids settling or blockage. Therefore, this may be handled by a regular supply of N_2 as carrier gas with intermittent pulsing which may prevent it from solid accumulation [27]. Furthermore, the use of excessive pressure to control feed by pinch valve might result a sleeve damage or failure [85].


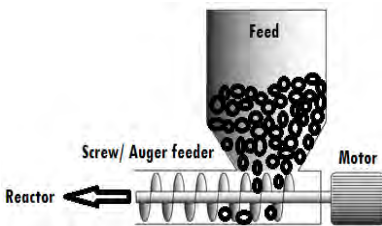
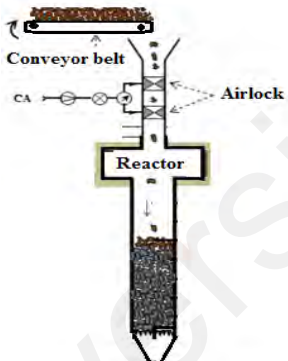
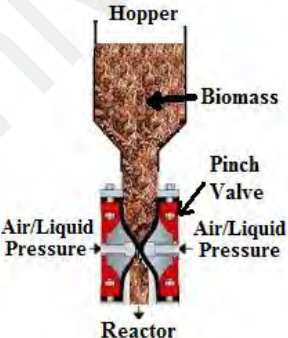
Hopper/lock hopper has some technical feed flowing issues which are flow instability, slow feed flow, material bridging stops the flow, flushing when the material is not effectively unified. All the mentioned limits may restrict its feasible use as feeder

in the pyrolysis process [86]. Also, conveyor belts are not regularly used in pyrolysis of biomass due to less feed control. Among the feeding equipment, screw/auger feeder was found to be the most suitable equipment in handling and controlling different samples of solid materials over a wide range of feeding rates [87]. In addition, the selection of good feeding equipment should also account for parameters such as type of material, particle size, particle shape, bulk density, good feed control and energy required to drive the feeding system [88].

In addition, special design strategy is needed for material that has sensitivity to temperature, like Kraft lignin, meat, bone meal, rubber, tire or plastic can cause the melt during the feeding. Actually, feeding system remains hot due to some of the following reasons such as: the direct (heat conduction) or indirect (heat flux) contact between the reactor and the feeding system. One main reason is unexpected hot vapor entrance into the feeder due to the elevation of pyrolytic gas/vapor pressure. In addition, internal friction between feed and device especially in auger/screw feeding system may face the problem due to screw flight rotation that occurred when the screw is twisting the feed causing some interlocking and arching of particles between the screw tips can melt the particles in the feed line [81].

To overcome these problems there are some strategies that can be applied, such as: installation of insulation system, create special coating on the feeder and feed line, the use of N_2 as a gas purging or water cooling the tube/jackets may be employed. [89]. Installation of insulation for feeding devices can be done by using the techniques of coating or wrapping the layers of insulation like fiberglass, mineral wool or char coating has been used [89]. In addition, the use of N_2 in feeding system will also benefit to maintain the ambient temperature in feedline and feeder [81]. Furthermore, the used of water cooling tube in feeding system is also recommended by many researchers to avoid the feed melt during pyrolysis processes [90].

Table 2. 2: Different types of biomass feeding equipment.

Feeding System	Drawing	Features	Ref.
Hopper /Lock hopper Free fall feeding		<ul style="list-style-type: none"> - Simple feeding method using free fall gravitational force. - Less consistency due to formation of ratholes. - Simple construction. - compatibility with other feeding mechanisms. - Low energy consumption and cost effective. 	[81]
Screw or Auger feeder		<ul style="list-style-type: none"> - Easy to operate - Efficient way to move semi-solid materials. - It can handle variety of materials like wood chips, MSW and many others. - Generally used for their considerable ability to seal and resist backpressure. - Simple to install and less maintenance. 	[81, 83, 84, 91]
Conveyor belt		<ul style="list-style-type: none"> - Use for open mechanical feeding system. - It can handle with different type and size of materials. - Suitable for the long-distance mass transfer. - Simple construction. - High efficiency. - Low power requirements. - Economic in upkeep. - More failure chances due to the improper alignment of idlers, belt running off at tail pulley. - Excessive wear on bottom of belt and corrosion in the frame. 	[26, 84]
Pinch valve		<ul style="list-style-type: none"> - Not suitable at excessive temperature and pressure. - Interior walls adheres when pinch close for many hours. - Feed inconsistency due to problem in actuator. 	[85, 92]

2.6 Discussion on Current Status of Pyrolysis Reactor Technology

Different configurations of pyrolysis reactor have been studied on laboratory scale and attempted to upgrade for commercialization due to high market interest [93]. Several reactors have been developed based on the continuous and semi-continuous modes to produce liquid oil like bubbling fluidized bed reactor (Dynamotive), circulating fluidized bed reactor (Ensyn and Fortrum), conical spouted bed reactor, rotary cone reactor (BTG), auger reactor (Lurgi together with Karlsruhe and Abritech), ablative reactor and auger/screw reactor to produce high liquid fuels [93-95].

2.6.1 Bubbling fluidized bed reactor

Bubbling fluidized bed (BFB) was first used in fast pyrolysis of biomass [96]. In past decades, the BFB reactor technology was commonly implemented in semi-continuous and continuous pyrolysis. Additionally, BFBs behave like a boiling fluid in which bubbles of gas rise rapidly and burst on the bed surface. These bubbles comprise of small amount solid particles either sand or biomass material. BFB is hydrodynamically stable for smaller biomass particle size (0.5–2 mm) and is used with an inert helium or nitrogen for fluidization and sand for destruction of biomass particles to achieve good heat transfer, trap char particles and temperature control [97]. Furthermore, BFB showed consistent performance with high liquid yield ranging from 70-75 wt. % as can be seen in Table 2.3 [40]. However, the use of this reactor will lead to fine char contamination of about 15 wt. % in liquid product, which is typically dependent on the reactor shape and fluidizing gas velocities [31].

Table 2. 3: Bubbling fluidized bed reactor.

S. N	Reactor Type & Dimensions	Mode	Feedstock & Particle size (mm)	Feeding system & Feeding rate	Heating system & Heating rate (°C/min)	Temp: (°C)	Residence time (Sec :)	Cooling system (°C)	Purging Gas	Gas output utilization	Yield (wt. %)			Ref:
											Oil	Char	Gas	
1.	Bubbling fluidized bed NM	Continuous	Stover and Corn cob 0.25-2 mm	Hopper and Screw ± 0.85 kg/h	Cylindrical Furnace 6.6kW 10	40-550	NM	Cooling tower & Condenser chain	N ₂ 20 ml/m	Atmosphere	51.1- 66.9	NM	10.8	[98]
2.	Bubbling fluidized bed L= 530 mm I.D=80 mm	Continuous	Beech sawdust 1.2 and 1.8 Wheat straw 0.8 & 2.0	Two Screw feeder 1.5 kg/h	Three adjustable electric heaters 10	500	1-1.5	Glass condenser Nitrogen and dry ice	N ₂ 0.3-0.4m/s	Atmosphere	60 – 70 51 - 60	NM 23	NM NM	[99]
3.	Bubbling fluidized bed reactor with mechanical stirrer L = 0.58 m I.D = 0.078 m	Continuous	Kraft lignin powder slugs, including silica sand, lignin and birch bark chars	pneumatically activated pinch valve 600g/h	Electric heaters NM	550	1.7	Fractional condensation system consisting Cyclone condenser	N ₂	Atmosphere	32.3 - 43	21.5 - 34.6	31.7 - 36	[100]
4.	Bench scale Bubbling fluidized bed reactor L = 500 mm O.D = ¾ inch	Continuous	Municipal solid waste 0.5-1.5mm	N ₂ Stream NM	NM NM	500-550	NM	Ice bucket	N ₂	To the extractor	45-50	32	NM	[101]
5.	Bubbling fluidized bed L = 0.58 m I.D = 0.078 m	Continuous	Birch bark sawdust 1 mm	Slug injector feeder 600 g/h	Electric heater	500-550	1.66	Two cyclonic (1and 3) condenser	N ₂	Atmosphere	34	25	59	[102]

Table 2.3: Continued...

S. N	Reactor Type & Dimensions	Mode	Feedstock & Particle size (mm)	Feeding system & Feeding rate	Heating system & Heating rate (°C/min)	Temp: (°C)	Residence time (Sec:)	Cooling system (°C)	Purging Gas	Gas output utilization	Yield (wt. %)			Ref:
											Oil	Char	Gas	
1.	Bubbling fluidized bed reactor L = 0.65 m I.D = 600, 0.075 m	Continuous	Kraft lignin 200 g NM	Injector tube and Pinch valve open 10 Sec NM	Three irradiative electric heaters NM	450-600	1.5	Ice-water-cooled jacket	N ₂ 5.2 × 10-4 to 4.3 × 10-4 kg/s	Atmosphere	32	NM	NM	[27]
2.	Bubbling fluidized bed L= 0.58 m D=0.076 m	Continuous	Tucuma (Aculeatum) seed < 2	Slug feeder 0.2kg/min	Four radiative electric heaters NM	400-600	1.4	Chiller	N ₂ 2.87 × 10-4N m ³ /s	Atmosphere	60	NM	NM	[103]
3.	Bubbling fluidized bed L = 305 mm I.D = 41 mm	Continuous	Spruce Salix MiscanthusW heat straw NM	Screw feeder NM	Insulated heater 10	460-475	NM	Intensive cooler	N ₂	Atmosphere	68.1 62.1 56.1 59.2	11.4 16.2 21.8 21.5	20.5 21.7 22.1 19.3	[104]
			< 0.5											

To manage this problem, a single or series of cyclone separators were usually used in the gas stream for continuous fine char separation. Typical configuration of cyclone separator is shown in Figure 2.1 for the removal of fine char dispersed in vapors by high gas velocities during fast pyrolysis [31].

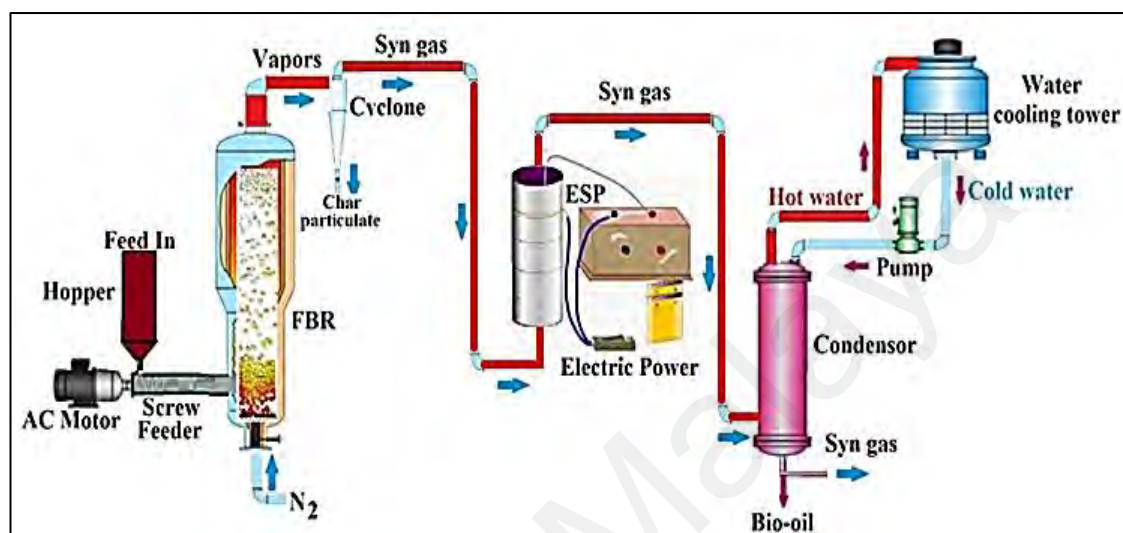


Figure 2. 1: Bubbling fluidized bed reactor with particulate separation facility. Redrawn based on [31].

Considerable development has been done by various groups on these types of reactors for continuous fast pyrolysis process. Waterloo Flash Pyrolysis Process (WFPP) has been developed by Scott and his group at the University of Waterloo, Canada, in the 1980's and 1990's. This was the first demonstration of fluidized bed fast pyrolysis process with capacity of 200 kg/day. With this reactor design, a maximum bio-oil yield of 80wt. % was obtained with clean aspen poplar wood particle size of 0.1 mm and short gas/vapor residence time of < 1 s. In addition, process was scaled up to 3 kg/h pilot plant due to higher liquid yield. WFPP provided great inspiration for the development of several other commercial scale pyrolysis reactors [36]. Due to the promising process in producing higher liquid yield, commercialization of BFBs technology was proactively ventured by Canadian company: Dynamotive Energy Systems Corporation [31].

In 2005, Dynamotive built the first demonstration scale plant with wood waste processing capacity of 100 dry tonnes/day and another plant operated in 2006 with 200 tonnes/day capacity to produce bio-oil [105]. Biomass Engineering Ltd. (UK) is another group which has built BFBs plant with capacity of 6 ton/day in UK, and 14 to 24 tonnes/day plant was built in China. Agri-Therm (Canada) presented the portable design in 2010 of BFBs to convert agricultural biomass waste with capacity of 10 t/day to convert bio-oil [40, 106]. Different BFBs manufacturing companies such as Waterloo, RTI, Dynamotive, Biomass Engineering Ltd. (UK) and Agri-Therm (Canada) were involved in improving the continuous fast pyrolysis reactor technologies. In contrast to other reactor fabricating groups, Agri-Therm has developed a portable pyrolyzer with capacity of 10 t/day which may decrease the cost of biomass collection, handling, equipment and workers for bio-oil production [107].

2.6.2 Circulating fluidized bed reactor

The working principle of circulating fluidized beds (CFBs) is relatively different from bubbling fluidized beds (BFBs). The major difference in CFBs and BFBs is the vapor/gas residence time of 0.5-1 s and 2-3 s, respectively with considerably higher energy recovery [19]. It has been noted that the 15 wt. % byproduct char produced during pyrolysis contains about 25% of unconverted biomass feed to bio-oil fuel energy which is normally used to provide the process heat in CFBs for heating the sand in char combustor for waste energy recovery as shown in Figure 2.2 [19]. The shorter residence time leads to the increase of bio-oil yield with rapid elimination of organic gasses from biomass material [108]. Moreover, BFBs do not facilitate the use of bio char and syngas stream for energy recovery. In addition, CFBs pyrolysis utilize char and non-condensable gases which make them more energy efficient, feasible and economical way for high energy recovery [31].

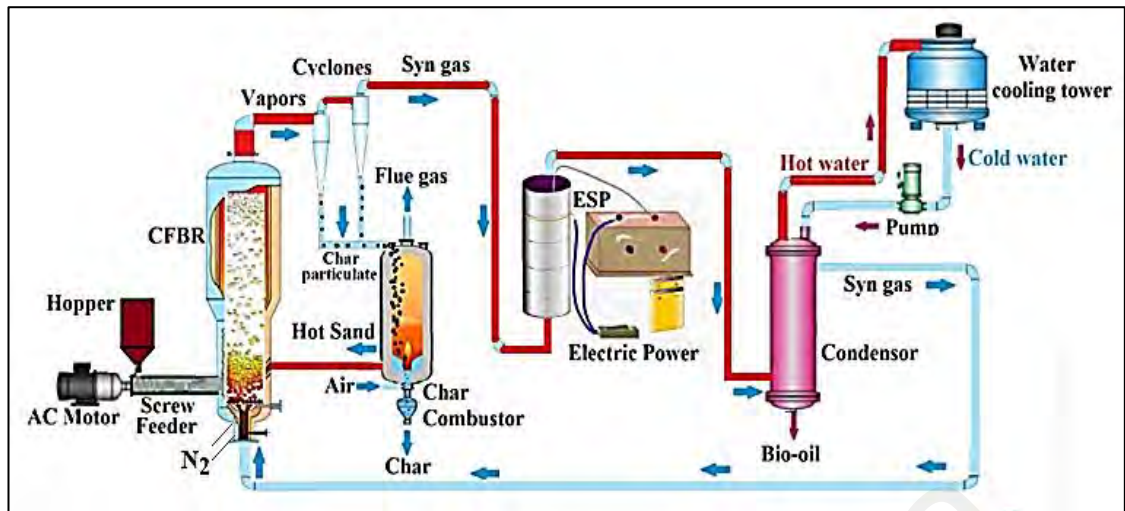


Figure 2. 2: Schematic diagram of a circulating fluidized bed reactor. Redrawn based on [19].

The CFB system operates under high particle flux and high superficial gas velocity, which are typically of 10–1000 kg/m²s and 2–12 m/s respectively. These operation conditions were chosen to avoid a distinct interface between the dilute region and the dense bed inside the riser. Thus, gas velocities above the bubbling point was chosen for contacting. The circulating fluidized bed (CFB) uses high fluid velocity to provide better gas-solid contact by providing more intense mixing of the fluid with the intention that better quality of product can be obtained. However, the high gas velocities and the recirculation of solids may make the CFB system much more expensive in term of power requirement and investment compared to conventional fluidized bed reactors [106].

In the past, CFB technology has been widely used in biomass continuous pyrolysis can be seen in Table 2.4. Ensyn (Canada) has built CFB plant with biomass processing capacity of 100 ton/day in 2007 [40]. In addition, the same company announced new projects in 2013 for Europe, North and South America and Asia, with increased processing capacity of 150 to 400 t/d for continuous liquid production [36]. Enverget is a joint project between Ensyn and Honeywell/UOP which started in 2008 to improve Ensyn’s capacity and to install Robin Tacchi Plants to develop a technology that permits

the pyrolysis oil to be improved with a mixed stock for handling in fossil-refinery process [40].

In addition, Valmet and Fortum jointly constructed the first CFBs plant on commercial scale to produce advanced biomass-based fuels in March 2012. This plant was started in 2013 and worked as a part of combined heat and power plant. It produces 50,000 tons of bio-oil every year which fulfills the heating needs of more than 10,000 family units [109]. Peters et al. investigated fast pyrolysis processes of hybrid poplar woodchips in circulating fluid-bed through Aspen plus simulation. Based on their simulation results, it has an exergetic efficiency of 71.2% and suggested that overall plant efficiency of 73.2 % can be achieved by improving dryer and the heat exchanger section [50]. Furthermore, Manon et al. conducted CFB experiments and studied the yields of oil, gas and char in relation to the operating parameters. They observed a maximum bio-oil yield of 65 wt.% with considerably short residence time of 0.5 s at 500°C. The residence time of the biomass particles in the riser section is more dependent on the fluidization velocity. The CFB biomass pyrolysis appeared to be an economically and feasible option for biomass utilization [110].

Table 2. 4: Circulating fluidized bed reactor.

S. N	Reactor Type & Dimensions	Mode	Char combustor & Dimensions	Feedstock & Particle size (mm)	Feeding system & Feeding rate	Heating system & Heating rate (°C/min)	Temp: (°C)	Vapor residence time (Sec :)	Cooling system	Purging Gas	Non-condensable gas	Yield (wt. %)			Ref:
												Oil	Char	Gas	
1.	Circulating fluidized bed L = 800 mm Square cross-section = 212 X 212 mm	Continuous	Silica sand 0.16 mm L = 800 mm Square cross-section = 212 X 212 mm	Sewage sludge 2 Pig compost 2 Woodchip 2	Screw conveyor Feeder 1-1.5 kg/h	3 Electric heaters NM	500	1	Chiller 3°C	N ₂	Atmosphere	45.2 44.4 39.7	NM	NM	[111]
2.	Batch and Circulating fluidized bed L = 300 cm I.D. = 8 cm	Continuous	Combustion chamber was a fluidized bed 500×310×1500 mm stainless steel cube box	Corn sunflower residue < 0.3	NM 12 kg/hr	Radiation heater And Non-condensable pyrolysis gas NM 100	500	> 0.5	Condenser	N ₂	Recirculated to Reactor	60 – 65	NM	NM	[110]
3.	Circulating fluidized bed I.D = 100 mm	Continuous	Combustion chamber was a fluidized bed NM	Quartz sand Pine wood powder 0.41, 0.38 and 0.73 mm	Rotary feeder NM	External heating through shredded charcoal powder NM	450-550	1.5	Water-cooled condenser	NM	Recirculated to the Reactor	NM	NM	NM	[112]

NM = Not Mentioned.

Table 2.4: Continued

S. N	Reactor Type & Dimensions	Mode	Char combustor & Dimensions	Feedstock & Particle size (mm)	Feeding system & Feeding rate	Heating system & Heating rate (°C/min)	Temp: (°C)	Vapor residence time (Sec:)	Cooling system	Purging Gas	Non-condensable gas	Yield (wt. %)			Ref.
												Oil	Char	Gas	
1.	Bench-scale Circulating fluidized bed Downer reactor L = 3m I.D = 0.039m	Continuous	Riser Combustor L = 7m ID = 0.086m	Quartz sand 0.25	Screw feeder 4 kg/h	12 electric heaters/60 kW	673K/400 °C	1	Fast quencher	N ₂	Recirculated hot sands to the reactor	(WS) 45	46	9	[113]
				Wheat straw (WS) & Acid treated wheat (ATWS) straw 0.18- 0.28								(ATWS) 56	40	5	
2.	Circulating fluid-bed L= 500 mm I.D =14 mm	Semi-continuous	Char combustor L = 152mm I.D = 51 mm	Sawdust NM Sand =0.075–0.212 mm	Feeding tube 100g/h	NM NM	400–600	NM	water-cooled condenser (double tube heat exchanger)	N ₂ 2L/min	Recirculated to the Reactor	67	18	15	[114]

2.6.3 Conical spouted bed reactor

Conical spouted bed reactor (CSBR) has been successfully used in pyrolysis for several biomass materials [115]. The CSBR has been proven to be a substitute for fluidized bed and an acceptable reactor for biomass fast pyrolysis [116]. It consists of three zones which are spout region, annular space and fountain as shown in Figure 2.3 [117].

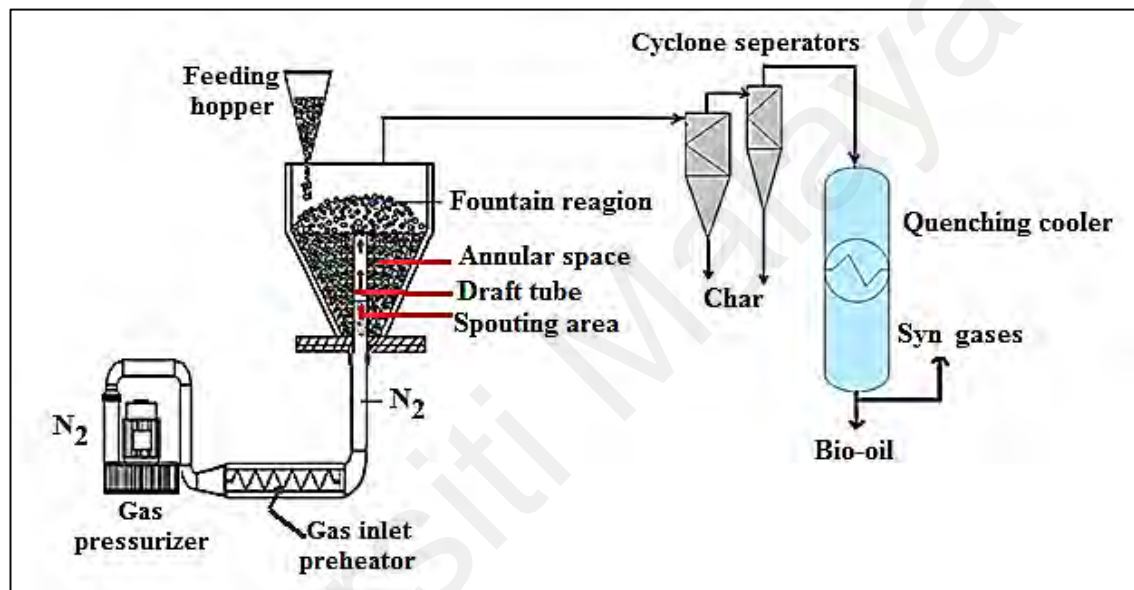


Figure 2. 3: Schematic diagram of a conical spouted bed reactor.

Generally, CSBs comprise of a central lean solid phase (spout). Solid particles enter in a fluid jet penetrating the bed from below, and a downward-moving thick solid phase (annulus) produces a counter-current flow between the solid and gas phase. At the bottom of the annular phase, solids transport downwards about the spout. While the upward-moving gas velocity or aeration rate in vertical aeration section of loop-seal (U_a) m/s in the annular phase is less than minimum fluidization velocity (U_{mf}) m/s. As the axial distance in the bed increases, U_a increases due to gas cross-flow from the spout phase to the annular phase across the axis of the bed. Additional cross-flow from the spout phase above the critical height will travel in the form of bubbles in the annular phase. The overall solid circulation in the bed was enabled as a result of radially non-uniform bubble

flow. Furthermore, bubble causing solid material move downwards to the annular phase, where it is entrained into the spout. Then, at a certain height when the spout jet breaks down, the material is able to link the bubbling bed above the spout [118].

The CSBR is based on the conical geometry with facility of handling considerably coarse particles > 1 mm which enables less pressure drop and reduces grinding energy [119]. The fountain region consists of different density materials in which lower density (bio-char) particles were designated by higher trajectories, while the heavier particles (sand and used biomass) reach lesser heights. Based on this separation method, the removal of char from the reactor is possible through an adjacent pipe placed higher than the bed surface [120]. The CSBR allows continuous operation by selectively removing the bio-char from the bed, which avoids its accumulation in the pyrolysis reactor. In addition, the disadvantages of CSBR are the high-pressure gas requirements for spouting and attrition of the material which increase the cost of the process [116]. Fernandez et al. studied the influence of excess gas velocity for spouting and char separation. They found that with the increase of gas velocity, char separation from the reactor was improved while the cost of the process was also noticeably increased [119].

Fernandez et al. observed the attrition in CSBR using sand for several bed heights and gas flow rates. The predicted attrition rate constant depends exponentially on excess gas velocity over that for minimum spouting. Furthermore, a sharp reduction in attrition has been observed when operating with a draft tube and increased temperature, which is attributed to the less vigorous gas–solid contact and the resulting reduction in particle breakage and higher liquid yields [121]. Additionally, temperature is a key parameter of CSBR that resulted in higher bio-oil yield. Alvarez et al. performed flash pyrolysis of sewage sludge in a CSBR supported by continuous biomass feed and char removal. The effect of temperature on product yields and composition were studied in the range of 450–

600°C. A maximum liquid yield of 77 wt.% at 500°C was obtained on dry and ash free basis is mentioned in Table 2.5 [122].

Furthermore, the parameter that restricts the scaling-up of spouted beds is the ratio between the reactor inlet diameter and particle diameter. In fact, the inlet diameter should exceed 20–30 times the average particle diameter to achieve spouting grade. The use of a draft tube can support in scaling-up of spouted beds due to its advantages such as greater flexibility, lower gas flow and pressure drop [117]. Nevertheless, a draft tube changes the hydrodynamics and solid circulation flow rate of spouted beds. In addition, minimum spouting velocity, pressure drop, solid circulation pattern, particle cycle time and gas distribution are dependent on the type of draft tube used. Consequently, it supports in handling particles of irregular surface and fine materials with no agglomeration problems. Additionally, selection and installation of a draft tube is the typical solution of this problem [116].

Table 2. 5: Conical spouted bed reactor.

S. N	Reactor Type & Dimensions	Mode of operation	Feedstock & Particle size (mm)	Feeding system & Feeding rate	Heating system & Heating rate (°C/min)	Temp: (°C)	Residence time (Sec :)	Cooling system (°C)	Purging Gas	Non-condensable gas	Yield (wt. %)			Ref.
											Oil	Char	Gas	
1.	Conical spouted bed U.D = 242 mm A = 32° C.H = 330 mm T.H = 1030 mm B.D = 52 mm Pilot plant	Continuous	Pinewood sawdust 0.1–2.3	Two Screw feeders 25kg/h	Two separate resistance NM	440-565	NM	Air-cooled heat exchanger	N ₂	Recirculated to fluidize the bed	65.8	15.4	18.8	[119]
2.	Conical spouted bed Upper section L = 34 cm D = 20.05 cm A = 28°	Continuous Vacuum 1, 0.5 & 0.25	Scrap tires NM	Hopper with PLC control system. 3 g/min	Electric heater NM	425-500	NM	Double shell glass tube condenser cooled by tap water.	N ₂ 30 L/min	Atmosphere	36-42	34-35	5-7	[123]
3.	Conical spouted bed Height = 34 cm L.C = 20.05cm B.dia = 12.3cm A = 28o	Continuous	Rice husk 0.63-1	Vertical shaft connected to a piston placed below the material bed 200g/h	NM NM	400-600	NM	Condenser	N ₂ 10 ml/min	Atmosphere	70	25	10	[32]
4.	Conical spouted bed H.C = 34 cm D = 12.3 cm B D = 2 cm A = 280°	Continuous	Sewage sludge 0.5 – 3 Sand 0.63-1	Piston 300g/h	Electric heater	450-600	1800	Double-shell tube condenser	N ₂ 14 L/min	Atmosphere	77	13	10	[122]
5.	Conical spouted bed NM	Continuous	Populusnigra wood sawdust Dia 3mm & length between 5 and 15 mm	2 screw feeder 25 kg/h and 6 kg of sand	NM 15	425–525	NM	Condensation Tower and Heat exchanger	Start up with N ₂ after non-condensable gases	Sent to reactor as fluidizing agent.	69	21	10	[120]

2.6.4 Rotary cone reactor

Rotary cone reactor (RCR) technology was invented 20 years ago at the University of Twente Netherlands and then further developed by Biomass Technology Group (BTG) in 1998. In 2007 BTG designed a modified RCR pyrolysis technology for commercialization [141]. The RCR is fairly different than the bubbling and circulating fluidized bed reactors. The configuration of RCR consists of a secondary bubbling fluid bed combustor assisted by air and non-condensable gases to combust the bio-char for heating and recirculating the sand as shown in Figure 2.4. A more complex integrated operation of three subsystems is necessary: rotating cone pyrolyzer, riser for sand recycling, and char combustor. In this type of reactor, the mixing of biomass and hot sand as “heat carrier” medium can be achieved by mechanical action through centrifugation (at ~10 Hz) which drives hot sand and biomass rather than gas fluidization [31].

Furthermore, char and sand are dropped into a separate fluid bed combustor where char is burned to heat the sand and formerly dropped back into the RCR. Additionally, condensable gas vapors are cooled and collected by conventional methods like liquefaction by condensation whereas non-condensable hot gas stream is used to promote the heat transfer rate and mixing within the RCR. In addition, RCR can typically produce a liquid yield of 60-70 wt.% [31]. The RCR pyrolysis technology was commercialized through the work of BTG Netherlands and in year 2006. They have installed a biomass processing plant in Malaysia with capacity of 50 ton/day. However, due to some technical reasons this plant is currently out of operation [40]. In addition, one more plant was installed in 2013 by BTG in Malaysia [29] and it operates on palm oil empty fruit bunches with 5.5-ton daily capacity.

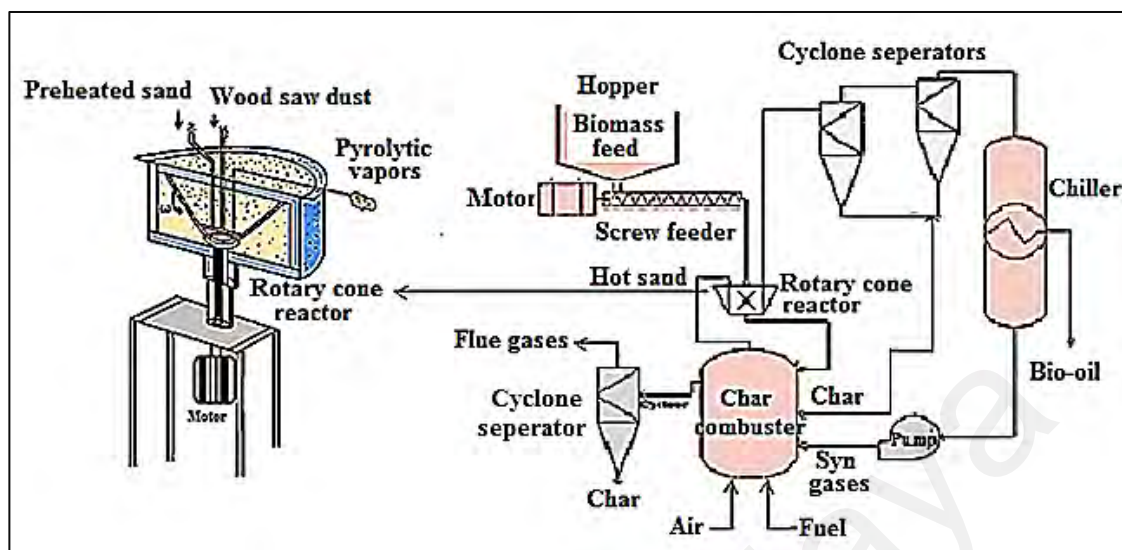


Figure 2. 4: Schematic diagram of rotary cone reactor. Redrawn based on [31].

Furthermore, BTG is trying to develop a biomass processing plant in 2015 [124] with capacity of 20,000 and 25,000 tons/year in Europe for pyrolysis oil, process steam, electricity, and aqueous organic acids. Similarly, N.V (Belgium/Netherlands) installed an industrial scale plant with 100 kg/h and 1500 kg/h biomass processing capacity for bio-oil production. Moreover, Belgium and Holland are manufacturing two semi-continuous pyrolysis plants with estimated production capacity of 5 tons/day [40]. RCR typically obtained liquid yield in range of 60 to 70 wt.% on dry feed basis as seen in Table 2.5 [31]. Correspondingly, Westerhout et al. obtained 66 wt.% of liquid yield from polyethylene waste in a pilot plant based on RCR technology [125]. Furthermore, Wagenaar et al. also observed the similar tendencies during flash pyrolysis of Poplar and straw in a RCR and found maximal liquid yield of 70 wt.% at optimal reactor condition [126]

Table 2. 6: Rotary cone reactor.

S. N	Reactor Type & Dimensions	Mode of operation	Feedstock & Particle size (mm)	Feeding system & Feeding rate	Heating system & Heating rate (°C/min)	Temp: (°C)	Residence time (Sec:)	Cooling system (°C)	Purging Gas	Reactor Cone (rpm)	Non-condensable gas	Yield (wt. %)			Ref:
												Oil	Char	Gas	
1.	Rotating cone Top cone angle = $\pi/2$ Top Dia =650 mm Bottom Dia= 200 mm Cone speed = 6-15 Hz	Continuous	Wood-dust 0.2	Vibratory feeder	Electric resistance	500-700	0.49, 0.65 and 30	Ice cooled Bath	NM	NM	Atmosphere	70	NM	NM	[127]
	Sand 1.0		2 g/s	NM											
2.	Rotating cone Top cone angle = $\pi/2$ Top Dia =650 mm Bottom Dia = 210 mm Cone speed = 300 rpm	Continuous	Poplar, straw and Sand	Vibratory screen feeder	NM	500	1.0	Water to air heat exchanger	NM	300	Atmosphere	70	15	15	[126]
	1-3		200 kg/hr	NM											
3.	Self-made rotating cone Cone speed = 85- 120 rpm	Continuous	Wood shatter 20, 30, 40 Sand 0.5	Screw feeder 4kg/h	NM 1.0-100	550	NM	First and second stage condenser	N2= NM He = 33.9mL/min	100 & 120	Atmosphere	54.83	NM	NM	[128]

NM = Not Mentioned.

Table 2.6: Continued

S. N	Reactor Type & Dimensions	Mode of operation	Feedstock & Particle size (mm)	Feeding system & Feeding rate	Heating system & Heating rate (°C/min)	Temp: (°C)	Residence time (Sec:)	Cooling system (°C)	Purging Gas	Reactor Cone (rpm/Hz)	Non-condensable gas	Yield (wt. %)			Ref:
												Oil	Char	Gas	
1.	Modified rotating cone reactor with static stirrer Cone height =20mm Cone speed = 6, 8, 12 Hz	Continuous	Coal 2.0 and 4.0 Sand 0.63	Hopper and feeder machine	Electrical heating baking oven	400-600	3	condenser	N ₂	6, 8 and 12Hz	Atmosphere	NM	NM	NM	[129]
2.	Continuous Rotating Cone Top cone angle = $\pi/2$ Top Dia =650 mm Bottom Dia = 210 mm Cone speed = 6-15 Hz	Continuous	Plastic waste <0.5 Sand 0.1-0.3	Riser Plastic 1 g/s Sand mass (0-108g/s)	3-kW Electric heater	750	NM	NM	Nitrogen 13.5 Nm ³ /h	600	Atmosphere	51	NM	NM	[125]

NM = Not Mentioned.

2.6.5 Ablative reactor

The concept of ablative pyrolysis technology was pioneered by “national renewable energy laboratory” in Colorado, USA in 1980’s. Moreover, a new demonstrative design was introduced by Pytec Thermo-chemische Anlagen GmbH. After that an ablative pilot plant was built in 2002 with processing capacity of 6 t/d (dry woody biomass) and operated in Hamburg, Germany [36]. Ablative pyrolysis is considerably different in concept as related with other methods of fast pyrolysis. The working principle of ablative reactor is similar to the melting of butter on a hot pan. The high heat transferred from the reactor surface causes wood to ‘melt’ under the action of external pressure. As the wood is pressed mechanically on rotating hot plate surface, the residual oil is evaporated and pyrolytic vapors are possibly collected with rapid cooling can be seen in Figure 2.5.

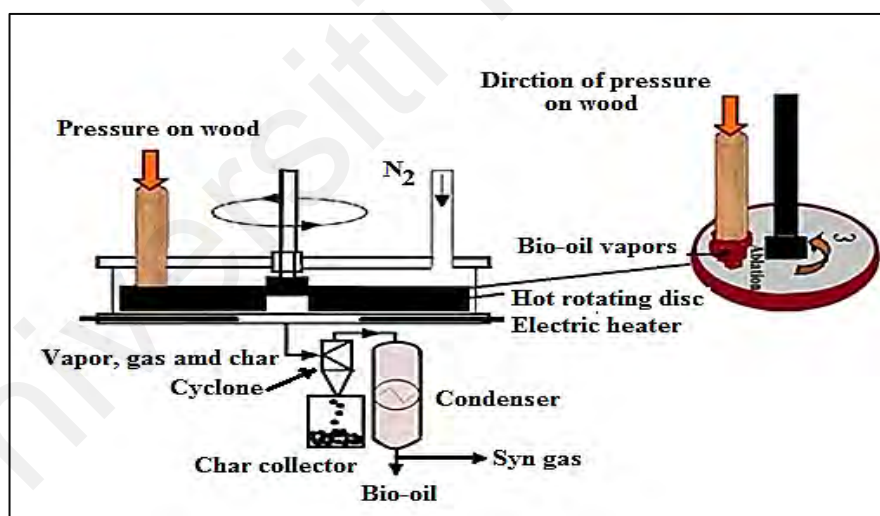


Figure 2. 5: Schematic diagram of an ablative reactor. Redrawn based on [31].

Through ablative technology, a 70-75% liquid yield were typically obtained in N₂ environment [31]. Peacocke & Bridgwater conducted comparative study between ablative and fluidized bed reactor technology. Product yields followed the same general trends with a maximum organic’s liquid yield around 500– 515°C for both fluid bed 59.4 wt.% and ablative reactor 62.1 wt.% at 502°C. However, higher char quantity was observed in

fluidized bed reactor. Furthermore, gaseous product varies in fluidized bed with temperature which suggests that secondary vapor cracking is more dominant in the fluid bed reactor than ablative reactor as can be seen in Table 2.7 [130].

The main advantage of using this technology is that large biomass particles might be easily pyrolyzed. Furthermore, rate of reaction in ablative reactor is strongly dependent on the applied pressure, reactor surface temperature and the contact between biomass and hot surface [131]. A common difficulty during ablation is mechanical dependability and high heat losses in surroundings, because the metal hot plate is exposed to ambient atmosphere. Furthermore, it needs considerably higher temperature than the required pyrolysis temperature. In addition, the higher degree of char formation leads to contaminated liquid product [132] which needs post-treatment of liquid oil for char removal and good quality product [131]. Furthermore, upgrading of ablative pyrolysis processes is difficult because with the increase of reactor size the ratio between the wall surface and reactor volume decreases which made its large scale implementation to be not feasible [133].

Table 2. 7: Ablative reactor.

S. N	Reactor Type & Dimensions	Mode of operation	Feedstock & Particle size (mm)	Feeding system & Feeding rate	Heating system & Heating rate (°C/min)	Temp: (°C)	Residence time (Sec:)	Cooling system (°C)	Purging Gas	Pressure (Mpa)	Non-condensable gas	Yield (wt. %)			Ref.
												Oil	Char	Gas	
1.	Ablative NM	Continuous	Pine wood 1-3.35	3 kg/h	NM	450-600	1	NM	NM	NM	NM	62.1	NM	NM	[130]
2.	Ablative Disc Dia = 7.5 cm	NM	Beech Wood Dia = 8	NM 3 m/s	Four gas burner 5 MW/m ²	500-900	Wood	NM	Argon NM	0.1-3.5	NM	NM	NM	NM	[134]
3.	Mobile Ablative I.D = 0.30 m I.L = 0.42 m	Continuous	Wood chips 2×2, 5×15, 10×20 and 35×200	Fixed Bowel	Three 1kW cartage heaters for plate and Two band heaters (Chromalox HBT 120) each 2kW NM	300-700	1.0	Double pipe condenser	Helium 35mL/m	0.15	Atmos- phere	60	20-22	20-18	[135]

NM = Not Mentioned.

Table 2.7: Continued

S. N	Reactor Type & Dimensions	Mode of operation	Feedstock & Particle size (mm)	Feeding system & Feeding rate	Heating system & Heating rate (°C/min)	Temp: (°C)	Residence time (Sec:)	Cooling system (°C)	Purging Gas	Pressure (Mpa)	Non-conductible gas	Yield (wt. %)			Ref.
												Oil	Char	Gas	
4.	Ablative I.D = 256 mm I.L= 65 mm Volume = 0.0034 m ³	Continuous	Wood >3.35 mm	Screw feeder 2.5 kg/h	Two Electric resistance heater Reactor wall= 2.25 kW Reactor base 11.4 W cm ⁻²	450-600	1.7 – 6.92	Three ice-cooled condensers	N ₂	0.1	Fume hood	81	NM	NM	[136]
	Rotating speeds = 200 r.p.m														
5.	Ablative Vol=82 x 200 mm Rotating speeds = 10,000 -20,000 rpm	Continuous	Wheat straw 0.6 mm	Screw feeder 24 g/min	Electric resistance heater	480-620	NM	Tap water condenser	N ₂	NM	Atmosph here		Wheat straw 52.8	21.3	[137]
	Pine wood 0.6 mm		Pine 60.8										14.0		
6.	Ablative I.D = 258 mm	Continuous	Pine wood 6.35 mm	2 kg/h	Electric resistance heater	500-600	NM	Two ice cooled condenser	N ₂	NM	Atmosph here		65.9	18.3 - 28.4	[136]

NM = Not Mentioned.

2.6.6 Auger/screw reactor

Screw/Augers reactor technology was adapted from Lurgi-Ruhrgas (LR) process and developed in the 1950s [33]. It comprises of single [138], twin [139] or triple [140] screw system. Hot sand and biomass particles are feeds at one end of an auger/screw through an oxygen free cylindrical heated tube. A channel through the tube raises the feedstock to the desired pyrolysis temperature ranging from 400°C to 800°C which causes it to devolatilize the biomass. Char is produced as byproduct and gases are condensed as bio-oil, with non-condensable vapor collected as bio-gas. In this design the vapor residence time can be altered by changing the length or rotation of screw in heated zone through which vapors passes before entering in the condensing zone can be seen in Figure 2.6 [1], while sand as heating medium is reheated in a separate vessel. Auger reactor offers many advantages such as their compact design and lower process temperature (400°C) [141]. Several auger/screw configurations have been studied in literature, while the influence of operating parameters on the product yields and composition has not yet been fully discussed [25].

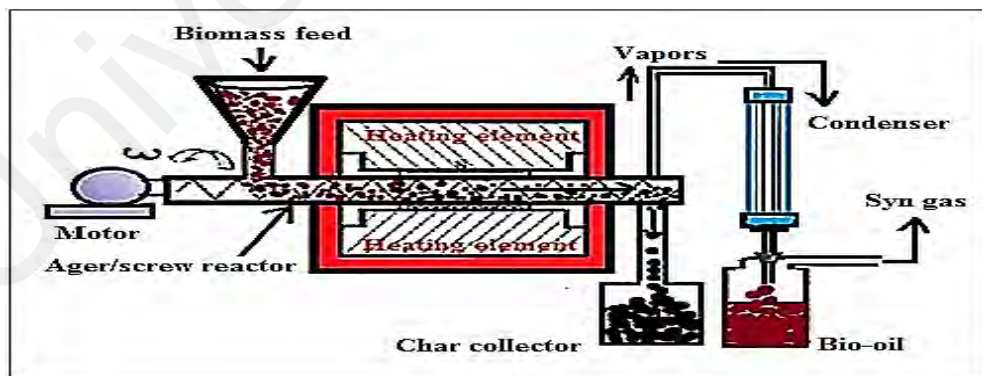


Figure 2. 6: Schematic diagram of an auger/screw reactor pyrolysis.

In recent years, Puy et al. used auger/screw reactor for bio-oil production from forestry waste (Pine wood chips). Liquid yield of 59 wt.% was obtained with N₂ flow rate

of 5L/min and residence times of > 2 min at temperature of 500°C. [25]. Raclavska et al. investigated the effect of increasing temperatures: 500, 550, 600, and 650°C on brown coal, biomass pellets and used tires in 4-meter length semi-continuous triple-screw reactor for bio-oil yield. They found that the yields were significantly increased with the increasing of temperature up to some extent. Followed by biomass (26.41wt.% gas, 48.68 wt.% liquid, 24.91wt% char) at 500 °C, coal (31.93 wt.% gas, 47.76 wt.% liquid, 20.31 wt.% char) 550 °C and for tires (18 wt.% gas, 42 wt.% liquid, 40 wt.% char) at 500°C, respectively [140]. Similarly, Agirre et al., performed pyrolysis in a semi-continuous, semi-pilot scale double screw Auger reactor (2.3-meter length) to produce substitute petroleum coke through carbonization process through charcoal. In addition, considerable reduction in charcoal was observed by increasing carbonization temperature from 527-927°C. The maximum charcoal yield left the reactor about 38% at 855°C with 3h residence time. Furthermore, increasing temperature resulted additional gas formation and reduced charcoal yield ~ 28% at 880°C [142].

Veses et al. studied catalytic pyrolysis of wood biomass of 15 mm in an auger reactor using calcium-based catalysts (CaO and CaO.MgO) for bio-oil upgrading. N₂ was used as carrier gas, with a flow of 5 L/min and 7 min residence time for 2 h. It was noted that char, gas and liquid yields were not significantly affected when more CaO or CaO.MgO catalysts were added. In addition, self-sustained system was proposed for biomass drying over non-condensable gas and char combustion [143]. Furthermore, screw/auger reactor technology is not yet been proven for large scale commercial pyrolysis process due to less controllability and liquid production can be seen in Table 2.8 [141].

Table 2. 8: Auger/screw reactor.

S. N	Reactor Type & Dimensions	Mode of operation	Feedstock & Particle size (mm)	Feeding system & Feeding rate	Heating system & Heating rate (°C/min)	Temp: (°C)	Residence time (Sec:)	Cooling system (°C)	Purging Gas	Non-conductible gas	Yield (wt. %)			Ref.	
											Oil	Char	Gas		
1.	Screw/auger NM	Continuous	Wheat straw, saw dust, flax straw and poultry. NM	Hopper 200g/min	Electric heater NM	400–550	1	Condenser	NA	Atmosphere	Wheat straw 43.5 Sawdust 55.5 Flax straw 28.7 Poultry 48.0	NM	NM	NM	[24]
2.	Single screw/auger NM	Continuous	Pine Wood chips =15 sand + catalyst = < 0.3 and 15	NM	Muffle furnace NM	400–500	7200	NM	Static air and N2	NM	48	22	30	[138]	
3.	Twin-screw screw/auger reactor NM	Continuous	Eucalyptus grandis lignocellulose < 5	Hopper and Screw 8.1 kg/h	Furnace	500-600	< 2	Single pass, counter-current shell and tube Heat exchanger	N2 1.6 m ³ /h	Atmosphere	68.3	NM	NM	[139]	
4.	Single screw/auger NM	Continuous	Pine woodchips 15mm	Two screw feeders	Three Electric Furnace NM	450	4	Condenser	N2 5 L/min	Burned to atmosphere	48–50	25–27	26–27	[143]	

NM = Not Mentioned.

Table 2.8: Continued

S. N	Reactor Type & Dimensions	Mode of operation	Feedstock & Particle size (mm)	Feeding system & Feeding rate	Heating system & Heating rate (°C/min)	Temp: (°C)	Residence time (Sec:)	Cooling system (°C)	Purging Gas	Non-conductible gas	Yield (wt. %)			Ref.
											Oil	Char	Gas	
5.	Triple-Screw screw/auger reactor and stirrer. L = 4m	Semi-Continuous	Biomass, Coal and Tires NM	NM 20 kg/h	Five atmospheric gas burners NM	500, 550, 600, and 650	NM	NM	N ₂	NM	Biomass 48.68 Coal 42.00 Tire 42.00	24.91 47.00 40.00	26.41 11.00 18.00	[140]
6.	Screw/auger 22 x 2.5 x 1.5 (Lx W x H) inch	Semi-continuous	Forestry waste (Pine wood chips) 20	Screw feeder 3.9, 4.8 and 6.9 kg/h	Electrical furnaces NM	500, 550, 600, 700, and 800	NM	Condenser	N ₂ 5L/min	Burner before sent to atmosphere	59	19-26	15-22	[25]

2.7 Overview of pyrolysis reactor technologies

A range of fast or flash pyrolysis technologies for the production of liquids in high yield has the potential for high reactor specific throughputs with reduced equipment size, costs and improved controllability. Table 2.9 presents an overview of pyrolysis reactor technologies. Based on Table 2.9, bubbling fluidized bed (BFB) reactor was generally used for bio-oil production because of simple design and easy operation. With this technology, a significant liquid yield of 67% – 70% has been reported by many researchers. However, due to high carbon conservation, extended solid residence time, low ash transfer, difficulties in char removal, small particle sizes and high gas fluidizing velocity, it has exorbitant process cost [98]. For circulating fluidized beds (CFB) reactors, they are similar to bubbling fluidized beds. However rather than having bed material remain suspended in one reactor, CFBs have a separate combustion reactor used to re-heat the sand which is continuously recirculated. As with fluidized beds, the CFB reactor was well understood that it gives liquid yield of 70% – 75% and is currently used in several industries on commercial scales. Due to small particle size and high gas fluidization velocity requirement, it also has exorbitant process cost [50].

Furthermore, CSB reactor has been successfully used in pyrolysis for several biomass materials [115]. The CSB reactor has been proven to be a substitute for fluidized bed and can produce up to 70% of liquid yield [116]. In addition, because of its complex design, high gas fluidization requirement and difficult operation has restricted it for large scale bio-oil production. However, rotating cone reactor is quite different than the bubbling fluidized or circulating fluidized bed reactors. Biomass is mechanically mixed in a rotating cone with a bulk solid heat transfer medium. On the other hand, heat transfer to biomass through contact with hot solid material or hot gas, ablative pyrolysis is a completely different approach.

The major benefit of this design is that much larger biomass particles with no carrier gas requirement can produce a maximum liquid yield of 70%. Nevertheless, it is a complex mechanical design which makes its scale up a challenge. Furthermore, high reactor cost, low reaction rate, high pressure requirement and more heat losses also restricted it from large scale industrial development [136]. Screw/auger system is compact but requires inert gas, lower process temperature (400°C) and can yield around 30% – 59 % liquid product. It works on continuous process but most of the moving parts are in hot zone so heat transfer in large scale is not suitable. For this reason, it has not been proven yet for large scale commercialization [25, 141].

Table 2. 9: Overview of pyrolysis reactor technology.

S. No.	Reactor type	Process	Advantage	Disadvantage	Bio-oil (wt. %)	Reference
1.	Bubbling fluidized bed	Continuous	<ul style="list-style-type: none"> - High heat transfer rates. - Good solid mixing. - ~ 2-3 s. particle residence time. - Higher liquid yield. 	<ul style="list-style-type: none"> - Requires small particle size. - Char transfer with vapors on top. - Char accumulation in the bed. 	51 - 67	[20, 98, 133]
2.	Circulating fluidized bed	Continuous	<ul style="list-style-type: none"> - High heat transfer rates. - Less solid residence time from 0.5-1.0s is needed. - Handle particle size up to 2mm. 	<ul style="list-style-type: none"> - Need smaller particle size than bubbling fluidized bed. - High abrasion of char layer. - More chances of reactor wear. 	75-80	[20, 133]
3.	Conical spouted bed	Continuous	<ul style="list-style-type: none"> - Valid for fast and flash pyrolysis. - High capacity of mass and heat transfer rate. - It is an alternative to fluidized beds. - Attaining high bio-oil yields. 	<ul style="list-style-type: none"> - Tube blockage risk. - Extended recirculation time. - Particle entrainment from the bed. - Design complexity. - Difficult to scaling up. 	60-80	[144-146]
4.	Rotating cone	Continuous	<ul style="list-style-type: none"> - Solid and biomass mixing by rotating action. - No carrier gas requirement. - Fast reactor heating. - Short solids residence time. 	<ul style="list-style-type: none"> - Extreme rotational speeds. - Particle inclusion due to high rotation. - Gas phase Channeling. 	70	[126, 127]
5.	Ablative	Continuous	<ul style="list-style-type: none"> - Permits larger size of feed particle. - Compact equipment size. - No inert gas is required. - Better controllability. - High throughputs. - Compact and simple design. 	<ul style="list-style-type: none"> - High pressure requirement. - Char removal is difficult. - High mechanical char abrasion. - Heat supply is complex. 	53.4 - 76	[133, 136]
6.	Screw/Auger	Semi-continuous	<ul style="list-style-type: none"> - Low process temperature. - Continuous process. - Low repairs. 	<ul style="list-style-type: none"> - Plugging risk. - Moving parts in the hot zone. - Heat transfer on large scale is not possible. - Not proven yet for large scale. 	65 – 75	[25, 141, 143, 147]

2.7.1 Effect of operating parameters

In this review, we discussed in detail about operating parameters and their effects on liquid yield during pyrolysis. These parameters include particle size, feeding rate, heating rate, temperature and residence time. Operating parameters are not only responsible to maximize the liquid yield but also effecting pyrolysis efficiency and composition of product quality [73, 148].

2.7.2 Effect of particle size

Biomass is a poor conductive of heat energy which may cause delay in heat transfer rate during pyrolysis. Effect of feed particle size is an important parameter to minimize the heat transfer problem in order to get significantly higher liquid yield [73]. Employing large particle size may lead to decrease in fluidization properties, reactor hydrodynamics, heating rate, solid residence time, which contribute to produce more char and less liquid yield. In this connection, average biomass particle sizes of less than 3 mm is more appropriate to attain high heating rates and liquid yield [149]. Bridgwater reported the use of average particle size of 1.3 mm with temperature range of 470-540°C and 0.88 s residence time has resulted in a maximum liquid yield of 54 wt. % [21]. Abnisa et al. also observed similar results when using 1-2 mm particle size of palm leaf and produced 46.7 wt.% liquid yield [3]. Similarly, from pine wood 50 wt.% of liquid yield with 1-2 mm particle size was also stated [150]. One more researcher investigated the effect of particle size from 0.81-5.6 mm at 500°C with Australian oil mallee woody biomass and determined that the increase of particle size from 0.3 to 1.5 mm has considerably decreased the bio-oil quantity [23].

Many researchers stated that coarse particle size >2 mm may be responsible for increasing the probability of secondary pyrolysis reaction. Furthermore, this may lead to more char formation and less quantity of liquid yield. Sensoz et al. observed the effect of biomass particle size of 0.224-0.425, 0.425-0.6, 0.6-0.85 and 0.85-1.8 mm. The results showed that the highest liquid yield (46.10 wt.%) was obtained with the biggest particle size of 0.85-1.8 mm [151]. Furthermore, with 2 mm particle size of Pine wood, Yildiza et al. reported that a yield of 58.9 wt.% for oil [150]. Literature showed that particle size approximately 2 mm is necessary to produce significantly higher liquid yield [19].

2.7.3 Effect of feed rate

The effect of feeding rate on product formation has been rarely discussed. The feeding rate can effect on the fluidization behavior, heat transfer rate, vapor residence time and secondary reaction. In addition, the higher feeding rate may decrease pyrolytic vapor movement and will lead the secondary cracking reaction. To set the higher feeding rate, preheating or well drying of material is needed to decrease the time of energy consumption by material. Qingang et al. used 42% cellulose, 34% hemicellulose, 24% lignin and 0.5 mm particle size with different biomass feed rates ranging from 1.6 to 2.7 kg/h. They observed that below 1.92 kg/h, biomass feed rate has negligible effect on all pyrolytic products. This can be attributed to the sufficient heat supply from the reactor walls for biomass decomposition. However, increasing the feeding rate more than 1.92 kg/h, to some extent negative effect of biomass feed rate on tar and biochar yield was observed. It can be explained as, at high biomass feeding rate, adequate heat cannot be delivered to biomass in a limited time earlier to biomass particles exit from the reactor zone. Therefore, biomass

feed rate needs to be retained at a reasonable level for confirming the suitable product yields [152].

In regard to the feeding rate effect, Aghdas et al. have performed a study by using eucalyptus wood in pyrolysis fluidized system. The effect of biomass feeding rate on the product distribution was studied at temperature of 450°C and the result was shown in Figure 2.7. It can be seen that the higher liquid yield of 70 wt. % was attained at 90 g/min feeding rate. However, further increase in feeding rate 100 g/h depicted clear decline in liquid yield to 66 wt.% and an increase in char yield from 15 wt.% to 20 wt.% [153]. These finding showed that feeding rate is an important parameter in getting higher liquid product.

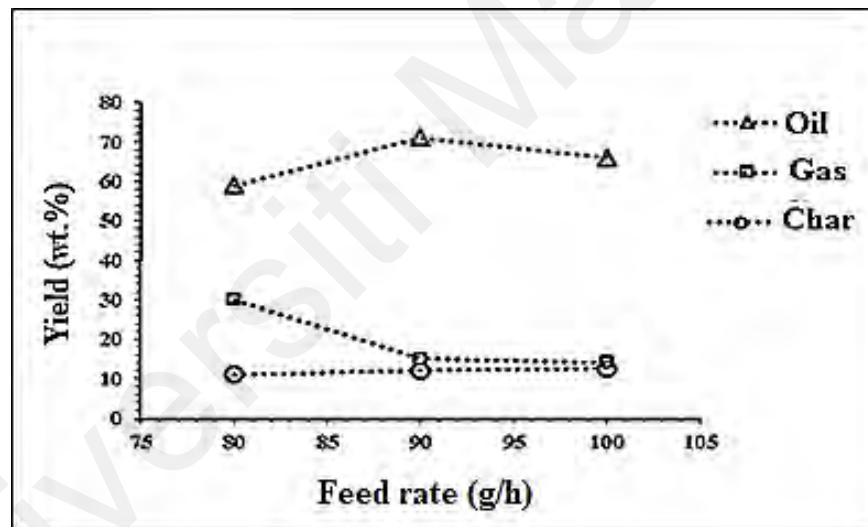


Figure 2. 7: Effect of feeding rate on pyrolytic products yield at 450°C. Redrawn based on [153].

2.7.4 Effect of heating rate

The elementary features of the fast pyrolysis are heating rate of biomass [93] and the final temperature [37]. The “fast pyrolysis” is characterized by high heating rates and short vapor residence times [148]. Heating rate has excessive rank in converting biomass to liquid, gas and char yield in continuous fast pyrolysis [149]. Depending on the heating rate, pyrolysis of biomass can be divided into three main kinds which include: slow, fast and flash

pyrolysis [14]. In slow pyrolysis, it has longer vapor residence time from 5 to 30 min and lower heating rates about 5 to 20°C/min and final temperature up to 500°C [154] results in formation of char, gas and 35%–50% liquid product [1]. In addition, Brech et al. also performed slow pyrolysis of different biomasses with slower heating rate of 5°C/min and obtained same range of liquid yield about 40 wt. % with final pyrolysis temperature of 500°C [155]. Contrariwise, fast pyrolysis process has higher heating rate (10-200°C/s), shorter vapor residence time (0.5-1.0 s), fast cooling of vapors for high bio-oil yield from 60-75 wt. % and good control of reaction temperature of 500°C. While, flash pyrolysis process is described by significantly higher heating rate of >1000°C/s or above that with shorter residence times of < 0.5 s and < 0.2mm particle size and temperature ranging from 450 to 1000°C [1]. For pyrolysis, limitation in heat transfer is often associated with the conduction of heat from the reactor to the biomass while limitation in mass transfer is often associated with the flow dynamics of biomass within pyrolysis reactor which can also be affected by the biomass particle size. Therefore, higher heating rate may be required to overcome the heat and mass transfer limitations and can bring out the bio-oil at a higher temperature and problem of coking in the reactor bed can be reduced which resulting maximum oil yield [14, 156].

Akkouche et al. investigated the effect of different heating rates ranging from 5 to 40°C/min. They observed that the effect of increasing heating rate resulted in an increase of gas yield from 6.4% to 14.8%; oil yield from 45.8% to 58.8% and char yield from 38.8% to 26.4% [144]. Similar effects of heating rates were also observed by Roy et al. [147]. Zhang et al. also investigated the effect of higher heating rate on pine sample and detected higher heating rate encouraged the evaporation rate of volatiles from the particle surface during

pyrolysis [157]. However, Kan et al. observed rapid increase in liquid yield for pyrolysis of cottonseed cake when elevating the heating rate from 5°C/min (26 wt. %) to 300°C/min (35 wt. %), whereas no noticeable variation of liquid yield was found when further increasing the heating rate from 300°C/min to 700°C/min [14].

Many scientists have been performed the experiments to observe the effect of heating rates on liquid oil yield in many studies. Salehi et al. observed that an increase in heating rate from 500°C/min to 700°C/min has increased the bio-oil yields. However, on further heating rate from 700 to 1000°C/min, no additional increase in bio-oil yield was observed. Generally, smaller particle size may encourage heat and mass transfer to form uniform temperature within the particles during pyrolysis and improving the liquid yield [14]. Hence, particle size and type of the feed stock has great effect in limiting the biomass conversion [156]. Consequently, more bio-char formation typically takes place at fairly low temperatures and lower heating rate. The high heating rate is benefiting in getting higher liquid yield production and less bio-char formation during pyrolysis process [158]. Therefore, heating rates of up to 1000°C/min have been recommended for higher oil yield [73].

2.7.5 Effect of temperature

Temperature is the main parameter which affects the amount of heat for biomass disintegration. Variations in the biomass products (liquid, gas and char) and composition are the main function of temperature and kind of biomass feedstock selected. The woody biomass mostly transformed into products by vapor residence time of 10 to 30 second at 500°C temperature around liquid yield of 50% on dry feed basis [31]. Typically, at reduced

temperature $< 300^{\circ}\text{C}$, disintegration at heteroatom positions inside the biomass structure occurs which causes the heavy tar formation. At higher temperature $> 455^{\circ}\text{C}$, adequate disintegration of biomass causes high molecular disordering which results in production of several types of useful compounds in the liquid yield. At such high temperature, pyrolysis reactions modify the product composition. This adjustments of pyrolysis temperature may reduce the char formation and will support in higher liquid yields [14].

Heidari et al. studied the influence of temperature on fast pyrolysis of *Eucalyptus* wood pyrolysis in continuous fluidized bed reactor. They observed a decline in bio oil yield with increasing temperature whereas gas yield was considerably increased from 29.4 to 48.4 wt.% by increasing the reaction temperature from 450 to 600°C. Additionally, the amount of char yield reduced from 19.7 to 14.2 wt.%. Furthermore, due to rising temperature secondary cracking of pyrolysis vapors decreased the liquid yield and increase the gas yields was also noticed [159]. Similarly, some other researcher also observed the influence of temperature on fast pyrolysis of Polystyrene type plastic waste. At 400°C, the yields of liquid, gas and char were 76, 8 and 16 wt.% respectively. Upon further increasing temperature from 400 to 450°C, bio-oil and gas yields have increased to 80.8 and 13 wt.% with a lesser char yield (6.2 wt.%) [160]. The liquid yields were determined from rapeseed cake on the basis of increasing temperatures 350, 400, 450 and 550°C via a home-built lab-scale semi-continuous pyrolysis reactor. They found that increasing temperature leads to higher liquid yields of 28.3, 34.3, 53.4 and 58.2 wt.%, respectively [161]. Therefore, it is stated that temperature is an important parameter which play key role in getting pyrolytic yields.

2.7.6 Effect of vapor residence time

The effect of inert gas as fluidization medium during continuous fast pyrolysis has great influence in controlling reactor hydrodynamics which lead to higher products liquid and gas [9]. Gartzen et al. observed the effect of sweeping gas flow rate using scrap tire around 9.5 L/min and obtained significantly higher bio-oil yield of 72 wt.% during pyrolysis [162]. Heideri et al. investigated the effect of nitrogen as inert gas flow rate of 12.6 L/min as fluidizing medium in fast pyrolysis of *Eucalyptus grandis*. It was observed that bio-oil yield decreased from 61.1% to 59.9% due to higher gas fluidization. This showed that the increasing nitrogen flow rate aided in sweeping out the vapors, causing reduction of residence time in both reactor and condenser which resulted a decreased liquid yield [159]. Similar tendencies were also observed by Alvarez et al., with sewage sludge of 14 L/min inert gas as fluidization medium and detected 62 wt.% bio-oil yield [122]. However, the oil yield typically decreased with considerably higher sweep gas flow rates. This suggests that higher sweep flow rates may stop reactions between lighter pyrolysis products, which are suitable for higher liquid production. This can be the possible explanation of low liquid yields at higher flow gas rates of inert gas fluidization medium [73]. Inert fluidizing gas also provides safety from material combustion, vapor control and good flow properties [163].

2.8 Condensation

Condensation is an important step in the production of pyrolysis oil. Without this step, only the char and gas products can be obtained from the process. The vapors generated during the process pass through the condensation unit to improve the heat transfer rate and change the physical state of matter from the gas phase into the liquid phase [9]. Some major

condensing fluids such as water, air, liquid nitrogen, refrigerants (hydro chlorofluorocarbons (HCFCs), Freon-12, R-410A, R-407C and R-134a), ice [164], chemicals (dry-ice/acetone) [165] and Ammonia (NH₃) or R-717 were commonly used [166].

There are many uses of condenser in different process industries. Moreover, electrostatic precipitator-cum-condenser [167], one-step fractional, multi-step (staged) condenser [168], shell & tube heat exchanger, plate type condenser, air below forced draft cooler, coil type glass condenser and heat exchangers were generally used for vapor/gas condensation are shown in Figure 2.8. Hwang et al. used two different types and combinations shell & tube and direct contact condenser in biomass fast pyrolysis. They found that direct contact condenser showed good conversion in getting high liquid yield [169]. Similarly, Gooty et al. used a series of three condensers. As a result of the high efficiency, the water fractions of the fractionated bio-oil were decreased to < 1 wt.% [170].

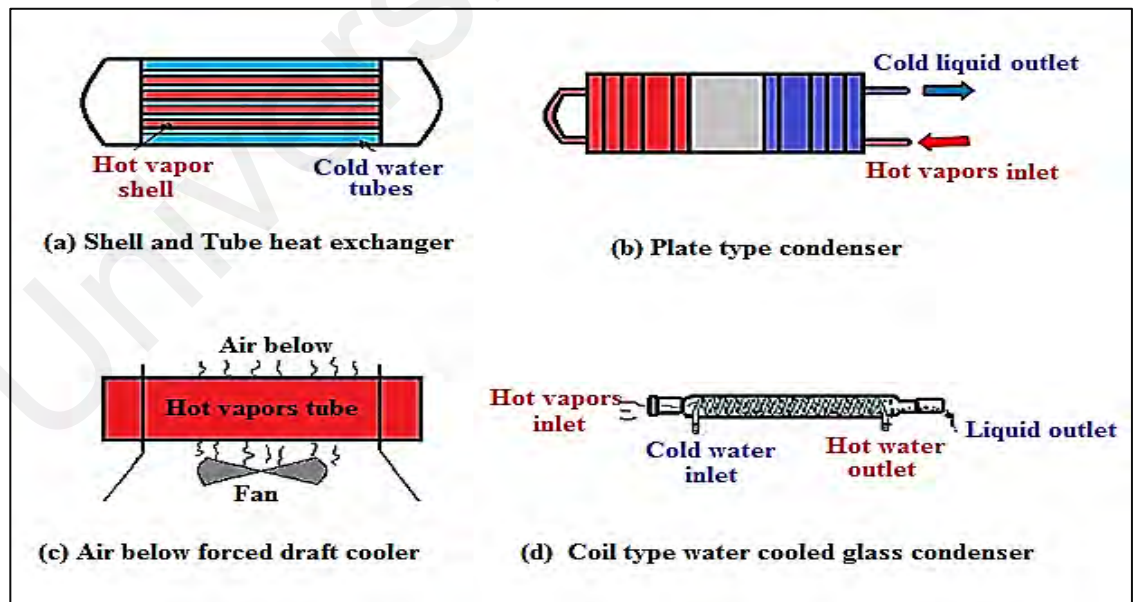


Figure 2. 8: Types of different condensers used in pyrolysis. Redrawn based on [169].

2.9 Additional particulate separation devices

Pyrolysis reactor designers extended that biomass particle size of less than 2 mm with short residence time and high gas fluidization velocity may achieve about 70–75 wt.% liquid yield. However, high gas fluidization conveys the decomposed biomass with pyrolytic gas stream [1]. Removal of particulates from pyrolytic gas stream requires either deposition or attachment with the separation medium. For selection of suitable separation unit, a detailed study is essential [171]. Generally particulates separation falls into four main types; cyclone separator, electrostatic precipitator, filters and scrubbers [172]. Various size of particulate are found in pyrolytic gas stream from 0.5 μm to 5 μm so selection of particulate separation device has important role in getting good quality product [173].

2.9.1 Cyclone separator

The cyclones are a kind of centrifugal separation devices. It is a static device that uses centrifugal force to separate particulates from a vapor or gas stream. The vapor/gas stream enters near the top of tangential inlet of cyclone separator and causes incoming gas and particles to circulate along the internal walls by centrifugal force of the cyclone separator. Eventually the particulates will dropdown to the bottom of the cyclone can be seen in Figure 2.9 [174].

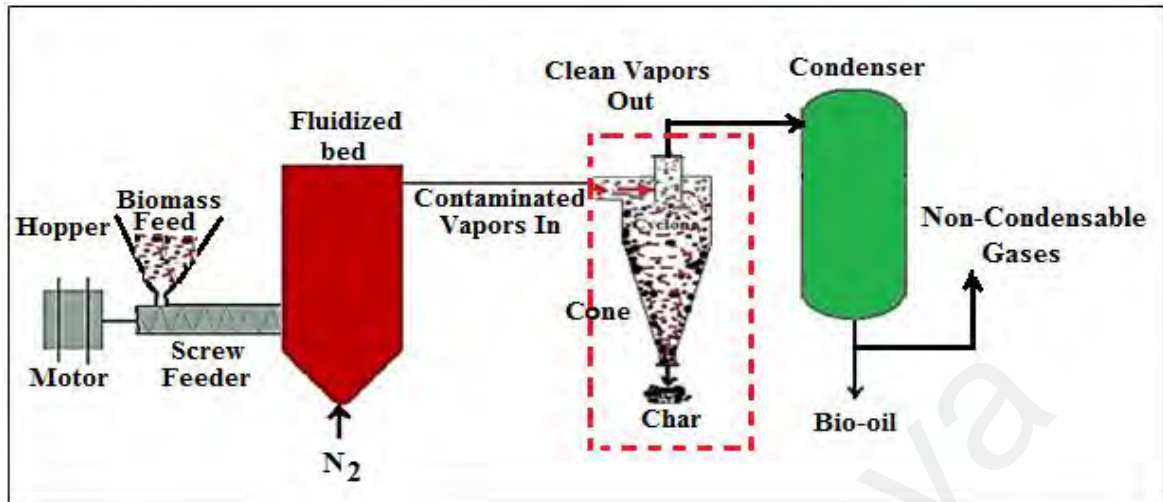


Figure 2. 9: Cyclone separator. Redrawn based on [174].

Cyclone separation was found to be effective for particulates removal from pyrolysis vapors. Lappas et al., used series of cyclones to separate the entrained solids from pyrolytic gas stream in a circulation fluid bed reactor during flash pyrolysis of lignocellulose from 0.2 - 0.4 mm particle size [175]. Sembiring et al. separated char from the gas stream in two series of cyclones during pyrolysis of empty fruit bunches using 0.21mm particle size in fluidized bed reactor [108]. Additionally, cyclones are more appropriate for particulates removal in continuous and semi-continuous pyrolysis process at higher temperature condition [174].

2.9.2 Electrostatic precipitators (ESPs)

ESP is a method of fine particulate collection that uses electrostatic forces and contains discharge wires and collecting plates. A high voltage about 440V AC is supplied to the discharge wires to form an electrical field between the wires and the collecting plates, which ionizes the gas stream around the discharge wires to supply ions. When gas contains an aerosol (dust, mist) flows among the collecting plates and the discharge wires, the aerosol particles in the gas are charged by the ions. The Coulomb force produced by the electric field

causes the particles to be charged and collected on the collecting plates and in this way particulate separation is achieved [176]. The working mechanism of ESPs can be seen in Figure 2.10. In addition, some advantages of ESPs are low operating cost and high efficiency. Furthermore, it can separate smaller particulates at large gas flow rates with low pressure losses [176], and also able to remove dry as well as wet particles (mist/smog) and with excellent temperature flexibility [177].

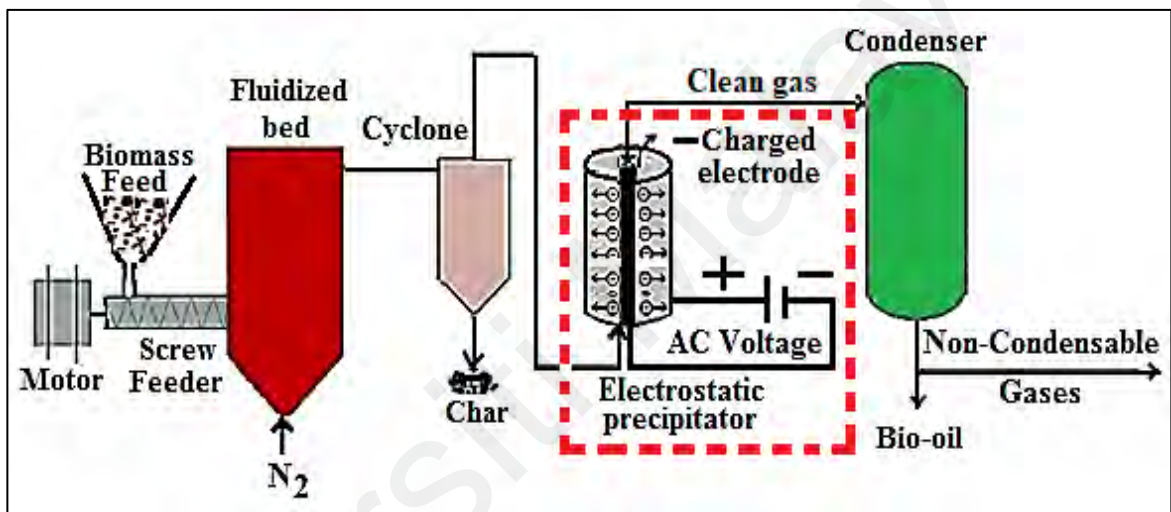


Figure 2. 10: Electrostatic Precipitator. Redrawn based on [177].

For particulates removal, Pattiya et al. installed the ESPs combined with other devices: two cyclone separators, a hot filter for solid collection, and a cotton wool filter. All of the particulates which obtained from different separation devices were then accumulated and defined as a char. The authors found that particulate matter was still present in the bio-oil. The large char particles dropped into the char pot 1, whereas char fines were carried over together with the pyrolysis vapor by the nitrogen flow passing the two cyclone separators and the hot filter where the majority of char fines were captured and then kept in the char pots 2 and 3. The pyrolysis vapor subsequently flew through the water-cooled condenser and

the ESP and was condensed into liquid product. Based on the current study we can say that for good quality liquid product, cyclone separators cannot completely serve the separation purpose of fine particulates so some additional separation devices must be installed for separation of very fine particulates as can be seen in Figure 2.11.

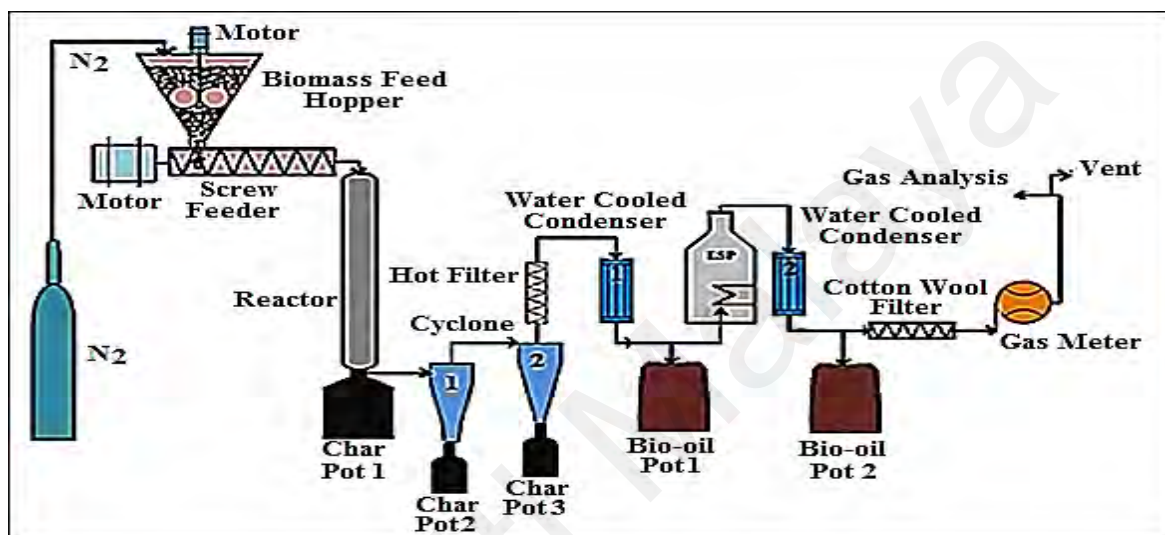


Figure 2. 11: Combination of devices for particulate separation. Redrawn based on [165].

Solids in bio-oil are char fines that could not be removed from the vapor in the separation process because of the low efficiency of the cyclones and hot filter. The char fines could also lower the bio-oil stability, which is normally measured by changes in viscosity over the period of time, because char fines containing active catalysts such as alkali and alkaline earth metals for polymerization reactions. This could increase the bio-oil molecular weight and therefore its viscosity [165]. Furthermore, Bridgwater suggested a typical configuration of electrostatic precipitators for removal of fines (aerosols) from bio-oil product [31]. Meier and Faix performed fast pyrolysis of lignocellulosic material in bubbling fluidized bed and circulating fluidized bed reactor. For fine solid particles, aerosol separation quencher in combination with electrostatic precipitator were used and a liquid yield of 70%

on dry wood basis was obtained [178]. These advantages have attracted great attention of ESPs to be used in fast pyrolysis.

2.9.3 Filters

Pyrolysis oil contains solids (char) which may increase the probability of plugging in downstream equipment. The fine chars from bio-oil can be removed in pyrolysis process by incorporating the hot pyrolysis vapor filters are shown in Figure 2.12 [179].

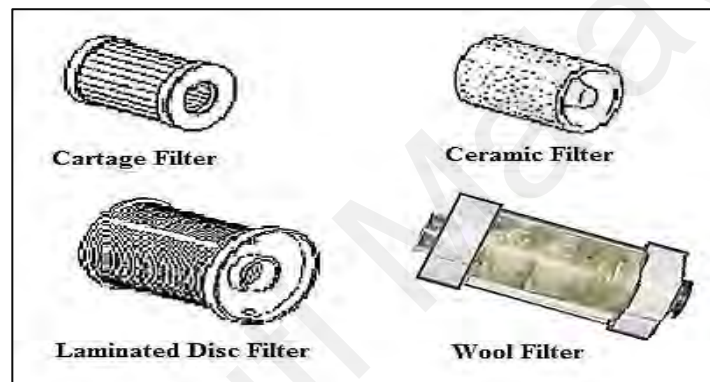


Figure 2. 12: Type of filters used in vapor purification during pyrolysis.

The filtration of hot pyrolysis vapors can be achieved by installing filters inside or outside of the pyrolysis reactor [179]. Hoekstra et al. and Chen et al. used ceramic or glass and metal filters [41, 180] inside a fluidized bed reactor with pore sizes of 10–15 μm and 6 μm . They found that the bio-oil found from hot filtration had lower solids, alkali metals and ash contents than that attained from the cyclone separation [179]. The disadvantages of these type of filters are the erosion when they are exposed for long time and pressure drop in fluidizing medium [179]. In addition, conventional fine char collection with a bag filter is less used in fast pyrolysis due to high fluidizing gas temperature. For particulates removal during biomass pyrolysis, Chen et al. used bag filter at the outer region of the rotary kiln reactor. The common drawback of this type of filter is the bio-char accumulation on the filter

medium after extensive run which leads to pressure drop [181]. For the improvement of bio-oil properties Paenpong et al. examined with increase of 1-2 filtration stages and filter medium size and found that the liquid yield was decreased from 57.7 to 42.0 wt.%. However, the bio-oil obtained through hot filtration showed lower solids, alkali metals and ash contents than that obtained from the cyclone separation. In addition, the hot filtered bio-oil was more stable than the cyclone separated bio-oil in terms of molecular weight change [179].

2.10 Outlooks on pyrolysis reactor technologies

This review showed that many researchers have studied and optimized the potency of the current semi-continuous and continuous pyrolysis reactor technologies along with feed treatment methods, feeding systems and effect of operating parameters on product recovery. It is perceived that thermal treatment of biomass through drying has shown a substantial decrease in the moisture content, increase in the grinding ability and improved the liquid product properties. Alternatively, physical treatment was shown to increase the interfacial surface area of biomass in order to avoid coagulation and increase the heat and mass transfer rate during pyrolysis. It has been found that screw/auger feeding system is more suitable in terms of efficiency and can provide good feed control in comparison to the other feeding equipment. The roles of operating parameters, for instance heating rate, temperature, feeding rate, gas flow rate, and reaction/residence time were studied in which temperature was found to be the most significant parameter in affecting liquid product yield.

Furthermore, it was found that different reactor types resulted in different liquid yields: BFB (67% – 70 wt. %), CFB (70 – 75 wt.%), CSBR (70 wt.%), RC reactor (65 wt.%), ablative reactor (70 wt.%) and screw/auger reactor (30 – 59 wt.%). However, due to high

carbon conservation, increased solid residence time, low ash transfer, problems in char removal, small particle sizes and high gas fluidizing velocity are the general causes of its limitations. In this regard BFB and CFB are expensive processes and require further liquid refining which makes them even more costly. Contrariwise, CSBR has been proven as a substitute for BFB and CFB. However, this technology has limited upgradation prospects on large scale bio-oil production due to its complex design, high gas fluidization requirement and difficult handling operation. Additionally, RCR technology is mostly dependent on centrifugal force. The hot sand and biomass are transported up in a conical bed by the centrifugal force created by the rotation of the cone without support of any sweeping or carrier gas.

However, ablative reactor can handle much larger biomass particle size with no carrier gas. Nonetheless, it is also a complex mechanical design which posed as a challenge for its scalability. In addition, higher reactor cost, elevated pressure and higher heat losses, restricted this technology for its industrialization. Finally, the screw/auger reactor operates at 400°C on continuous mode, but its upgradation is difficult as the moving parts of the reactor are in contact of hot zone, so high heat transfer rate on large scale liquid production is not possible. Thus, it is not been proven yet for large scale commercialization and further research is needed. Therefore, by considering all types of the reactors, design aspects, facilities, advantages and disadvantages, the designing of a more efficient semi-continuous or continuous pyrolysis reactor would certainly be of great need and advantage in the field of pyrolysis process.

CHAPTER 3: METHODOLOGY

3.1 Introduction

Novel Helical Screw Fluidized Bed Reactor (HSFBR) is developed and palm shell (PS) for bio-oil production is used. The performance of novel HSFBR is investigated for high particle dynamics, heat transfer rate, high liquid and low char yield with improved properties heating rate, temperature, particle size, feed rate, pyrolysis time and vapor residence time are described.

- **Part 1:** Designing of fluidized bed reactor for oil palm solid waste pyrolysis and experimental procedure using helical screw as a new concept for fluidization for improved oil production.
- **Part 2:** To determine whether there was an improvement in the quantity and quality of the oil production by using the helical screw fluidized bed reactor.
- **Part 3:** To explore the performance of helical screw fluidized bed reactor in slow, medium and fast pyrolysis modes.
- **Part 4:** Effect of temperature and feed rate on pyrolysis oil produced by helical screw fluidized bed reactor.
- **Part 5:** Palm shell pyrolysis in a novel helical screw fluidized bed reactor: Effect of particle size, pyrolysis time and vapor residence time on bio-oil yield and characteristics.

3.2 Material

Palm shell (PS) was obtained from Felcra Palm oil Mill Sdn. Bhd., Bota, Perak, Malaysia. The sample was treated by drying under the sun for a day and subsequently

grinded to obtain the desired particle size of 1–2 mm. The drying process was again performed in an oven at 105°C for 24 h to remove the moisture content. Prior to use, the samples were then stored in a desiccator to keep them free of moisture.

3.3 Part 1: Designing of fluidized bed reactor for oil palm solid waste pyrolysis and experimental procedure using helical screw as a new concept for fluidization for improved oil production.

In this section, the design features and experimental set up of helical screw fluidized bed reactor (HSFBR) along with main operating temperatures monitored during the pyrolysis process are discussed. The existing reactor setup is provided in appendix B, while Figure 3.1 illustrates the design features and experimental set up of helical screw fluidized bed reactor (HSFBR) along with main operating temperatures monitored during the pyrolysis process. The reactor was made from stainless steel (CS309) of 5 mm thickness with an internal diameter of 228 mm and total length of 1,524 mm. A helical screw of stainless steel (CS309) with total length of 1,550 mm including 6 flights with each pitch distance of 95.25 mm and an external diameter of 203.2 mm was used. The helical screw was powered by an AC motor to rotate the helical screw within the reactor shell as shown in Figure 3.1. A perforated steel screen (CS309) plate of 132.4 mm diameter with 1.5 mm pore size was fitted inside the reactor bottommost to arrest the solid material for a short period of time until biomass particles are reduced to 1-2 mm and to pass through the sieve pores to the by-product biochar collector. For biomass control feeding, an auger feeding system of stainless steel 304 was used. Furthermore, for a continuous by-product biochar collection, a char collector was connected at the bottom of the reactor system.

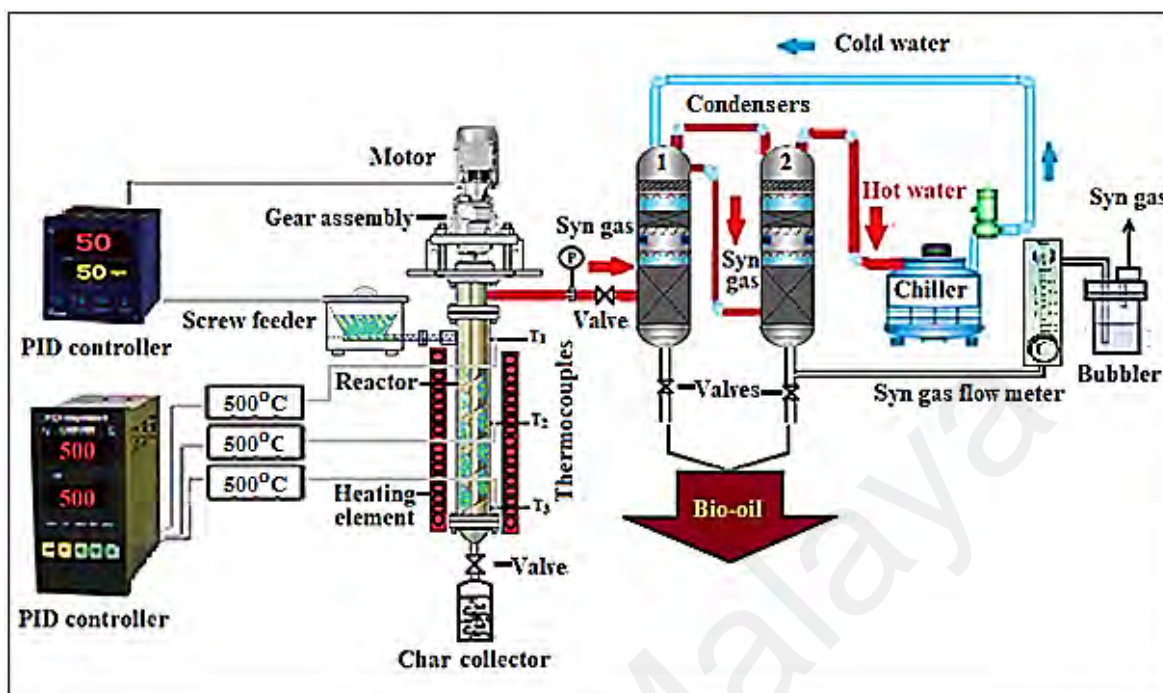


Figure 3. 1: Schematic diagram of novel helical screw fluidized bed pyrolysis reactor:

A pressure gauge of 7 bar/100 psi was installed between the reactor and condenser line to constantly monitor the vapor pressure. A series of two stainless steel condensers was installed with each condenser length of 1371.6 mm and outside diameter of 228.6 mm. A chiller was used to provide the chilled water at 5°C as cooling medium temperature for rapid pyrolysis vapor condensation in order to avoid from the secondary vapor cracking. Three series of experiments were carried out using 300 g of PS.

The experiment was started by charging 300 g of PS (particle size of 1–2 mm) into the reactor. The reactor then was heated using a two-zone electric furnace at 1.5 KW for each of the zone heaters. The temperature process was monitored by using three K-type thermocouples T₁- T₃ attached to the reactor shell with equal height of 1742.66 mm. The PID temperature controller (KT-1130, Korea CHINO Co.) was used to maintain a constant heating rate to observe the isothermal reaction condition. Furthermore, Mechanical

fluidization was performed by adjusting the helical screw rotation speed from 25, 50, 75 and 100 rpm and the temperature was set constantly at 500°C.

Minimum fluidization velocity can be found by monitoring the pressure drop of inert gas across the bed. While, in case of fluidization condition using mechanical device a helical screw was used as a substitute of inert gas for fluidization. Therefore, no pressure drop was observed. On the other hand, torque applied is related to minimum fluidization velocity (V_{mf}) equal to gas minimum fluidization velocity of 5 l/min when the bed height is strained to increased.

The first setting of the experiment was adjusted at 0 rpm, indicating that no particle movement exists inside the reactor system during pyrolysis at the heating rate of 10 °C/min. The second setting was operated in helical screw rotation at 50 rpm with the help of the AC motor. After the desired temperature was obtained as per first setting, then experiment continued for 60 min to condense all pyrolysis vapors.

Furthermore, the condensed pyrolysis vapors were collected at 5°C in a series of condensers, whereas non-condensable gases remained under the controlled flow rate of 5 cc/min with air passing through the bubbler to minimize air pollution in the surrounding environment. However, the char by-product accumulated in the char collector installed at the bottom of the reactor. Additionally, bio-oil and bio-char were collected for the yield calculation and additional analysis of their physicochemical features. The product yield bio-oil was calculated using Eq. (3.1), as followed:

$$Y_p = \frac{X_1}{X_2} \times 100 \quad (3.1)$$

Where, Y_p is the product yield, X_1 is the mass of the desired product, and X_2 is the initial weight of the raw material. The gas yield was determined by subtraction: gas yield =

100 – (liquid yield + char yield). Each pyrolysis experiment with or without rpm condition was performed three times under the same conditions to take the average and consistency of the results.

The below given parts: 2, 3,4 and 5 are discussed in chapter 4 of result and discussion.

3.4 Characterization

In this section for product characterization several analyses were made to investigate the effect of operating parameters as listed in Part 2, Part 3, Part 4 and Part 5 is presented in Table 3.1. Prior to characterization, the liquid collected from the condensation unit was stored in a separating funnel for 48 h. Each layer that formed during the separation process was then investigated for different parameters, such as pH, density, viscosity, and water content, of the main liquid product using the following analytical instruments and techniques are mentioned below.

Table 3.1: Product characterization.

Analysis	Method
pH analysis	The pH was determined at room temperature by using the Metrohm 827 pH meter and following the ASTM E70 standard.
Density analysis	The density was determined by using a pycnometer (volume: 25 mL) at room temperature following the ASTM D4052 standard.
Viscosity analysis	Furthermore, the viscosity of the liquid product was determined using a rotational viscometer (model: DV-II + Pro EXTRA) with 20 rpm at room temperature according to ASTM D445 standard.

Table 3.1 cont....

Analysis	Method
Water content analysis	The Karl–Fischer titration method was used to measure the water content in the liquid samples by using a 737 Karl–Fisher coulometer from Metrohm according to the ASTM E 203-96 standard [182]. Hydranal-coulomat AG (80ml) and Hydranal-coulomat CG (5ml) were used as anolyte and catholyte reagents, correspondingly.
Ultimate analysis	Ultimate analysis of bio-oil and by-product biochar was performed using Perkin-Elmer 2400 CHNS/O following ASTM D 5373 standard. Carbon, hydrogen, oxygen, nitrogen and sulfur data obtained from this analysis using combustion tube and reduction tube.
FTIR analysis	Perkin–Elmer Spectrum 400 spectrometer with ATR assembly was used for FTIR analysis of bio-oil and by-product char. The samples were scanned in the range of 400–4000 cm^{-1} with a resolution of 4 cm^{-1} .
GC/MS analysis	GC/MS of bio-oil was conducted with Shimadzu model no. QP2010 equipped with DB-5 MS column (30m x 0.25mm x 0.25 μm). The injector temperature of GC/MS was set about 250°C and oven temperature was programmed at 60°C for 1 minute and then increased to 300°C with a heating rate of 10°C/min and maintained for 20 minutes. Helium was used as carrier gas with a flow rate of 1.5 mL/min. The detector temperature was set at 230°C. Sample was injected into the column with a split ratio of 1:30. The identification of the chemical composition of bio-oil was performed by comparing the sample chromatogram with the database in the GC/MS library.
TGA/DTG analysis	The TGA/DTG analysis of by-product char was performed using TGA Q500 to investigate for two different purposes which were proximate analysis and thermal properties of the samples. Around 10 mg of sample was used for this analysis and heated in an alumina crucible under N_2 atmosphere from 30 to 800°C with a heating rate of 20°C/min. Moisture content was estimated from the weight loss initial temperature of 150°C. Volatile matter was determined by the calculation of the weight loss data between 150 to 450°C. Ash content was determined from available residue over combustion temperature of 800°C.

Table 3.1 cont....

Analysis	Method
Fixed carbon analysis	<p>The percentage of fixed carbon in by-product char was calculated by Eq. (3.1).</p> $\text{Fixed carbon (\%)} = 100 - [\text{Moisture (\%)}] + [\text{Volatile matter (\%)}] + [\text{Ash (\%)}] \quad (3.1)$ <p>Table 4.14 lists the different fuel properties of bio-oil, including flash point, fire point, dew point, pour point, higher heating value (HHV), and lower heating value (LHV), that characterize the liquid sample.</p>
Flash Point analysis	<p>The flash point test was performed according to the (ASTM D93-97) standard by using the HFP 360 Pensky–Martens closed cup manual tester.</p>
Fire point analysis	<p>The fire point test was performed following the (ASTM D93) standard by using the Pensky–Marten open cup tester.</p>
Pour point analysis	<p>The pour point of the bio-oil was determined according to the ASTM–D97-17b method.</p>
HHV and LHV analysis	<p>The following equations show that the HHV of the bio-oil and char was obtained by ultimate analysis according to the Dulong formula, whereas LHV was calculated by using Eq. (3.2), as proposed by Oasmaa [183].</p> $\text{HHV (MJ/kg)} = \frac{338.2 \times C + 1442.8 \times \left(H - \frac{O}{8}\right)}{1000} \quad (3.2)$ $\text{LHV (MJ/kg)} = \text{HHV} - 0.218 \times H \quad (3.3)$ <p>For reliability of data standard deviation (SD) of variances was calculated using Eq. (3.4).</p> $\text{Standard Deviation} = (SD)$
Data analysis	$= S^2 = \frac{\sum (x - \bar{x})^2}{n - 1} \quad (3.4)$
Product syn gas analysis	<p>The collected syngas product was analyzed using Rosemount Analytical X-STREAMTM (UK) apparatus.</p>

All testing experiments were carefully repeated three times to avoid the margin of errors.

CHAPTER 4: RESULTS AND DISCUSSION

4.1 Part 2: Novel helical screw-fluidized bed reactor for bio-oil production in slow pyrolysis mode: A Preliminary study

4.1.1 Introduction

The oil from biomass can be produced by different modes of pyrolysis; fast and slow pyrolysis. In terms of yield, fast pyrolysis is more superior than slow pyrolysis due to the rapid heating rate ($>100^{\circ}\text{C}/\text{min}$) and few seconds of vapor/gas residence time ($< 2\text{s}$) released from hot zone reactor [184]. This process mode can produce liquid yield up to 75wt.% from biomass wood on a dry-feed basis with small particle sizes of ~ 2 or less than 3mm [2, 31]. In contrast to fast pyrolysis, the liquid yield from slow pyrolysis was found low around ~ 30 wt.% [184]. To improve the yield, the researcher tried to modify the reactor design and there are various slow pyrolysis reactor types have been developed includes vacuum pyrolyzers, bubbling fluidized beds, augers and heated kilns of various types [185]. Although the concept design is different, the behind reason is same which is to obtain the high liquid yield with low operation cost.

Most of the concepts in slow pyrolysis reactor are focused on how to improve the heat transfer rate from the heat source to material. There are several attempts to improve the heat transfer rate which mainly can be classified into two categories: the addition of transfer medium and the addition of mechanical device. Generally inert gases (N_2 , He and Ar) [186] and quartz sand [1] are commonly used as a heat transfer medium to increase the heat transfer rate through the collision mechanism. However, this strategy has some drawback since it needs; inert gas preheating system, pressurization system to help the fluidization, and fines

separation system, which may lead to increase the processes cost. Conversely, the addition of mechanical device in slow pyrolysis reactor is found to be more feasible option since it only needs cost for design, installation and maintenance. Agitation, rotation, vibration and mass transportation are some of mechanical idea that has been successfully used in slow pyrolysis reactor [187, 188].

However, none of the researcher has tried to develop the fluidization idea using mechanical device. Compared to other methods, the concept of fluidization can provide more hydrodynamic or mass transfer rate during the pyrolysis process [189]. As a result, the particles interaction will increase and lead to improve the heat transfer rate. This concept has proven to have a good performance in producing the high liquid yield, where the product can be obtained in the range of 39-44 wt. % [1, 190]. The fluidization is generally occurred by helping the gas velocity. The minimum fluidization condition can be established when the bed of material start to expands δU with minimum fluidization velocity U_{mf} , and as a result the bed height will increase from initial H_i to final height H_o . The minimum fluidization velocity U_{mf} for particulate fluidization can be written as, $U_{mf} = \delta U = \delta H = H_o - H_i$. Whereas, δU is the change in velocity which lead to expand the bed and will increase the bed height δH [191]. To replace the gas velocity, the proper design of mechanical device with providing the number of flights to up lift the material is potential to create the fluidization condition. The good thing of mechanical device is no pressure drop during the process, because it is supported by gear system which has capability to maintain the fluidizing condition till the process complete.

This research aims to investigate the performance of novel HSFBR to produce bio-oil derived from biomass. The process was performed in slow pyrolysis mode with the

heating rate of 10°C/min to achieve the reaction temperature of 500°C. The effect of helical rotation speed on the liquid yield and product quality were studied. In addition, some important findings were discussed in this paper including some technical notes and characterization of liquid product.

4.1.2 Product yields

The liquid yield from this study was higher than other slow-pyrolysis studies that used gas fluidization systems, where the yield was found competed when it compared fast-pyrolysis mode, as shown in Table 4.1. The works conducted by [192] and [193] show that the maximum liquid yield obtained in slow-pyrolysis mode may vary in the range of 30–48 wt.% by using fluidized bed reactor with both works performed under the nitrogen environment. The high liquid yield obtained in this study is associated with the helical screw fluidization characteristics, and the heating rate was improved by good mixing and collision property between particle–particle and particle–reactor shell [194, 195]. This result was consistent with the study by Valentina et al. who studied the fluidization behavior of biomass by using the mixer system inside mechanically fluidized reactor. They noted that good mixing is crucial to achieve effective heat transfer characteristics between the heaters and the bed, and between the bed and the biomass particles [196].

Table 4. 1: Comparison of pyrolysis products using different fluidization system with slow and fast pyrolysis mode at a reaction temperature of 500°C.

Ref.	Reactor type	Pyrolysis mode	Heating rate (°C/min)	Other key parameters	Bio-oil phases		Product yields		
					(wt. %)				
					Org.	Aqua.	Oil	Char	Gas
This study	Helical reactor with fixed bed condition	Slow	10	- Temp: 500°C - τ : 0 rpm	16.80	21.60	38.4	35.5	26.1
This study	Helical reactor with fluidization condition	Slow	10	- Temp: 500°C - τ : 50 rpm	24.00	27.60	51.6	26.6	21.8
[192]	Fluidized bed	Slow	10	- Temp: 500°C - N ₂ : 0.2 L/min	NM	NM	48.1	36.4	15.5
[193]	Fluidized bed	Slow	5	- Temp: 500°C - N ₂ : 1 L/min	12.1	18.6	30.7	31.2	38.1
[197]	Fluidized bed	Fast	NM	- Temp: 500°C - N ₂ : 13.3 L/min	NM	NM	57.8	25.9	16.3
[198]	Fluidized bed	Fast	NM	- Temp: 500°C - N ₂ : 5-6 L/min	30.26	21.7	51.9	24.8	23.3
[198]	Fluidized bed	Fast	NM	- Temp: 500°C - N ₂ : 5-6 L/min	27.1	20.6	47.8	27.8	24.4
[198]	Fluidized bed	Fast	NM	- Temp: 500°C - N ₂ : 5-6 L/min	36.6	17.4	54.0	28.9	17.1

Note: τ = Torque, NM = Not mentioned.

In gas fluidization system, bed fluidization condition and short vapor residence time are two parameters that need to be carefully adjusted to obtain the high liquid yields. These two parameters actually controlled by an inert gas flow rate. The high gas fluidization velocity is desired to achieve the good hydrodynamic condition in the reactor. However, this condition also lead to reduction in vapor residence time of the reactor and condenser, resulting decreased liquid yield [199]. This contradiction can be eliminated by introducing the mechanical fluidization technique, wherein no inert gas is required in the fluidization process.

4.1.3 Effect of helical screw rotation

Some additional experiments were performed to obtain an accurate description of the effect of the helical screw rotation. The experiments were focused on the increasing speed of the helical screw rotation, wherein the additional rotation speeds of 25, 75, and 100 rpm were evaluated. Table 4.2 provides the results of the experiment together with those under 0 and 50 rpm conditions.

Table 4. 2: Effect of helical screw rotation on the distribution of slow pyrolysis products.

Helical Screw torque (rpm)	Reactor Pressure (psi)	Products (wt. %)		
		Liquid	Char	Gas
0	1.0	38.40	35.50	26.10
25	1.2	44.00	30.33	25.67
50	3.0	51.60	26.60	21.80
75	3.2	45.00	23.33	31.67
100	3.5	43.00	15.34	41.66

The results show that the liquid yield increased linearly with the increase of rotation speed. The maximum liquid yield was obtained under the 50-rpm condition. However, the yield then gradually decreased when the rotation speed was greater than 50 rpm and increased to 100 rpm. Notably, the increase in rotation speed also increased the corresponding pressure inside the reactor. As a consequence, the non-condensable gas released from the condenser also increased significantly. Section 4.2.3 of Table 4.2 shows that this phenomenon led to the sharp increase in gas product from 21.80 at 50 rpm to 41.66 at 100 rpm. Thus, the proper adjustment in the rotation speed is needed to maximize the liquid yield product.

4.1.4 Effect of reactor design on slow pyrolysis performance

4.1.4.1 Effect of helical design on pyrolysis time

Figure. 4.1 shows the correlation between temperature and time profile obtained at different setting of the experiment (0 and 50 rpm). The temperature was recorded in minutes at different time to reach the pyrolysis temperature of 500°C. Without the influence of helical screw at no rotation 0 rpm inside of the reactor, the final temperature of 500°C was achieved in 50 min. However, when the helical screw was operated at 50 rpm, a significant decrease in total pyrolysis time of 20 min was observed. This condition is efficient because the pyrolysis process can be completed in a short period of time, thus also indicating the effect on the reduced energy consumption.

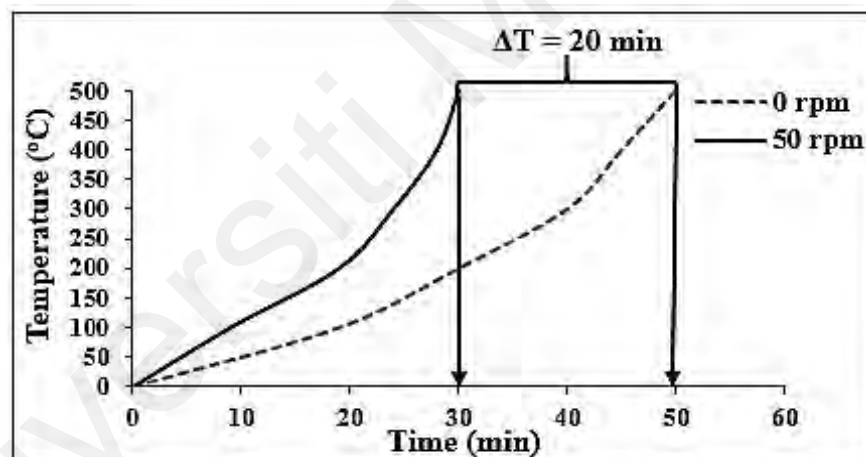


Figure 4. 1: Effect of helical screw rpm on pyrolysis time.

The improvement in pyrolysis time was caused by the presence of helical screw, which improved the reactor hydrodynamics and changed the bed entropy through the high dispersion of biomass particles. The dispersion process avoids the agglomeration of the particles that can cause the temperature reduction. Ralph et al. [200] stated that the onset of agglomeration has been indicated by a decrease in reactor temperature and pressure as the bed defluidized. In addition, based on the additional experiment mentioned in Section 3.2,

the increase in rpm speed has led to decrease in pyrolysis time. When the helical screw was operated at 25, 50, 75 and 100 rpm, a significant decrease in total pyrolysis time was observed at 40, 30, 25 and 20 min, respectively.

4.1.4.2 Effect of helical design on pyrolysis pressure

The pressure inside the reactor can indicate the production of vapors during the pyrolysis of biomass. The release of high vapors tends to produce higher yield of liquid product [201]. Figure 4.2 shows that the use of helical screw reactor at 50 rpm have two main positive contributions, namely, early production and high quantity of vapor.

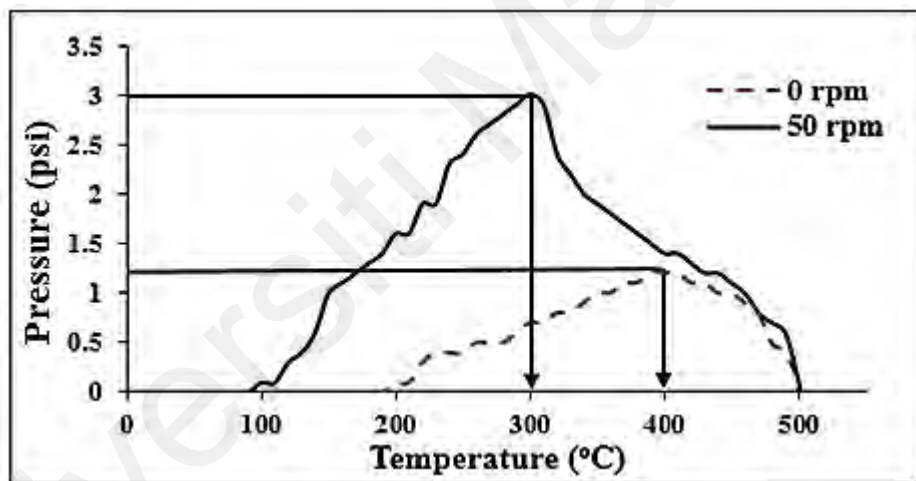


Figure 4. 2: Effect of helical design on pyrolysis pressure.

Figure 4.2 presents that the early formation of vapors of 0.1 psi vapour pressure under 50-rpm condition was observed at 100°C, whereas the initial pressure was observed when temperature reached 190°C. The vapors will basically tend to release when the biomass obtains the sufficient amount of heat at high temperature. This condition of vaporization is called endothermic reaction [202]. The rate of endothermic reaction can be improved by using several approaches, such as adjusting the reactant concentration, increasing the

pressure or temperature, using a catalyst, and introducing the stirring system. The use of stirring in the reactor significantly promotes the fluidity and permeability of the granular layer by convective heat transfer and collisional heat transfer between the particles [203]. Moreover, when the rate of endothermic reaction was improved by the helical screw, the maximum breakdown of biomass material provided high pyrolysis vapor/gas production [201].

4.1.4.3 Distribution of liquid product based on the type of phase

The high water content in the biomass obtained the bio-oil from the existing moistness in the feedstock and dehydration reactions in pyrolysis [31]. Figure 4.3 shows that the liquid products obtained from single-phase 0 and 50 rpm settings initially appeared dark brown, viscous, and free-flowing liquid with pungent smell.

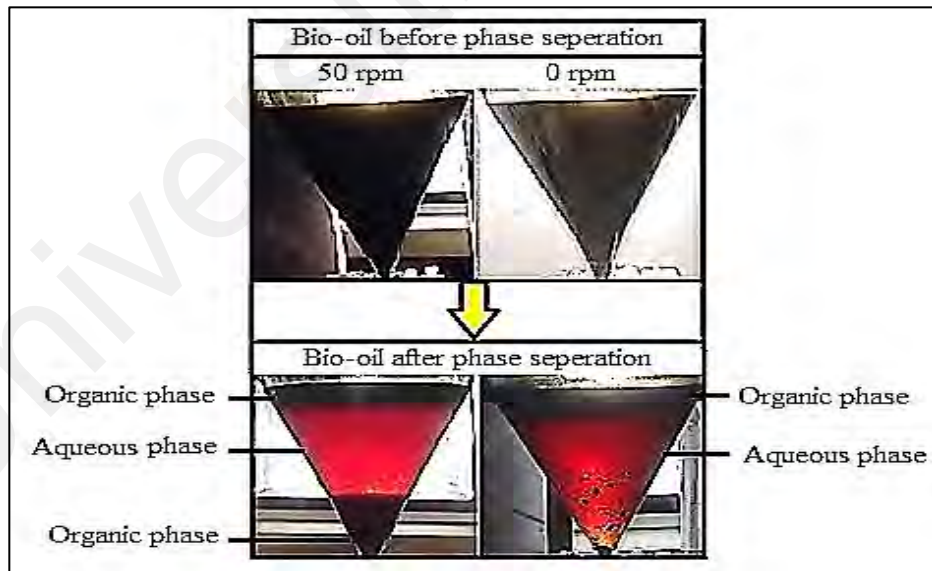


Figure 4. 3: Separation of bio-oil phases obtained with 0 and 50 rpm conditions.

For 0-rpm condition, the top black layer was considered in the organic phase, whereas the bottom reddish brown layer was in the aqueous phase. By contrast, the liquid

product was divided into three layers when 50-rpm condition was applied. Similar indications for three phases were also reported in other studies [204]. The top and bottom layers were defined as the organic phases, and the middle layer was the aqueous phase. Table 4.3 presents the details of the liquid distribution based on the type of phase derived from 0- and 50-rpm settings. Table 4.3, that the aqueous and organic phases with 0-rpm condition were quantified as 21.6 and 16.8 wt. %, respectively. Under 50-rpm condition, the total organic and aqueous phases were obtained at 24 and ~27.6 wt. %, respectively. The helical screw provided high bed hydrodynamics during the pyrolysis process, causing the contact between the nascent char particle and vapor.

Table 4. 3: Distribution of bio-oil yield based on the type of phase.

Ref:	Reactor type	Parameters	Pyrolysis mode	Bio-oil phases (wt. %)		Total bio-oil yield (wt. %)
				Org:	Aqua:	
This study	Helical screw reactor with fixed bed condition.	- Temp: 500°C - τ : 0 rpm	Slow	16.8	21.6	38.4
This study	Helical screw reactor with fluidization condition.	- Temp: 500°C - τ : 50 rpm	Slow	16+8=24	27.6	51.6
[205]	Auger reactor.	- Temp: 450°C - N ₂ : for purging	Slow	12.0	37.0	49.0
[206]	Fluidized bed reactor.	- Temp: 500°C - N ₂ : 0. 2 L/min	Fast	21.5	29.9	51.4
[198]	Fluidized bed reactor	- Temp: 500°C - N ₂ : 5-6 L/min	Fast	30.26	21.7	51.9
[198]	Fluidized bed reactor	- Temp: 500°C - N ₂ : 5-6 L/min	Fast	27.1	20.6	47.8

This phenomenon allowed the nascent char as the catalyst to promote the secondary cracking of pyrolysis vapors and the secondary formation of the solid organics [207]. In this

study, the formation of solid organics can be clearly observed as bottom organic yield increase at 50-rpm condition. The findings of this phenomenon were similar to those of other researchers; Zhu et al. indicated that the organic phase increased from 4.25% to 8.31% when the bio-char was used as the catalyst in the pyrolysis of the Douglas biomass. The elemental analysis result shows that the solid organics under the 50-rpm condition contained a majority of carbon content at ~56.40 wt. %.

For fuel production, the organic phase is preferred because it has higher calorific value compared with the aqueous phase. Wang et al. derived an organic phase from the pyrolysis of biomass that can be easily upgraded to transport fuel [208]. As a comparative study, Yang et al. performed biomass pyrolysis by using barley straw via the auger reactor and obtained a total liquid yield of ~49 wt. % with organic and aqueous phases of ~12 and 37 wt. %, respectively [205]. Peerapon et al. produced the liquid oil derived from the oil palm empty fruit bunch by using the fluidized bed reactor with N₂ atmosphere; they produced a total liquid yield of ~51.4 wt. % containing 21.5 wt. % and 29.9 wt. % of organic and aqueous phases, respectively [206]. This study clearly shows that the use of the helical screw reactor at 50-rpm condition provided a significant amount of organic phase in slow-pyrolysis mode that is more effective than other reactors and was able to obtain high-yielding liquids without the influence of N₂ gas.

4.1.5 Characterization

4.1.5.1 Characterization of liquid product

Table 4.4 shows that the liquid organic phase density of 1030 kg/m³ was observed with 0-rpm condition and slightly increased to 1040 kg/m³ when the speed of the helical screw was adjusted to 50 rpm. Furthermore, the viscosity of the liquid product at 0 rpm was

attained at ~1.8 cP, whereas it increased significantly to 23.10 cP when the helical screw was operated at the speed of 50 rpm. Most researchers agree that the increase in bio-oil viscosity was caused by the removal of water content from the liquid product [187].

This finding is supported by the result of the water content analysis, wherein the water content was significantly decreased from 12.4% to 4.7% under 50-rpm condition. The pH values of the liquid organic phase obtained at 0 and 50 rpm were 2.8 and 3.5, respectively, which are consistent with other findings [183]. High pH value is leads to the corrosion of the engine due to the high content of phenols [15], which were also major compounds in this study.

Table 4. 4: Physical and chemical properties of bio-oil (organic phase) produced at 0 and 50 rpm settings.

Properties	Bio-oil (organic phase)	
	Value	
	0 rpm	50 rpm
Density (kg/m ³) at 27°C	1030	1040
Viscosity (Cp) with 50 rpm at 27°C	1.8	23.10
Water content (%)	12.44	4.71
pH at 27°C	2.90	3.50
Ultimate analysis		
C	65.34	76.82
H	12.18	12.36
N	6.57	9.46
S	0.92	0.92
O (by difference)	14.99	0.44
HHV (MJ/kg)	36.96	43.73
LHV (MJ/kg)	33.69	41.03

Notably, on the basis of the ultimate analysis, the use of the helical speed at 50 rpm improved the quality of the organic phase, especially the carbon and oxygen contents. The carbon content significantly increased at 17.5%, in which the oxygen content was significantly reduced at ~97%. These results may be attributed to the nascent char, which

served as the catalyst during pyrolysis. Jahirul et al. [1] explained that the char produced during pyrolysis can serve as a vapor-cracking catalyst. Similarly, Bridgewater [31] also described that the char acts as an effective vapor cracking catalyst. Shoujie et al. investigated the bio-char catalyst in the pyrolysis of sawdust and found that the quality of bio-oil was improved clearly, wherein the concentration of the hydrocarbon compounds was increased with the increase of bio-char catalyst loading [209].

From this study, the performance of the helical screw fluidization at 50-rpm increased the contact between the vapors and char surface during pyrolysis. In addition, the liquid produced at 50-rpm exhibited high HHV value at ~ 43.73 MJ/kg, indicating that the liquid produced from the helical screw reactor will have comparable calorific value with the diesel fuel (45 MJ/kg) [210].

4.1.5.2 FTIR analysis of liquid product

Figure 4.4 presents the FTIR spectra of the bio-oil (organic phase) samples derived from PS at 0-rpm and 50-rpm conditions, and Table 4.5 lists the identified functional groups.

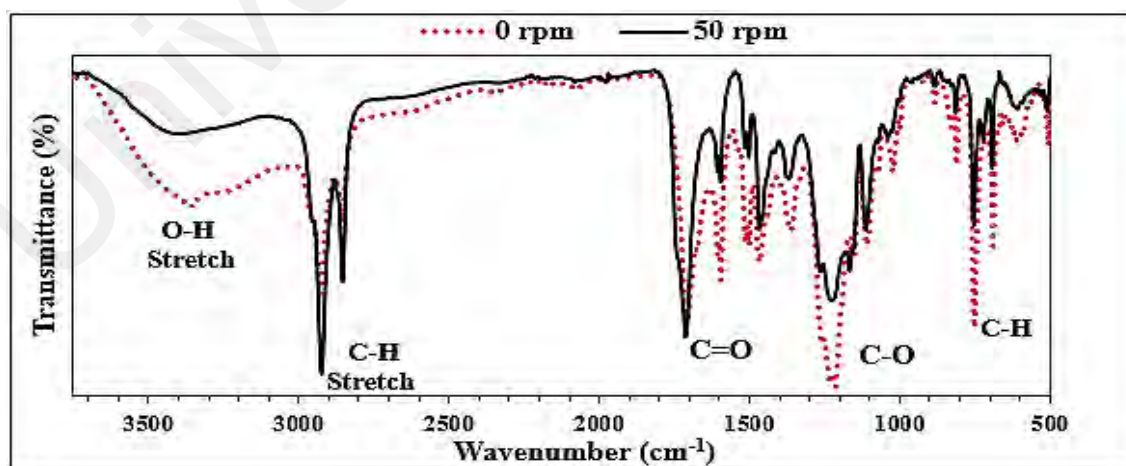


Figure 4. 4: FTIR spectra of the bio oil (organic phase) attained at 0 and 50 rpm torque.

The FTIR results indicated that the quality of bio-oil (organic phase) improved when the process performed by using the helical screw at 50-rpm torque. Among the compounds present, phenol is the major compound detected at the O-H stretching vibration between 3200 to 3600 cm^{-1} that was caused was by the phenol and alcohol group in bio-oil organic phase. Mostly, phenols are responsible to the thermal instability since high O_2 content in the bio-oil product [16].

Table 4. 5: Functional group compositions of bio-oil (organic phase) derived from palm shell.

Group	Absorbance (cm^{-1})	Class of compounds
Alcohols/ Phenol	3200 - 3600	O–H Stretch
Alkanes	2950 - 2800	C–H Stretch
Ketone	1760 - 1658	C=O Stretch
Carboxylic acids	1320 - 1135	C–O Stretch
Aromatics	900 - 675	C–H Bend

Figure 4.4, shows that the significant improvement was clearly observed when phenol was remarkably reduced at 50 rpm because it can enhance the energy density of the liquid product [211]. Apart from the sharp absorption peak from 2950 cm^{-1} to 2800 cm^{-1} with the C-H stretching vibration, the presence of alkanes increased in value when 50 rpm was used. Therefore, the increase in the alkane group can be explained by the helical screw that improved the mass and heat transfer rate of the feed and cracked more bonds that influenced the fuel quality as shown in Table 4.5. However, when 0-rpm condition was applied, a blunt alkane peak was observed. The second major peak occurred between 1750–1658 cm^{-1} , thus indicating the presence of the ketone group that signifies the CO stretching vibration. The third corresponding strongest peaks from 1320–1135 cm^{-1} revealed the

presence of the carboxylic acid group with the CO stretching vibration. The fourth major peak represents the aromatic group in the low frequency region from 900 cm^{-1} to 675 cm^{-1} , thereby indicating the CH bending vibration.

4.1.5.3 GC/MS analysis of liquid product

The results of GC/MS analysis show that alcohol was the highest chemical group detected in the organic phase, followed by alkyls, aromatics, aldehydes, alkenes, ketones, and carboxylic acids. Table 4.6 shows that the alcohol group significantly contributed to the oxygenated compounds in the bio-oil at $>50\%$ and was dominated by phenol at 48% . However, the total of alcohols was drastically reduced from 58% to 39% when the helical screw was used at 50-rpm . The phenomenon of the oxygenated compound reduction can also be observed for furfural compounds (aldehydes), wherein no furfural compound was detected in the organic phase that was produced at the 50-rpm condition.

An increase in hydrocarbon-based chemicals also became an important analysis. The increase in hydrocarbon-based chemicals was clearly observed for alkyls and alkenes. The total increase in alkyls from 11% to 19% was observed, whereas a significant increase in alkenes was recorded from 4% to 7% . Alkyls are advantageous for high-quality bio-oils due to their high carbon and hydrogen contents that bring the favorable effect of HHV improvement [212]. Moreover, the high percentage area of aromatics was also observed for the organic phase produced at the 50-rpm condition. The greatest proportion of aromatics was mainly derived from toluene at 18% .

Table 4. 6: Main compounds detected by GC/MS analysis of bio-oil (organic phase) attained at 0 and 50 rpm.

Identified compounds and group	Chemical Formula	Relative content (%)		Identified compounds and group	Chemical Formula	Relative content (%)	
		0 rpm	50 rpm			0 rpm	50 rpm
Aromatics				Ketones			
Toluene	C ₇ H ₈	9.649	18.664	Cyclohexanone	C ₆ H ₁₀ O	0.514	1.521
1,2,4-Trimethoxybenzene	C ₉ H ₁₂ O ₃	1.019	ND	7-Oxabicyclo[2.2.1]heptane	C ₆ H ₁₀ O	0.572	1.245
Benzene, 1,2,3-trimethoxy-5-methyl-	C ₁₀ H ₁₄ O ₃	1.122	ND	7-Oxabicyclo[4.1.0]heptane	C ₆ H ₁₀ O	0.513	1.846
Total		11.790	18.664	2-Cyclopenten-1-one, 2-methyl	C ₆ H ₈ O	0.173	ND
Alkyls				Total		1.772	4.612
Heptane	C ₇ H ₁₆	0.376	0.644	Alkenes			
Cyclohexane, methyl-	C ₇ H ₁₄	5.791	9.542	Cyclohexene	C ₆ H ₁₀	4.072	7.899
Cyclopentane, ethyl-	C ₇ H ₁₄	2.145	3.555	2-Hexene, 4-methyl-, (E)-	C ₇ H ₁₄	0.532	ND
Norbornane	C ₇ H ₁₂	3.230	5.635	Total		4.604	7.899
Cyclopentane, 1,2-dimethyl-, cis-	C ₇ H ₁₄	ND	0.381	Aldehydes			
Total		11.542	19.757	5-Hexenal	C ₆ H ₁₀ O	3.157	7.738
Alcohols				Hexanal	C ₆ H ₁₀ O	0.256	0.552
Cyclohexanol	C ₆ H ₁₂ O	0.678	1.665	Furfural	C ₅ H ₄ O ₂	4.597	ND
Phenol	C ₆ H ₆ O	48.305	37.782	Total		8.010	9.068
Phenol, 2-methyl-	C ₇ H ₈ O	1.973	ND	Carboxylic acids			
Phenol, 2-methoxy-	C ₇ H ₈ O ₂	2.961	ND	Dodecanoic acid, methyl ester	C ₁₃ H ₂₆ O ₂	1.312	ND
Creosol	C ₈ H ₁₀ O ₂	1.104	ND	Dodecanoic acid	C ₁₃ H ₂₆ O ₂	0.175	ND
Phenol, 4-ethyl-2-methoxy-	C ₉ H ₁₂ O ₂	1.218	ND	2,4-Hexadienedioic acid, 3,4-diethyl-, dimethyl	C ₁₂ H ₁₈ O ₄	0.730	ND
Phenol, 2,6-dimethoxy-	C ₁₁ H ₁₄ O ₃	1.907	ND	Methyl tetradecanoate	C ₁₅ H ₃₀ O ₂	0.463	ND
Phenol, 2,6-dimethoxy-4-(2-propenyl)-	C ₁₁ H ₁₄ O ₃	0.096	ND	Total		2.680	0.0
Total		58.242	39.447	Grand Total (%)		98.64	99.44

4.1.5.4 Characterization of bio-oil (organic phase) for fuel properties

Pyrolysis oil is derived from thermal degradation of biomass must be tested for fuel specifications before it is used in turbines, boilers and in automobiles [213]. Focusing on these bio-oil applications, some of the fuel properties of bio-oil rich organic phase attained from 0- and 50-rpm were tested for flash point, fire point, dew point, pour point, HHV and LHV under ASTM standards, and Table 4.7 presented results.

Table 4. 7: Characterization of bio-oil (organic phase) for fuel properties.

Condition	Flash Point	Fire point	Dew point	Pour point	HHV	LHV
					(°C)	
0 rpm	69	78	80	12	36.96	33.69
50 rpm	60	70	65	7	43.73	41.03

Table 4.7 shows that the fuel properties of bio-oils were different between the liquids produced at 0- and 50-rpm conditions. The values of flash, fire, dew, and pour points were higher in the liquid produced at 0 rpm compared with those at 50 rpm. The flash point values of 0 and 50-rpm were significant at 69°C and 60°C, respectively. The low flashpoint of the 50-rpm sample showed high fuel volatility and high energy content, which may provide support in fuel ignition. The low fire point of 70°C obtained at the 50-rpm condition indicates that the liquid contains increased volatiles and has good fuel ignition properties due to the high energy density [214]. The dew and pour points of the liquid produced at the 50-rpm condition were low at ~65°C and ~7°C, respectively. Furthermore, the LHV of the liquid organic phase samples with 0- and 50-rpm conditions were significant at 33.69 and 41.03 MJ/kg, respectively. The increment in LHV may be

due to the gradual decrease of water content when the reactor was operated at 50 rpm. These values are consistent with the literature and comparable to those of diesel fuel oil [215]. This study proves that the use of HSFBR increases not only the liquid yield but also improves the fuel properties, such as flash point and LHV, of the liquid organic phase.

4.1.5.5 Characterization of the by-products

Table 4.8 lists the characterization results of by-product char produced at 0 and 50 rpm with low heating rate of 10°C holds the higher carbon content with 60.12% and 57.45%, respectively. These results were higher compared with those from the fast pyrolysis of the biomass. Funke et al. [216] attempted to summarize the data from two different process scenarios related to the fast pyrolysis of the three different types of biomasses and observed that the carbon content can be obtained in the range of 43 wt.% to 49 wt.%. The high carbon percentage is important because it can contribute to increasing the HHV of char. Moreover, the use of the HSFBR can also reduce the ash content contained in the char by-product. Table 4.8 shows clearly that ~40% of the ash content in the char by-product was decreased when the HSFBR operated at a speed of 50 rpm. The low ash content is important if the char is considered for use as a solid fuel. Briefly, this study shows that the HSFBR can maintain the char quality similar to that produced from slow pyrolysis and reduce the ash content significantly.

Furthermore, the yield of the gas by-product decreased when the helical screw rotation speed was adjusted at the optimum condition (50 rpm). The researchers agree that the gas composition obtained from the pyrolysis process is dependent on the

composition of the feedstock used. In general, the gas product released during wood pyrolysis contains CO, CO₂, H₂, CH₄, C₂H₄, C₃H₆, and minor amounts of other hydrocarbons. Based on the literature and our previous study [217, 218]; the main gas components detected from the pyrolysis of palm shell at 500°C were CO, CO₂, and CH₄. The CO and CO₂ tended to produce at low temperature (150°C - 350°C), whereas CH₄ was released at high temperatures.

Table 4. 8: Ultimate and proximate analysis of by-product char obtained at 0 and 50 rpm.

Characteristics	Char value	
	0 rpm	50 rpm
Ultimate analysis (wt. %)		
C	60.12	57.45
H	9.21	9.62
N	0.42	0.28
S	0.92	0.67
O (by difference)	29.33	31.98
Proximate analysis (wt. %)		
Moisture content	2.9	2.2
Fixed carbon	82.6	74.3
Volatile matter (by difference)	10.5	21.1
Ash	4.0	2.4
HHV (MJ/kg)	31.3	27.5
LHV (MJ/kg)	29.3	25.4

4.1.5.6 FTIR analysis of by-product char

Figure 4.5 shows the FTIR spectra of by-product char at 0 and 50-rpm conditions have shown similar chemical groups. FTIR spectrum of by-product char at 0 rpm showed higher concentration of OH groups (greater intensity of the band at 1416 cm⁻¹) and a lower concentration of aromatic C=C (decreased intensity in the bands at 872–744 cm⁻¹) as compared to 50 rpm by-product char. The CH aromatic bands at 872-744 cm⁻¹ were also weaker due to the deformation of the adjacent H. In addition, the intensity of the

carboxyl group band at $1578\text{-}1760\text{ cm}^{-1}$ was decreased in the by-product char samples, possibly due to the degradation of the cellulose components during the pyrolysis. These results are attributed by higher level of oxygen content in 0 rpm by-product char consequently resulting the higher content of volatiles in the sample.

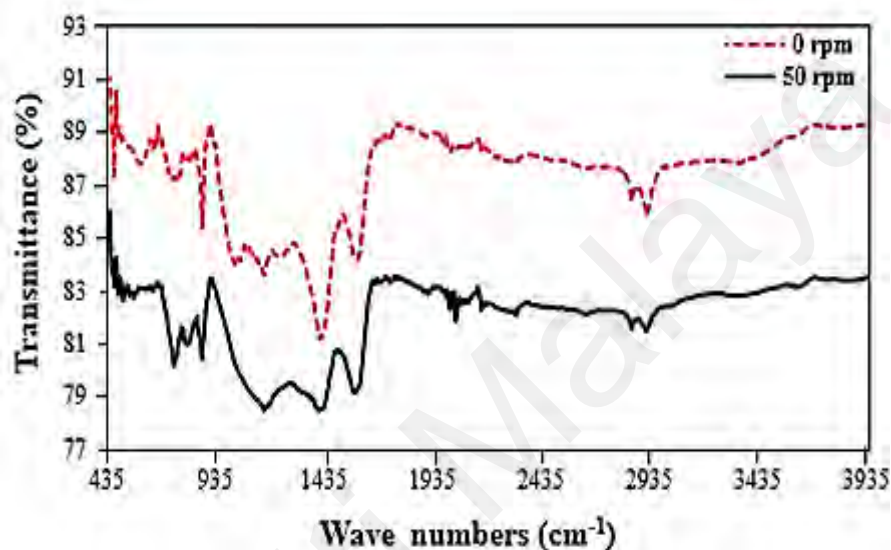


Figure 4. 5: FTIR spectra of by-product char obtained at 0 and 50 rpm condition.

However, by-product char produced with 50-rpm showed a decline in absorbance at $2313\text{-}2320\text{ cm}^{-1}$ ($\text{C}\equiv\text{C}$) compared to the spectra obtained from 0-rpm char product. On the other hand, the FTIR spectral intensity of $\text{C}\equiv\text{C}$ (alkynes) absorbance ($2313\text{-}2320\text{ cm}^{-1}$) was increased in carbonaceous chars, feasibly due to dehydrogenation. In addition, the intensities of the bands at $1578\text{-}1500\text{ cm}^{-1}$ for aromatic $\text{C}=\text{C}$ and adjacent H deformation were significantly higher in the by-product chars, which indicated the cracking of volatiles and conversion of aliphatic to aromatic compounds. This conversion can be attributed by extensive decrease in the intensities of the OH and CH alkyl peaks. The O-H stretching vibrations at $3600\text{-}3100\text{ cm}^{-1}$ in the FTIR spectra of the produced by-product

char were nearly absent after the carbonization process, probably due to the dehydration of the biomass together with the release of a large amount of water .

4.1.5.7 TGA/DTG analysis of by-product char

Figure 4.6 demonstrates the TGA curve and Figure 4.7 represents the DTG curve of by-product char obtained at 0 and 50-rpm. According to TGA of by-product char obtained at 0 rpm indicated four major weight loss curves that can be clearly shown in Figure 4.6.

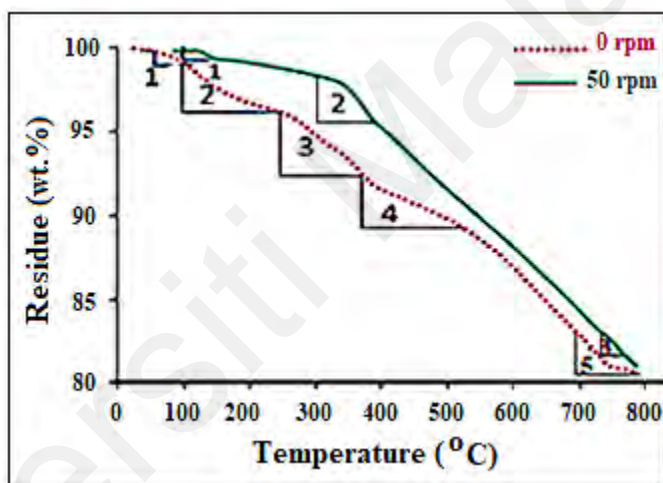


Figure 4. 6: Thermogravimetric analysis of by-product char obtained at 0 and 50 rpm.

The first and the second weight loss curves were observed at a temperature of 85°C and 125°C, respectively indicating the exclusion of moisture content and volatile matter. Whereas, the third curve is more prone to degradation of remaining hemicellulose and cellulose at 256°C. However, the fourth curve depicted substantial weight loss at 465°C which replicates the degradation of hemi cellulose and extent of lignin present in the char sample [219]. While, fifth degradation curve from 700-800°C revealed the complete decomposition of lignin with 98 % weight loss.

The TGA profile of by-product char sample attained with 50-rpm condition showed two adjacent weight loss curves from 100-150°C and one minor curve in temperature range from 700 to 800°C. The two adjacent weight loss curves from 100-150°C owing the removal of moisture content and volatiles. While, from 300-400°C temperature accounting the weight loss of total mass corresponds to cellulose present in the by-product char. Furthermore, no significant decomposition curve from 400 to 700°C was observed. While, minor weight loss noticed in temperature range of 700 to 800°C which is devoted to lignin content in the by-product char.

The DTG was performed to determine the thermal degradation behavior of remaining cellulose, hemicelluloses and lignin content in the by-product char obtained at 0 rpm and 50 rpm are shown in Figure 4.7.

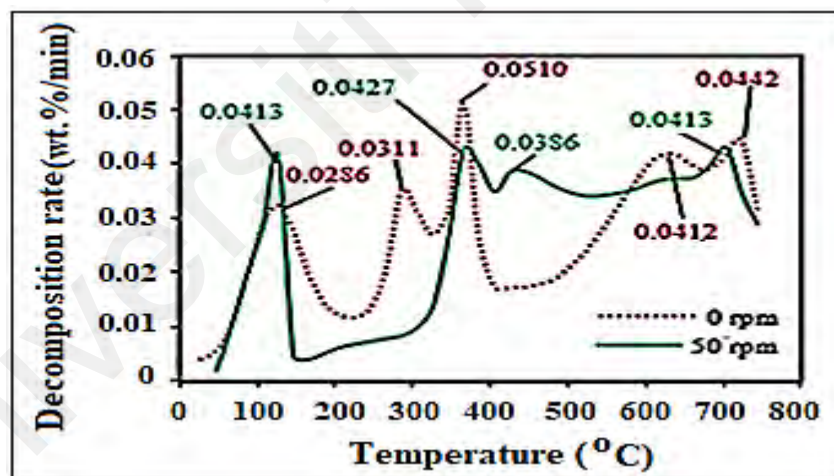


Figure 4. 7: DTG analysis of by-product char obtained at 0 and 50 rpm.

The DTG profile of by-product char with 0 rpm condition illustrated the degradation with five sharp peaks at different temperatures 145, 285, 365, 645 and 705°C with decomposition rate of 0.286, 0.031, 0.051, 0.041 and 0.044 wt. %/min, respectively. The initial decomposition rate from 145 to 200°C with 0.286 wt. %/min is related to the

hemicellulose. The main decomposition of by-product char with 0.031, 0.051, 0.041 and 0.044 wt. %/min occurred in the temperature range from 145°C to 600°C due to the remaining hemicellulose, cellulose and lignin at 0 rpm and can be explained by the low heat transfer rate due to stationary bed condition. Previous studies have been also shown the major weight loss of hemicellulose and cellulose occurred between 200–300°C due to fixed bed condition [220]. Furthermore, a significantly higher decomposition rate was observed at 365°C with 0.051 wt. %/min due to less conversion of lignin when pyrolysis was performed with fixed bed condition at 0 rpm.

Nevertheless, DTG curves at 50 rpm showed four main peaks at 125, 365, 445 and 705°C with low decomposition rates of 0.041, 0.042, 0.038 and 0.041 wt. %/min, respectively. The decomposition rate of 50 rpm by-product char was sharply decreased from 100 to 400°C due to more conversion of hemicellulose, cellulose and lignin to bio oil when pyrolysis was performed with helical screw with 50-rpm condition at 500°C. The low decomposition rate of lignin with 0.038 and 0.041 wt. %/min was noticed between 400 to 750°C. Thus, it can be determined that at 0 rpm by-product char indicated that the biomass was not sufficiently decomposed due to the static bed condition. While, minimum decomposition rate of by-product char at 50 rpm was observed due to helical screw which increased the bed particle dynamic and heating rate during the pyrolysis.

4.2 Part 3: Pyrolysis of Palm Shell using Helical Screw-Fluidized Bed Reactor: Effect of Heating Rate.

4.2.1 Phase separation

Figure 4.8 shows the phase separation process of liquid product obtained at heating rates of 75, 100, 125, 150, 175, 200, 225, 250 and 275°C/min.

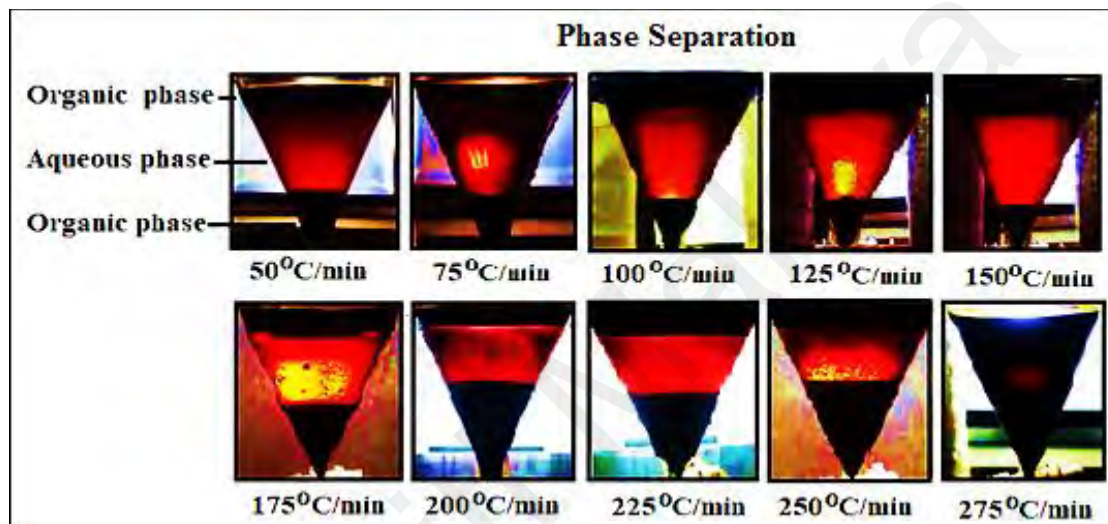


Figure 4. 8: Phase separation of bio-oil under the influence of polar affinity and gravity.

The bio-oil received at first hand was dark brown in color, viscous and free-flowing liquid with pungent smell. Phase separation process showed that, the liquid was divided into three layers with the top and bottom layers demarcated as the organic layers while the middle layer as the aqueous layer. The reason behind multilayers is attributed by the difference in density and the existence of oxygenated compounds in the liquid product. Therefore, bio-oil have a polar affinity and formed redistribution of the different phases [221]. Similar observation of three phases were also reported elsewhere due to differences of solubility or affinity between the two phases [222].

Furthermore, Table 4.9 depicted organic and aqueous phases quantified based on low (50, 75, 100, 125), medium (150, 175, 200) and high (225, 250 and 275°C/min) heating rates. For low pyrolysis heating rates (50 to 125 °C/min), the organic phase was obtained as from 25.23 to 28.14 wt.%, while the aqueous phase was noticed little higher from 30.61 to 34.21 wt.% in contrast to organic phase. The higher amount of aqueous phase in the bio-oil is due to the presence of moisture in the biomass and dehydration reactions during the pyrolysis [223].

Table 4. 9: Distribution and quantification of the bio-oil yield based on the type of phase.

Heating rate (°C/min)	Top Organic	Bottom Organic	Total Organic (wt. %)	Aqueous	Bio-oil yield
50	8	17.23	25.23	30.16	55.39
75	9	16.61	25.61	35.85	61.46
100	10.6	15.52	26.12	35.75	61.87
125	11.5	16.64	28.14	34.47	62.61
150	11	21.24	32.24	34.21	66.45
175	9	24.98	33.98	32.25	66.23
200	8.5	25.55	34.05	31.93	65.98
225	11	23.01	34.01	34.43	68.44
250	11	23.51	34.51	34.98	69.49
275	20.01	22.2	42.21	30.63	72.84

For medium heating rates (150 to 200°C/min), the organic phase was marginally increased from 28.14 wt.% to 34.05 wt.% while decrease in aqueous phase was observed from 34.21 wt.% to 31.93 wt.%. The increase in heating rate enabled sufficient disintegration of heavy lignin molecules present in the biomass. At high heating rates (225 to 275°C/min), higher organic yields were obtained from 34.01 wt.% to 42.21 wt.% and bio-oil from 68.44 wt.% to 72.84 wt.% was obtained. For fuel production, organic phase is the desired product, since it has high calorific value as compared to aqueous phase. Wang et al. also described that organic phase from pyrolysis of biomass can be upgraded to be used as transport fuel [224]. While, there is no evidence for usage of aqueous phase in fuel application or any

other use in the literature. This might be due to the high-water extent in aqueous phase which is an unfavorable property for bio-oil, thus receiving lesser attention for further research on its liquid fuel production. However, several aromatic compounds are still remaining in the aqueous phase; therefore, this area needs to be researched to maximize the liquid fuel recovery [225].

4.2.2 Influence of heating rate on product yields.

The influence of heating rate is summarized in Table 4.10. At low heating rates, bio-oil yield was gradually increased from 55.39 to 61.87 wt.% while byproduct biochar yield was slightly reduced from 35.45 wt.% to 24.32 wt.%. Likewise, Jordan et al. also informed that when heating rate was increased, the quantity of bio-oil was significantly increased [226]. These results indicated that when reactor was operated with low heating rate, a small increase in by-product biochar and minor reduction in gas yield were noticed. Bridgwater et al. also studied the effects of heating rate and noticed that when heating rate was increased from 20 to 100°C/min the bio-oil and gas yields were evidently increased, while by-product biochar yield was decreased [227, 228].

Table 4. 10: Influence of heating rate on pyrolysis yields.

Mode	Heating rate (°C/min)	Organic	Aqueous	Total Oil (wt. %)	By-product Biochar	Gas
Low	50	25.23	30.16	55.39	35.45	9.16
	75	25.61	35.85	61.46	25.65	12.89
	100	26.12	35.75	61.87	24.32	13.81
Medium	125	28.14	34.47	62.61	23.83	13.56
	150	32.24	34.21	66.45	19.21	14.34
	175	33.98	32.25	66.23	19.52	14.25
High	200	34.05	31.93	65.98	19.61	14.41
	225	34.01	34.43	68.44	15.87	15.69
	250	34.51	34.98	69.49	14.00	16.51
	275	42.21	30.63	72.84	11.98	15.18

At medium heating rates, bio-oil yield increases from 62.61 to 66.23 wt.%, by-product biochar yield decreased from 23.83 to 19.52 wt.% and gas yield was slightly increased from 13.56 to 14.25 wt.%. At high heating rates, bio-oil yield was further improved from 65.98 to 72.84 wt.% due to the rapid decomposition of biomass and quick release of volatiles. In addition, enrichment in volatiles is mainly because of extra tar decomposition at high heating rates [229]. Similar trend was also reported by Akhtar et al. where high heating rates cause quick release of volatile due to rapid endothermic decomposition of biomass to obtain higher liquid yield. Li et al. also described that increasing bio-oil yield may be due to the high heating rate which converts the biomass into more volatiles [230].

Present study shows the major improvement in formation of organic yield was basically linked with increasing heating rate as reported by Bridgwater [231]. Thus, standard deviation of bio-oil yield was found as $SD = 4.9$ due to the wide variation in heating rates. Therefore, high heating rate is essential to transform biomass to get more bio-oil yield.

4.2.3 Characterization of bio-oil

4.2.3.1 Physico-chemical properties of bio-oil at different heating rates

Heating rate has been found to significantly modify the composition and physicochemical properties of bio-oil which includes: density, viscosity, pH and water content. Physicochemical properties of bio-oil were measured at ambient temperature. Table 4.11 shows the effect of heating rate on physicochemical properties of bio-oil samples. In general, the density of bio-oil is higher than that of water/aqueous phase

which shows that it holds heavy fractions in the bio-oil [232]. The content of energy in bio-oil depends on its physicochemical properties such as density. The typical range of density of pyrolytic oil starts from 1000 to 1240 kg/m³ at 15 to 40°C [233]. Table 4.11 shows the minimum density of bio-oil organic phase was found to be around 1040 kg/m³ with low heating rate of 50°C/min, when the heating rate was increased to 75 and 100°C/min the density of bio-oil was consistently increased to 1042 and 1050 kg/m³, respectively. The increasing of density value is due to the presence of heavy hydrocarbon fractions in the bio-oil which might decrease the bio-oil quality.

Table 4. 11: Physico-chemical properties of bio-oil at different heating rates

Heating rate (°C/min)	Density (kg/m ³)	Viscosity (cP) @ 20 rpm	pH	Water content (wt. %)
50	1040	21.5	2.8	4.71
75	1042	25.2	2.5	4.68
100	1050	26.4	2.6	4.68
125	1050	27.4	2.6	4.60
150	1051	29.9	2.5	4.63
175	1052	29.9	2.6	4.04
200	1052	29.9	2.4	4.00
225	1055	29.9	2.6	3.43
250	1054	29.5	2.5	2.48
275	1053	29.9	2.6	2.44

At medium and high heating rates, there was only a small increase in density from 1050 to 1054 kg/m³. On the other side, a slight decrease in density from 1054 kg/m³ to 1053 kg/m³ was also noticed when heating rate was increased to 275°C/min. This small reduction in bio-oil density is attributed to the rapid decomposition of vapors and converted to plasma state. Kilinger et al. also indicated that the plasma decay of bio-oil vapors ionizes the hot gas-phase molecular compounds that typically condensed at downstream as liquid product and subsequently being swept out from the reactor outlet which thus decreases the bio-oil density [234].

Table 4.11 depicts that, at low heating rate of 50°C/min, viscosity of bio-oil is 21.5 cP. This low viscosity is due to the existence of water in organic phase produced by lignin decomposition. Nevertheless, by increasing the heating rate from 50 to 150°C/min, viscosity gradually increased from 21.5 to 27.4 cP, respectively. This increase was due to higher organic fraction in organic phase. Most of the researchers agreed that the increase in bio-oil viscosity is due to quick evolution of volatiles and removal of water content from the bio-oil [187]. This finding was supported by our results of water content analysis as shown in Table 4.11. Nevertheless, the viscosity of bio-oil organic phase was slightly decreased to 31 cP with 175-275°C/min heating rate. The decrease in viscosity can be due to the water content produced during lignin degradation at higher heating rates. Similar finding was also discussed by Yang et al. that, the presence of water content at high heating rate might reduce the viscosity of bio-oil [235].

Bio-oil acidity can be in pH range of 2.0 to 3.0 [236] due to the presence of carboxylic acids [237]. Table 4.11 represents the minimum and maximum pH value of liquid organic phase which is in the range of 2.4 to 2.8 obtained at different heating rates and is consistent with our previous findings [183]. The pH value was 2.8 at the heating rate of 50°C/min and as the heating rate was increased from 75 to 125°C/min the pH value was slightly reduced to 2.5 - 2.6 which could be due to the degradation of hemicellulose which might added the carboxylic acid in the bio-oil [238]. However, by further increasing the heating rate from 150 to 275°C/min, pH value remained in the range of 2.4 to 2.6.

Water content in pyrolysis oil mainly arises from bounded moisture present within the feedstock. While another source could be due to the dehydration reaction of

carbohydrates, subsequent formation of anhydrosugars such as levoglucosan and other glucopyranosides, and secondary reactions that occurred in the existence of inorganic components [226]. The purpose of investigation on the water content in the organic phase is to improve the bio-oil quality for fuel properties as presented in Table 4.11. Based on Table 4.11, the high-water contents in organic phase for low heating rates were quantified about 4.71 wt.% to 4.68 wt.% which would lead to adverse effects on calorific value, fuel stability, viscosity, pH and other liquid properties of bio-oil. Likewise, disadvantages of water content in bio-oil were also reported by Jahirul et al [239].

A slight decrease in water content from 4.60 wt.% to 4.04 wt.% was noted for medium heating rates. This is credited to the slight decomposition of oxygenated compounds. In addition, a further decrease in water content in bio-oil organic phase with high heating rates was observed from 4.04 to 2.44 wt.%. This decrease in water content is qualified by decomposition of biomass to volatiles through high heating rate. Wang et al. also described that in order to improve the bio-oil quality one may consider the reduction in water content, oxygenated compounds and acid content in bio-oil product [240].

4.2.3.2 Ultimate analysis of bio-oil at selected heating rates

It is emphasized that the use of increasing heating rate can improve the quality of organic phase, especially on the carbon and oxygen contents. Table 4.12 summarizes the results of ultimate analysis with selected heating rates.

Table 4. 12: Ultimate analysis of bio-oil at selected heating rates.

Heating rate (°C/min)	Ultimate analysis of bio-oil (organic Phase)					
	C	H	N	S	O*	HHV (MJ/kg)
50	71.6	10.0	7.3	0.8	0.3	41.97
150	76.8	12.4	9.5	0.9	0.4	43.79
275	77.4	12.7	8.8	0.9	0.2	44.41

* = by difference.

Results of ultimate analysis showed a significant change in bio-oil composition with increasing heating rate from 50°C/min to 275°C/min. The carbon content was noticeably increased from 71.6% to 77.4% while the oxygen content was reduced from 0.3% to 0.2% which might improve the calorific-value of bio-oil. Leng et al. also clarified that a low oxygen content in bio-oil improves the calorific-value [223]. These results showed that an increase in heating rate has improved the decomposition of PS biomass and produced more high molecular weight components like sugar and decreased the oxygen content. Sugar resulting from cellulose principally contributes about 67–79 wt.% in the bio-oil and the rest of the sugars are derived from hemicellulose [241]. This finding is supported by the result of the water content analysis, where the water content was reduced from 4.71% to 2.44% with 275°C/min higher heating condition and a higher degree of cross-linking high molecular weight components. Correspondingly, Sonil et al. reported that higher heating rate specified a higher degree of cross-linking and occurrence of high molecular weight components [242]. By increasing heating rate from 50°C/min to 275°C/min the endothermic reaction was improved, the maximum breakdown of biomass material provided high pyrolysis vapor/gas production [243]. Thus, HHV value of organic phase was improved from 41.97 MJ/kg to 44.41 MJ/kg which is comparative

with the HHV of diesel fuel (45 MJ/kg) [244]. For the reliability of results, standard deviation for HHV is found to be $SD = 1.28$. These results revealed good performance of novel helical screw fluidized bed reactor at low, medium and high heating rates.

4.2.3.3 FTIR analysis of bio-oil at different heating rates

Figure 4.9 shows the FTIR spectra of bio-oil organic phase attained with low, medium and high heating rates of 50, 150 and 275°C/min whereas Table 4.13 lists the recognized functional groups during this study.

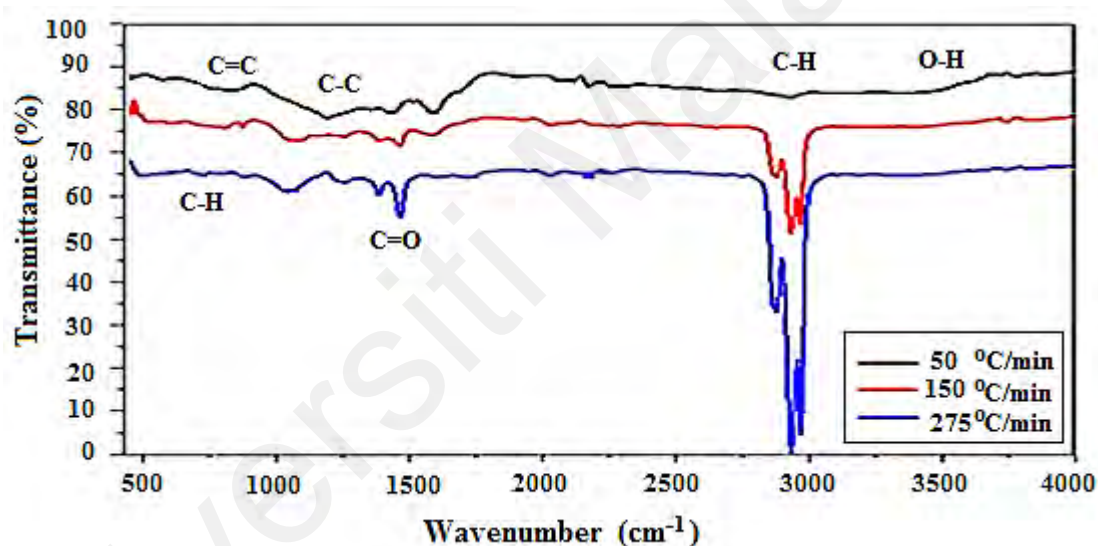


Figure 4. 9: FTIR spectra of the bio-oil (organic phase) attained at different heating rates.

The results of FTIR indicated that the quality of organic phase was significantly improved when the heating rate was gradually increased from 50 to 275°C/min. Between the 3200 cm⁻¹ to 3500cm⁻¹ low O-H stretching vibration attributed to the presence of phenol group in bio-oil organic phase. Generally, phenols are liable to thermal instability due to the high oxygen content in the liquid product [198]. The results of FTIR analysis clearly showed the substantial improvement when phenol was progressively decreased

as the heating rate was increased, since it can increase the liquid density [223] can be referred from Table 4.11 and HHV of the liquid product can be stated from Table 4.12.

Table 4. 13: Functional group composition of the bio-oil (organic phase) derived from PS.

Group	Absorbance (cm ⁻¹)	Class of compounds
Alcohols and Phenol	2600-3000	O-H Stretch
Alkenes	2850-3000	C-H Stretch
Ketones, aldehydes and carboxylic acid	~1750	C=O Stretch
Aromatic and alkenes	1400- 1500	C-C Stretch
Aromatics and alkenes	~750	C=C Stretch
Alkynes	~600	C-H Bending

The second most important and major peak at 2850-3000 ascribed the presence of alkenes group with C-H stretching. The third peak at 1750 cm⁻¹ indicated the presence of Ketone, aldehydes and carboxylic acid group that signifies the C=O stretching vibration. Beside that a fourth absorption peak from 1400 cm⁻¹ to 1500 cm⁻¹ with C-H stretching vibration indicated the presence of aromatic and alkenes compounds. Therefore, increase in aromatic group can be explained by the higher heating rate and high particle dynamics provided by helical screw which improved the mass and heat transfer rate of feed and cracked the more bonds which has influence on the fuel quality more specifically HHV that can be seen from Table 4.12. The fifth corresponding peak ~750 cm⁻¹ which revealed the presence of aromatics and alkenes with C=C Stretch stretching vibration. While the sixth peak represents the alkynes group in the low frequency region ~600 cm⁻¹ which specified the C-H bending.

4.2.3.4 GC-MS analysis of bio-oil

Results of GC/MS analysis of bio-oil attained with optimum heating rate of 275°C/min are shown in Table 4.14. The results of this analysis indicated the highest proportions of possible compounds were dodecanoic acid, trans-1,4-hexadiene, cyclohexane, methyl- and aromatic phenol-based compounds with 25.60 %, 9.30%, 9.43% and 8.65%, 5.28%, respectively. The total concentration of carboxylic acids was the highest around 39.47% in the organic phase. Due to the acidity of carboxylic acids in bio-oil it is corrosive and has adverse effect on engine and fuel properties which might reduce the HHV and cause corrosion to engine. Therefore, for upgradation of bio-oil through hydrodeoxygenation route by suitable catalyst is mandatory to get good quality fuel. In this regard, zeolites and alumina-based catalysts were extensively used in the upgrading of bio-oil for biofuel production [245-249]. Hence, more research is required to exploit the real potential of bio-oil as a green and renewable fuel [250]. Furthermore, the second major group in bio-oil was clearly observed for alkenes and alkynes with 20.90% and 14.68 %, respectively. Among these chemical components, phenolics, alkenes and alkynes are advantageous for high-quality bio-oils due to their high carbon and hydrogen contents that bring the favorable effect in HHV improvement [212]. The presence of these groups indicating the suitability of the oil to be considered for value-added chemicals. In addition, it is possible to eliminate the oxygenates from bio-oil to obtain higher-quality liquid fuel [251-254].

Table 4. 14: GC/MS analysis of bio-oil attained with optimum heating rate of 275°C/min.

GC/MS analysis of (organic phase) for major compounds			
	Identified compounds and group	Chemical Formula	Relative content (%)
	Esters		
1	Hexadecanoic acid, methyl	C ₁₆ H ₃₂ O ₂	5.378
2	9-Octadecenoic acid (Z)-, methyl	C ₁₉ H ₃₆ O ₂	2.199
3	Benzoic acid, perhydroquinolin-4-yl	C ₁₆ H ₂₁ NO ₂	1.688
4	Methyl stearate	C ₁₉ H ₃₈ O ₂	1.148
5	Octanoic acid, 4-tridecyl	C ₁₉ H ₃₈ O ₂	1.122
6	2-Octynoic acid, methyl ester	C ₉ H ₁₄ O ₂	1.065
7	Octadecanoic acid, propyl	C ₂₁ H ₄₂ O ₂	0.628
8	Dodecanoic acid, methyl ester	C ₁₃ H ₂₆ O ₂	0.259
	Total		13.487
	Carboxylic acid		
9	Dodecanoic acid	C ₁₂ H ₂₄ O ₂	25.606
10	Tetradecanoic acid	C ₁₄ H ₂₈ O ₂	3.460
11	cis-Vaccenic acid	C ₁₈ H ₃₄ O ₂	3.015
12	Methyl tetradecanoate	C ₁₅ H ₃₀ O ₂	2.785
13	2,4-Hexadienedioic acid, 3,4-diethyl-, dimethyl	C ₁₂ H ₁₈ O ₄	2.098
14	Octadecanoic acid	C ₁₈ H ₃₆ O ₂	1.206
15	cis-11-Eicosenoic acid	C ₂₀ H ₃₈ O ₂	1.165
16	3,5-Dimethoxy-4-hydroxyphenylacetic acid	C ₁₀ H ₁₂ O ₅	0.131
17	Allogibberic acid	C ₁₈ H ₂₀ O ₃	0.005
	Total		39.471
	Alkenes		
18	Cyclohexene	C ₆ H ₁₀	9.432
19	trans-1,4-Hexadiene	C ₆ H ₁₀	9.304
20	2-Hexene, 4-methyl-, (E)-	C ₇ H ₁₄	2.166
	Total		20.902
	Alkyl		
21	Cyclohexane, methyl-	C ₇ H ₁₄	14.231
22	Tridecane, 7-cyclohexyl-	C ₁₉ H ₃₈	0.45
	Total		14.681
	Aldehyde		
23	5-Hexenal	C ₆ H ₁₀ O	5.606
24	Cyclopentane acetaldehyde, 2-formyl-3-methyl-.alpha	C ₁₀ H ₁₂ O ₃	0.275
25	3,4-Hexadienal, 2-butyl-2-ethyl-5-methyl-	C ₁₃ H ₂₂ O	0.231
26	Benzaldehyde, (2,4-dinitrophenyl) hydrazone	C ₁₃ H ₁₀ N ₄ O ₄	0.059
	Total		6.171
	Phenol		
27	Phenol, 2,6-dimethoxy-	C ₈ H ₁₀ O ₃	3.923
28	Phenol, 2,6-dimethoxy-4-(2-propenyl)-	C ₁₁ H ₁₄ O ₃	1.365
	Total		5.288
	Grand Total		100

4.2.3.5 Characterization of bio-oil for fuel properties

Pyrolysis oil or bio-oil derived from thermal degradation of biomass must be tested for fuel properties before it is used as energy source in vehicles, boilers and turbines [213]. Focusing on these bio-oil applications, some of the fuel properties of bio-oil organic phase obtained at 50, 150 and 275°C/min heating rate were tested for fire point, flash point, dew point, pour point and HHV under ASTM standards are summarized in Table 4.15.

Table 4. 15: Characterization of bio-oil (organic phase) for fuel properties.

Heating rate (°C/min)	Fire point	Flash Point	Dew point (°C)	Pour point	HHV (MJ/kg)
50	72	66	69	9	41.79
150	67	64	66	8	43.79
275	65	60	63	6	44.41

Table 4.15 shows that the fuel properties of bio-oils organic phase were altered between the liquids formed at different heating rates. The values of fire, flash, dew, and pour points were higher in the liquid produced with 50°C/min heating rate compared with those at 275°C/min. The low fire point of 65°C attained with high heating rate of 275°C/min designates that the liquid covers adequate volatiles and presented good fuel ignition properties due to the high energy density [214]. The flash point values at 50°C/min and 275°C/min heating rate were at 66°C and 60°C, respectively. The low flashpoint at 275°C/min heating rate sample showed high fuel volatility and high energy content, which may give improved sustenance of the fuel ignition. The dew and pour points of the liquid attained at a heating rate 275°C/min were lower: 63°C and ~6°C, respectively. Furthermore, the HHV of the organic phase attained with 50°C/min and 275°C/min heating rate were 41.79 MJ/kg and 44.41 MJ/kg, respectively. The increment

in HHV may be due to the gradual decrease of water content when the pyrolysis was performed at 275°C/min heating rate. These values are consistent with the literature and comparable to those of diesel fuel oil [215]. In the light of these results this study proves that the use of HSFBR with 275°C/min heating rate increased not only the liquid yield but also improved the fuel properties, such as flash point and HHV of the bio-oil organic phase.

4.2.4 Characterization of by-products

4.2.4.1 Ultimate and proximate analysis of biochar

Table 4.16 lists the characterization results of by-product biochar produced at 50, 150 and 275°C/min heating rates. Remarkable results were obtained from the characterization of char by-product. The low pyrolysis mode mainly produces the by-product biochar, and its quality is normally higher than that of high pyrolysis by-product biochar.

Table 4. 16: Ultimate and proximate analysis of by-product biochar with different heating rates.

Characteristics	By-product biochar value		
	Heating rate (°C/min)		
	50	150	275
Ultimate analysis (wt. %)			
C	60.12	57.45	53.64
H	9.21	9.29	14.13
N	0.42	2.28	3.98
S	0.92	0.67	0.02
O (by difference)	29.33	30.31	28.23
Proximate analysis (wt. %)			
Moisture content	2.9	2.2	2.9
Fixed carbon	20.5	21.1	20.94
Volatile matter (by difference)	72.6	74.3	73.96
Ash	4.0	2.4	2.2
HHV (MJ/kg)	24.89	28.33	33.43
LHV (MJ/kg)	22.86	26.32	31.62

The results showed that carbon content of by-product biochar decreased when heating rate increased. Qian et al. indicated that, low pyrolysis has been shown to retain the highest biomass carbon content in the by-product biochar [255]. It can be observed that, the higher percentage of carbon in by-product char is essential, since it can contribute to increasing the HHV [256]. Moreover, the use of HSFBR with increasing heating rate have also reduced the ash content contained in the by-product biochar. The low ash content is important because it increases the energy output if the biochar is considered as a solid fuel [257]. Concisely, this study demonstrates that the HSFBR with higher heating rate can maintain the by-product char quality similar to that produced with low heating rate and decrease the ash content considerably.

4.2.4.2 FTIR analysis of biochar

Figure 4.10 shows the FTIR spectra of by-product biochar derived from PS attained with low, medium and high heating rates of 50, 150 and 275°C/min.

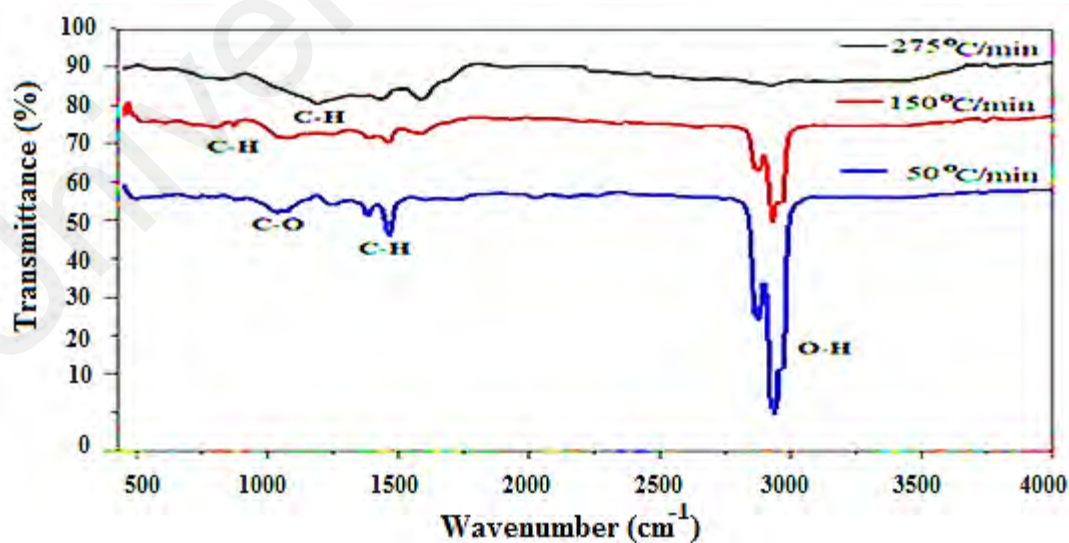


Figure 4. 10: FTIR spectra of the by-product biochar attained at different heating rates.

All biochars were found to have similar chemical groups. Table 4.17 represents the functional group composition of the by-product biochar derived from PS.

Table 4. 17: Functional group composition of the biochar derived from Palm Shell.

Group	Absorbance (cm ⁻¹)	Class of compounds
Alcohols/ Phenol	2750-3000	O-H Stretch
Aromatics	1450-1550	C-H Stretch
Alcohols	1000-1100	C-O Stretch
Alkynes	~600	C-H Bending

FTIR spectrum of by-product biochar with heating rates of 50°C/min showed the highest concentration of OH groups with intensity of the band in the range of 2750-3000 cm⁻¹, while a lower concentration of O-H group at 150 and 275°C/min heating rate was noticed. The C-H stretch at 1450-1550 cm⁻¹ were also weaker in 150 and 275°C/min due to the deformation of the adjacent C-O stretch. In addition, the intensity of alcohol group C-O stretch from 1000-1100 cm⁻¹ was higher in 50°C/min heating rate, while it was clearly reduced in the by-product biochar samples attained at 150 and 275°C/min. This may be due to the rapid degradation of the cellulose components and formation of vapors with increasing heating rates during the pyrolysis. Furthermore, very minor peak of C-H bending of alkynes group at 600 cm⁻¹ was observed at 50°C/min heating rate, however it was not detected in 150 and 275°C/min samples. These results are attributed to the formation of high content of volatiles during the high pyrolysis.

4.2.4.3 TGA/DTG analysis of biochar

The TGA/DTG analysis was performed to estimate the decomposition rate of PS by-product char at different conditions. Figure 4.11 shows (a) TGA analysis and (b) DTG peaks of by-product char attained at 50, 150 and 275°C/min heating rates. According to TGA analysis, four major weight loss curves can be clearly seen in all three samples.

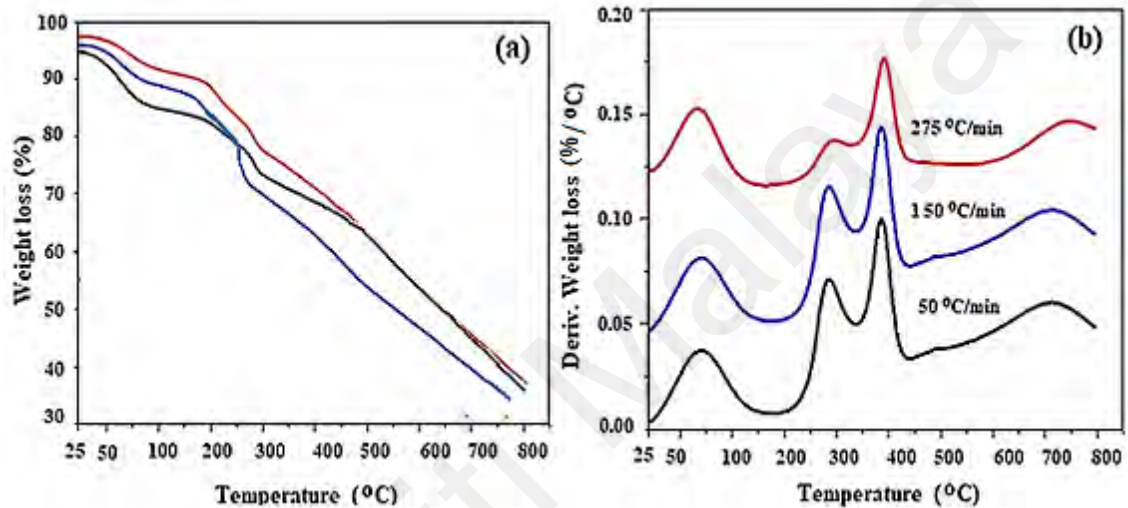


Figure 4. 11: (a) TGA analysis and (b) DTG analysis of bio-char attained at 50, 150 and 275°C/min heating rate.

The first and the second major weight loss curves were observed at a temperature of 100°C and 300°C, respectively showing the elimination of moisture content and volatile matter with 5% and 10% weight loss, respectively. The third curve is more inclined to disintegration of residual hemicellulose and cellulose in by-product char at 340-400°C with 50% weight loss. However, the fourth curve depicted substantial weight loss between 500-700°C which replicates the degradation of hemicellulose with 70% weight loss and extent of lignin present in the by-product biochar sample which further continued to complete the decomposition of lignin with 98% weight loss [219]. The DTG analysis of by-product biochar samples with 50, 150 and 275°C/min heating rate showed

the thermal degradation behavior of remaining cellulose, hemicelluloses and lignin content as shown in Figure 4.11 (b) and details of this analysis are summarized in Table 4.18.

Table 4. 18: DTG analysis of bio-char at different heating rates.

Peak No.	Heating rate (°C/min)			Peak Temperature (°C)	Content
	50	150	275		
	Derivative weight loss (%/°C)				
1	0.04	0.04	0.03	50	Moisture
2	0.06	0.06	0.02	150	Cellulose
3	0.10	0.09	0.06	200–300	Hemicellulose
4	0.53	0.05	0.04	700-800	Lignin

The DTG profile of by-product biochar with 50°C/min heating rate illustrated the high degradation rates followed by 0.04, 0.06, 0.10 and 0.53 wt.%/min, respectively of by-product biochar with four sharp peaks at different temperatures can be seen from Table 4.18. The first weight loss peak is due to moisture content while the second and third peak was due to cellulose and hemicellulose degradation. Earlier studies also revealed that the major weight loss of hemicellulose and cellulose take place from 200–300°C [220]. Furthermore, the fourth peak indicates that the lignin decomposition at elevated temperature from 700-800°C. Nevertheless, the decomposition rate of by-product biochar attained at 150°C/min heating rate depicted slightly less degradation rates with 0.04, 0.06, 0.9 and 0.05 wt.%/min, respectively. The low decomposition rates with 0.03, 0.02, 0.06 and 0.04 wt.%/min, respectively were also noticed for 275°C/min heating rate. This considerable decrease in degradation rate is attributed by high heating rate which decomposed the cellulose, hemicellulose and lignin during the pyrolysis process. Thus, it can be determined that by-product biochar produced via higher heating rate contains has a significantly lower lignin proportion.

4.2.4.4 Analysis of gas product

The vapor that is condensed in the cooling device is called bio-oil, and those vapors which are not condensed are non-condensable gas mixture that contains commonly CO, CO₂, H₂, and CH₄. The researchers agreed that the gas composition obtained from the pyrolysis process is dependent on the composition of the feedstock used [217, 218]. The gas composition and non-condensable gas yields attained at 50, 150 and 275°C/min heating rates are summarized in Table 4.19.

Table 4. 19: Distribution of gas products of PS at different heating rates.

Non-condensable gases	Heating rate (°C/min)		
	50	150	275
	Yield (wt. %)		
CO	2	2.1	4.17
CO ₂	0.8	2.2	4.5
H ₂	2.2	3.9	5.13
CH ₄	4.16	5.14	6.38
Total	9.16	13.34	20.18

PS with heating rate of 50°C/min showed the less production of non-condensable gas. It was described in the literature that gas formation can be assigned to high hemicellulose content in the biomass feed [258]. The increase in gas yield about 4.18 wt.% signifies the influence of increasing heating rate 150°C/min which improved the decomposition and formed more volatiles and increased the gas yield during pyrolysis. Besides, the gas yield was further increased from 13.34 to 20.18 wt.% when 275°C/min heating rate was applied. The gas produced from the pyrolysis of biomass has a significant calorific value; thus, it can be potentially used as gaseous fuels or to compensate the total energy requirements of the pyrolysis unit [258].

4.3 Part 4: Effect of temperature and feed rate on pyrolysis oil produced by novel helical screw fluidized bed reactor

4.3.1 Phase separation

Bio-oil derived at different temperatures showed differences in color shown in Figure 4.12. The bio-oil initially appeared as single-phase dark brown, viscous free flowing liquid with strong bitter smell. The presence of water in the bio-oil is due to existing moisture in the biomass and dehydration and degradation of lignin during pyrolysis [259].



Figure 4. 12: Phase separation of bio-oil with various temperatures under the influence of gravity.

Phase separation showed that, the liquid was divided into two layers and then three layers based on the pyrolytic temperature. The black color represents the organic or hydrocarbon phase, while yellowish red layer represents the aqueous phase. These multilayers are due to the density variation and the presence of oxygenated compounds which is attributed by pyrolytic temperature difference, therefore, bio oils have a polar affinity and formed distinct phases [221]. Lu et al. also reported that multi layers were due to the variance in solubility or polar affinity among the different phases [222].

4.3.2 Product yields

4.3.2.1 Effect of Temperature

Table 4.20 shows the product distributions of bio-oil after pyrolysis at various temperatures.

Table 4. 20: Influence of temperature on bio-oil yields.

Temperature (°C)	Product distribution (wt. %)				
	Organic	Aqueous	Bio-oil*	Biochar	Gas
400	16.00	23.10	39.10	50.00	10.90
450	23.50	30.20	53.70	34.80	11.50
500	42.21	30.63	72.84	11.98	15.18
550	41.00	27.34	68.34	10.60	21.06
600	37.20	28.31	65.51	12.60	21.89
650	31.60	33.80	65.40	11.60	23.00

* Bio-oil = organic + aqueous

At 400°C, the bio-oil yield was relatively low with a value of 39.1 wt.%, while by-product biochar value was higher with 50 wt.%. The higher value of by-product biochar can be attributed to the less decomposition of cellulose between 300-450°C [260]. As the temperature increased to 450°C, bio-oil yield increased to 53.7 wt. % while by-product biochar yield decreased from 50 to 34.8 wt.%. This could be attributed to the breaking of glycoside chain of polysaccharide which provides tar production. Similar effects of temperature at 450°C on product distribution are reported elsewhere [261]. Bio-oil yield drastically increased to 72.84 wt.% when temperature reached to 500°C and this could be attributed to the lignin decomposition between 250-500°C which is the major contributor of liquid at the end of pyrolysis [262, 263]. Conversely the by-product biochar yield was drastically reduced to 22.82 wt.%, while gas yield was slightly increased by approximately 3.68 wt.%. Similar trend was also reported by Bridgewater et al. [149] and Powar et al. [264]. However, a more increase in temperature to 550°C

caused reduction to some extent in bio-oil yield to 1.38 wt.% while the gas product yield increased to 5.88 wt. %. This variation in liquid and gas yields can be explained by the onset of secondary cracking of vapors at 550°C which resulted in decline of the liquid product yield and increase in the non-condensable gas yield [198]. Similar trend is observed as temperature was further increased to 650°C and was also reported by Powar et al. [264] According to Bridgwater et al., pyrolysis at adequate temperature of around 500°C with short vapor residence time of up to 2 s is desirable to avoid the secondary reactions in vapor phase in order to produce high liquid product [149, 265]. In addition, the effect of secondary reaction in vapor phase on bio-oil composition requires further investigation [266].

4.3.2.2 Effect of feed rate

The results of this study in Table 4.21 showed that when feed rate was approximately about 3 g/min the bio-oil, by-product biochar and gas yields are 70.73, 23.32 and 5.95wt.% respectively.

Table 4. 21: Effect of feed rates on pyrolytic yields.

Feed Rate (g/min)	Product distribution				
	Organics	Aqueous	Total Bio-oil	Char	Gas
	(wt.%)				
3	44.56	26.17	70.73	23.32	5.95
5	45.26	23.13	68.39	27.56	4.05
7	45.06	23.24	68.30	26.32	5.38
10	45.11	23.73	68.84	24.45	6.71
13	44.12	24.78	68.90	22.45	8.65
15	46.08	24.79	70.87	20.23	8.90
18	47.03	24.81	71.84	21.33	6.83
20	45.28	24.81	70.09	21.33	8.58
23	48.21	24.63	72.84	14.98	12.18
25	46.26	26.66	72.92	13.30	13.78

However, when the feed rate is in the range of 3-13 g/min it was observed that the liquid, by-product biochar and gas yields were relatively constant. This may be attributed by high heat transfer rate at low feed rate which resulted in faster devolatilization, leading the formation of gas and vapors. In addition, at low feed rate it may decrease the movement of pyrolytic vapor and boosts the secondary reaction which decrease the bio-oil yield [243]. This implies that fluidization with helical screw has resulted in high heat and mass transfer rate therefore reaction rates was not affected by the slow feed rates. These findings are comparable with previous studies performed with different feed rates [267]. However, by introducing more PS biomass feed rate above 13 g/min, a noticeable increase in bio-oil, gas yields and decrease in by-product biochar yield is observed. However, the formation of more condensable vapors and gas product with high feed rate is because of reduction in the vapor residence time inside the reactor, thus preventing from secondary cracking reactions which lead to the a higher bio-oil yield [268]. Heo et al. also reported that, low feed rate resulted in low bio-oil yield, while the higher feeding rates were seemed to be more promising for the production of bio-oil attributable to the low vapor residence times [269, 270].

4.3.3 Characterization of bio-oil

4.3.3.1 Effect of temperature on physicochemical properties of bio-oil.

The typical range of bio-oil density is from 1000 to 1240 kg/m³ at 15 to 40°C [233]. Based on Table 4.22, it can be seen that as pyrolysis temperature increased from 400-650°C, the density of bio-oils improved from 1089-1150 kg/cm³ and as the bio-oil density increases, the content of energy also increases. This result is in agreement with

the results obtained by Bardalai et al. The increase in density is related to increase in pyrolysis temperature and decrease in residence time which provided further biomass breakdown and more vapors [233].

Table 4. 22: Effect of temperature on physicochemical characteristics of bio-oil (organic phase).

Temperature (°C)	Density (kg/m ³)	Viscosity (cP) 20 rpm	pH	Water content (wt.%)
400	1089	14.6	2.6	4.7
450	1130	18.8	2.6	4.6
500	1150	25.6	2.9	2.4
550	1130	23.4	2.6	2.5
600	1126	21.3	2.8	2.4
650	1123	18.5	2.9	2.5

Tanvidkar et al. described that, the development of high liquid density product at high temperatures is linked to low residence time [271]. Viscosity, pH and water content are also important properties of bio-oil, which determine the flow quality or fluidity of the liquid. The viscosity of the bio-oil varies in a wide range as it is produced from various biomasses at different temperatures [272]. The viscosity, pH and water content of bio-oil in this work are ranging from 14.6-25.6 cP, 2.6-2.9 and 2.7-4.7 wt.%, respectively.

The results depicted a significant decrease in water content from 4.7-2.4 as higher pyrolysis temperature promotes further lignin dehydration. Qiang et al. found that, the high amount of water content present in the bio-oil lead to phase separation between aqueous phase and heavier organic phase which makes it difficult to be burnt [273]. Furthermore, high water quantity in the bio-oil can lower the heating value of the liquid, increase the ignition delay and decrease the combustion rate by decreasing adiabatic

flame temperature. Therefore, it is essential to control the water or moisture content to be below 10 wt.% [243, 274].

4.3.3.2 Effect of feed rate on physicochemical properties of bio-oil.

The effect of feed rate on the product distribution and bio-oil characteristics entirely depends on the particle size, feed rate, reactor configuration [268] and condensation system [233].

Table 4. 23: Effect of feed rate on physicochemical characteristics of bio-oil at 500°C.

Feed rate (g/min)	Density (kg/m ³)	Viscosity (cP) at 20 rpm	pH		Water content (wt. %)
			Organic phase		
Low	3	1089	15.8	2.7	6.4
	5	1120	16.6	2.8	5.5
	7	1120	16.9	3.0	4.3
Medium	10	1124	17.8	2.7	4.2
	13	1124	23.3	3.0	4.2
	15	1124	21.9	3.0	4.1
High	18	1127	22.9	3.1	4.0
	20	1170	23.3	3.1	3.9
	25	1254	23.8	3.6	2.5

Based on Table 4.23, it can be observed that that there is an increase in density, viscosity, pH and decrease in water content of bio-oil which indirectly improve the quality of bio-oil. In this HSFBR setup, fluidization efficiency, feed rate and residence time were all directly correlated and affected by the auger speed of the feeding system. With the increase in feed rate, fluidization effect was further increased which leads to better reactant mixing and pyrolysis efficiency to produce bio-oil of higher quality and quantity. In similar vein to this, PS biomass would also have lower residence time which minimizes secondary cracking reactions in producing gaseous products. The decrease in water content might be due to decrease in carbonyls that can be confirmed from GC-MS

analysis. This result is in agreement to the findings of Chung et al. [275]. The maximum density was observed at high feed rate from 18-25 g/min with high density from 1127-1254 kg/m³, viscosity 22.9-23, pH 3.1-3.6 and a decrease in water content from 4.0-2.5 wt.%.

4.3.3.3 Ultimate analysis of bio-oil at different temperatures

Table 4.24 summarizes the results of ultimate analysis at temperatures of 400, 500 and 650°C. The results showed that the HHV of bio-oil at 400°C was the lowest and this could be attributed to the low decomposition of biomass [276]. However, at temperature above 400°C, extensive biomass disintegration was noted which lead to higher de-volatilization of polymers and tar formation [277].

Table 4. 24: Ultimate analysis of bio-oil (organic phase) at different temperatures.

	Temperature (°C)	Ultimate analysis of bio-oil (Organic phase) (%)					HHV (MJ/kg)
		C	H	N	S	O*	
Low	400	71.60	10.37	14.7	0.03	3.30	38.52
Medium	500	76.80	11.40	8.37	0.03	3.40	41.83
High	650	79.55	11.83	6.16	0.03	2.43	43.13

* = by difference.

The higher value of HHV at 500°C could be attributed to the biomass decomposition that enhance the bio-oil quality. Hossain et al. showed that the increasing temperature improved the percentage of carbon content and HHV [278]. Similar effects of HHV by increasing the pyrolysis temperature have been reported elsewhere [259]. Therefore, when the temperature was further increased from 500°C to 650°C to a slight increase in HHV of bio-oil from (41.83 to 43.13MJ/kg) was observed. This can be attributed to the increase of carbon and hydrogen content as well as a noticeable decrease

of oxygen content as can be seen in Table 4.24. Anguruwa et al. reported that, the yield of bio-oil reduced with the increase in temperature, while calorific value increased with the increase in pyrolysis temperature.

4.3.3.4 Ultimate analysis of bio-oil at different feed rates

The feed rate can effect on the fluidization behavior and physicochemical properties of the liquid product. Table 4.25 reviews the results of ultimate analysis of bio-oil at selected low, medium and high feed rates.

Table 4. 25: Ultimate analysis of bio-oil (organic phase) at 500°C with different feed rate.

	Feed rate (g/min)	Ultimate analysis of bio-oil (Organic phase)					
		C H N S O*					HHV (MJ/kg)
Low	3	76.66	10.23	6.43	0.13	6.55	39.12
Medium	15	78.90	10.21	6.58	0.02	4.29	40.24
High	25	81.80	11.40	3.37	0.03	3.40	43.09

* = by difference.

The relationship between elemental properties and the biomass feed rate shows that HHV, carbon and hydrogen contents were increased while nitrogen, sulfur and oxygen contents were decreased when feed rate was increased. These improvements can be attributed to an adequate heat transfer rate from reactor shell to biomass particle interaction that was delivered by helical screw before biomass particles exit from the reactor hot zone. This result is consist with the findings of Guedes et al who described that feed rate correlates with the HHV [268]. Xiong et al. reported that, the lower feed rate may decrease pyrolytic vapor formation and movement which led to secondary cracking reactions, thus changing the elemental composition and physicochemical properties of bio-oil.

4.3.3.5 FTIR analysis of bio-oil attained at different temperatures and feed rates

Figure 4.13 (a) shows the FTIR spectra of bio-oil (organic phase) at pyrolysis temperatures of 400, 500 and 650°C and Figure 4.13 (b) shows the FTIR spectra of bio-oil (organic phase) at feed rates of 3, 15 and 25 g/min, respectively. The identified functional groups in bio-oil are summarized in Table 4.26.

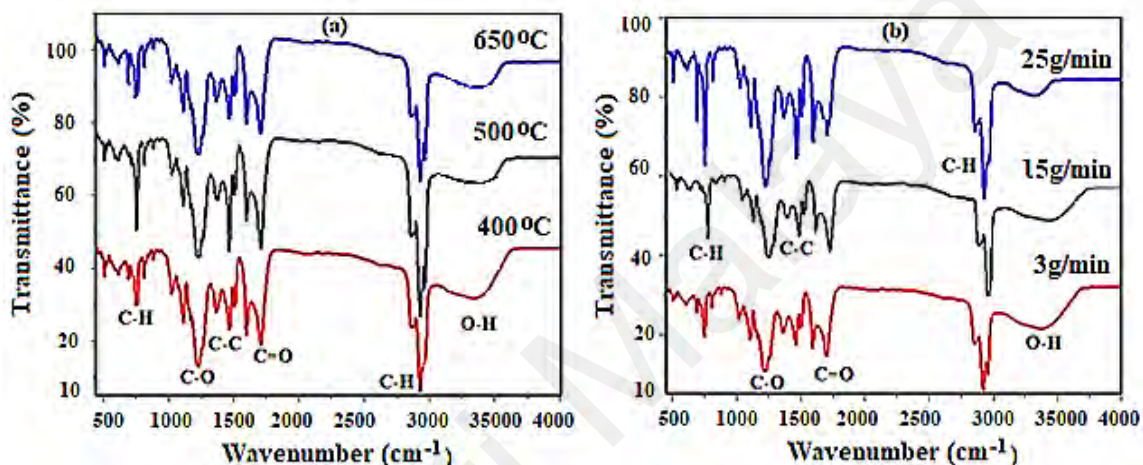


Figure 4. 13: FTIR spectra of organic phase attained at different (a) Temperatures and (b) Feed rates.

Table 4. 26: Functional group composition of the bio-oil (organic phase) attained at different temperatures and feed rates.

Group	Wavenumber (cm ⁻¹)	Class of compounds
Alcohols/ Phenols	3000-3500	O-H Stretch
Aromatics	2700 -3000	C-H Stretch
Ketones	~1750	C=O Stretch
Aromatics	~1500	C-C Stretch
Carboxylic	1200-1300	C-O Stretch
Aromatics	~750	C-H medium stretch

The FTIR band assessment indicated the organic phase consists of a number of atomic groups and structures. Band intensities reveal that the most abundant chemical bonds are O–H, C–C, C=O and C–H bonds. The FTIR spectrum of organic phase

obtained at 400, 500 and 650°C indicated O–H stretching vibration between 3000 cm^{-1} to 3500 cm^{-1} which is recognized by phenol group. Generally, phenols are liable for the thermal and chemical instabilities of bio-oil due to the high oxygen content in the liquid product [198, 252-254, 279]. The positive effect in reducing the phenol content will go to helical screw which provided high heat transfer rate and increased temperature from 400 to 500°C.

Furthermore, a considerable decrease in phenol and increase in aromatics were observed [279], since it can produce value-added chemicals such as aldehydes, acids which improved the energy density and HHV [259]. The results are in corroboration with ultimate analysis presented in Table 4.25. According to the Lyu et al. high temperature supports the formation of small aldehydes and acids, accompanied by a reduction of phenols [280]. Beside that a sharp absorption peak at 500°C from 1400–1500 cm^{-1} with C-H stretching vibration indicates the presence of alkanes which is high in contrast to the ones obtained at 400 and 650°C. The 1750 cm^{-1} band is ascribed to C=O stretching vibration in ketone shows the presence of acetyl derivative and aldehyde group [281]. The 1500 cm^{-1} band relates to C–C stretching, indicating the presence of aromatics. The peak in the range from 1200-1300 cm^{-1} with C–O stretching indicates the presence of carboxylic acid. The peak intensity increased when the temperature was increased to 650°C. Besides that, a medium C–H stretch was noticed which specifies the existence of aromatics at low frequency region of 750 cm^{-1} .

The O-H stretching vibration between 3000 cm^{-1} to 3500 cm^{-1} of phenol group showed a substantial reduction when feed rate was increased from 3 g/min to 25 g/min. This decrease in phenol group mainly attributed to the nascent char which cracked the

oxygenated compound. Hu et al. described that, the nascent char inside the reactor can serve as the catalyst which initiates the secondary cracking of phenol containing vapors and resulting in secondary formation of the bottom organics [207]. Besides that, C-H, C-C, C-O and C=O peaks at 750 cm^{-1} , 1500 cm^{-1} , $1200\text{-}1300\text{ cm}^{-1}$, 1750 cm^{-1} bands were shown to increase in peak intensity with the increase in feed rate, indicating higher formation of alkanes, aromatics, ketones and carboxylic acids at higher feeding rate. This improvement in aromatics is due to the extra decomposition of lignin caused by helical screw rotation which increased the particle-particle and particle-reactor shell interaction during the pyrolysis.

4.3.3.6 GC-MS analysis of bio-oil obtained at different temperatures

The results of GC/MS analysis of bio-oil obtained at 400, 500 and 650°C are shown in Table 4.27. Mostly aromatics, alkyls, alcohols, phenols were detected in the samples. The results of this analysis indicate the highest value of possible compounds in alkyls were heptane, methylcyclohexane, ethyl cyclopentane, norbornane and cis-1,2-dimethylcyclopentane respectively. However, at 400°C a high number of oxygenates such as: cyclohexanol, phenol, 2-methylphenol, 2-methoxyphenol, creosol, 4-ethyl-2-methoxyphenol and 2-,6-dimethoxyphenol were produced. The oxygenates content was reduced with the increase in pyrolysis temperature. From the results it is evidently appeared that 500°C is optimal temperature to obtain good product quality [282]. Between these chemical constituents, alkenes, aromatics and alkyls are valuable for high-quality bio-oils because of high carbon and hydrogen contents that bring the positive effect in HHV enhancement [212]. The existence of these groups signifying the

suitability of the oil to be considered for value-added chemicals (e.g., alkyls, aromatic, and alkenes) in bio-oils. In addition, it is necessary to exclude the oxygenates from bio-oil via catalytic upgrading processes such as hydrodeoxygenation, decarboxylation and decarbonylation to improve its energy content [246, 251, 252, 283].

Universiti Malaya

Table 4. 27: GC/MS analysis for the identification of compound existing in bio-oil (Organic phase) achieved at 400, 500 and 650°C.

Identified compounds and groups	Chemical Formula	Relative content (%)			Identified compounds and groups	Chemical Formula	Relative content (%)		
		Temperature (°C)					Temperature (°C)		
		400	500	650			400	500	650
Aromatics					Ketones				
Toluene	C ₇ H ₈	13.12	18.59	16.64	Cyclohexanone	C ₆ H ₁₀ O	2.51	1.32	1.52
Benzene, 1,2,4-trimethoxy-	C ₉ H ₁₂ O ₃	2.32	1.21	2.01	7-Oxabicyclo[2.2.1]heptane	C ₆ H ₁₀ O	2.57	1.03	1.24
Benzene, 1,2,3-trimethoxy-5-methyl-	C ₁₀ H ₁₄ O ₃	2.53	1.54	1.12	7-Oxabicyclo[4.1.0]heptane	C ₆ H ₁₀ O	3.52	0.37	1.84
Total		17.97	21.34	19.77	2,5-Dimethylfuran	C ₆ H ₈ O	3.16	1.34	4.10
Alkanes					Total				
Heptane	C ₇ H ₁₆	3.45	7.61	6.37			11.76	4.06	10.38
Cyclohexane, methyl-	C ₇ H ₁₄	4.12	8.51	7.79	Alkenes				
Cyclopentane, ethyl-	C ₇ H ₁₄	3.23	6.53	7.53	Cyclohexene	C ₆ H ₁₀	4.07	5.62	6.21
Norbornane	C ₇ H ₁₂	1.56	3.62	1.23	2-Hexene, 4-methyl-, (E)-	C ₇ H ₁₄	2.53	7.77	6.12
Cyclopentane, 1,2-dimethyl-, cis-	C ₇ H ₁₄	3.85	4.38	4.61	Total		6.60	13.39	12.33
Total		16.21	30.65	27.53	Aldehydes				
Alcohols and Phenols					5-Hexenal	C ₆ H ₁₀ O	4.1	3.15	2.70
Cyclohexanol	C ₆ H ₁₂ O	1.68	1.67	1.12	Hexanal	C ₆ H ₁₀ O	1.1	0.25	0.57
Phenol	C ₆ H ₆ O	17.30	15.35	13.44	Furfural	C ₅ H ₄ O ₂	2.3	1.3	1.52
Phenol, 2-methyl-	C ₇ H ₈ O	1.31	2.12	1.12	Total		7.5	4.7	4.79
Phenol, 2-methoxy-	C ₇ H ₈ O ₂	1.96	-	1.34	Esters				
Creosol	C ₈ H ₁₀ O ₂	1.10	-	1.11	Dodecanoic acid, methyl ester	C ₁₃ H ₂₆ O ₂	4.31	1.87	1.34
Phenol, 4-ethyl-2-methoxy-	C ₉ H ₁₂ O ₂	1.21	0.11	0.87	2,4-Hexadienedioic acid, 3,4-diethyl-, dimethyl ester, (E,Z)-	C ₁₂ H ₁₈ O ₄	3.73	2.73	1.87
Phenol, 2,6-dimethoxy-	C ₈ H ₁₀ O ₃	1.90	-	-	Tetradecanoic acid, methyl ester	C ₁₅ H ₃₀ O ₂	5.46	2.01	2.99
Total		26.46	19.25	19.00	Total		13.50	6.61	6.20
Grand Total							100	100	100

4.3.3.7 GC-MS analysis of bio-oil at different feed rates

Table 4.28 shows the compositions of bio-oil from PS pyrolysis at different feed rates as analyzed via GC/MS. A total of seven groups including 29 kinds of major compounds were identified. When feed rate was increased, the yields of deoxygenated products (aromatics, alkanes, alkenes) were increased while the yields of oxygenated products (alcohols, phenols, ketones, esters, aldehydes) were decreased. In addition, the yield ratio of deoxygenated non-aromatics (alkanes and alkenes) to deoxygenated aromatics were 2.04, 3.52 and 3.70 at the respective feeding rates of 3, 15 and 25 g/min. These changes in liquid product composition at higher feed rate is attributed to the enhanced heat transfer rate by particle-particle and particle-reactor hot shell interaction which triggered the greater extent of ring opening, dehydration and cracking of heavy oxygenated aromatics molecule [284]. The increase in selectivity for deoxygenated non-aromatics at higher feed rate is a favorable trend in producing liquid fuel of better quality as deoxygenated non-aromatics have higher HHV than their aromatic counterparts [254].

Table 4. 28: GC/MS analysis of bio-oil (Organic phase) produced at different feed rates.

Identified compounds and groups	Chemical Formula	Relative content (%)			Identified compounds and groups	Chemical Formula	Relative content (%)		
		Feed rate (g/min)					Feed rate (g/min)		
		3	15	25			3	15	25
Aromatics					Ketones				
Toluene	C ₇ H ₈	5.89	6.30	10.38	Cyclopentenone	C ₅ H ₆ O	2.21	1.01	1.67
Benzene, 1,2,4-trimethoxy	C ₉ H ₁₂ O ₃	3.32	4.34	1.21	Cyclohexanone	C ₆ H ₁₀ O	2.51	1.52	1.32
Benzene, 1,2,3-trimethoxy-5-methyl-	C ₁₀ H ₁₄ O ₃	4.53	3.12	2.52	7-Oxabicyclo[2.2.1]heptane	C ₆ H ₁₀ O	2.57	1.24	1.03
Total		13.74	13.76	14.11	7-Oxabicyclo[4.1.0]heptane	C ₆ H ₁₀ O	3.52	2.84	1.37
Alkanes					2,5-Dimethylfuran	C ₆ H ₈ O	3.16	3.10	2.34
Cyclohexane	C ₆ H ₁₂	5.23	6.01	8.21	Total		13.97	9.71	7.73
Heptane	C ₇ H ₁₆	3.45	6.37	7.61	Alkenes				
Cyclohexane, methyl-	C ₇ H ₁₄	4.12	7.79	8.51	Cyclohexene	C ₆ H ₁₀	4.07	5.21	5.62
Cyclopentane, ethyl-	C ₇ H ₁₄	5.23	7.53	6.53	2-Hexene, 4-methyl-, (E)-	C ₇ H ₁₄	2.53	6.12	7.77
Norbornane	C ₇ H ₁₂	3.56	2.23	3.71	Total		6.6	11.33	13.39
Cyclopentane, 1,2-dimethyl-, cis-	C ₇ H ₁₄	3.85	4.61	4.38	Aldehydes				
Total		25.44	34.54	38.95	5-Hexenal	C ₆ H ₁₀ O	4.10	2.15	2.70
Alcohols and Phenols					Hexanal	C ₆ H ₁₀ O	0.57	1.25	1.27
Cyclohexanol	C ₆ H ₁₂ O	1.68	1.12	1.67	Furfural	C ₅ H ₄ O ₂	3.40	1.30	1.52
Phenol	C ₆ H ₆ O	15.30	13.44	10.43	Total		8.07	4.70	5.49
Phenol, 2-methyl-	C ₇ H ₈ O	1.31	1.99	2.12	Esters				
Phenol, 2-methoxy-	C ₇ H ₈ O ₂	1.96	1.34	3.12	Dodecanoic acid, methyl ester	C ₁₃ H ₂₆ O ₂	4.31	2.14	1.34
Creosol	C ₈ H ₁₀ O ₂	2.7	3.11	3.44	2,4-Hexadienedioic acid, 3,4-diethyl-, dimethyl ester, (E,Z)-	C ₁₂ H ₁₈ O ₄	3.73	2.73	1.87
Phenol, 4-ethyl-2-methoxy-	C ₉ H ₁₂ O ₂	1.21	0.87	3.86	Tetradecanoic, methyl ester	C ₁₅ H ₃₀ O ₂	4.68	2.01	2.99
Phenol, 2,6-dimethoxy-	C ₁₁ H ₁₄ O ₃	1.90	3.54	2.88	Total		12.72	6.88	6.20
Total		26.06	30.41	27.52	Grand Total		100	100	100

4.3.4 Characterization of by-product biochar

4.3.4.1 Effect of temperature on physicochemical properties of by-product biochar

Table 4. 29: Ultimate and Proximate analysis of by-product biochar with different temperatures.

Characteristics	Byproduct biochar value		
	Temperature (°C/min)		
	400	500	650
Ultimate analysis (wt. %)			
C	60.98	54.64	57.45
H	2.73	8.57	7.21
N	0.43	1.97	1.28
S	0.03	0.02	0.67
O*	35.83	34.8	33.39
Proximate analysis (wt. %)			
Moisture content	4.90	7.94	8.20
Volatile matter (by difference)	72.85	70.21	69.59
Fixed carbon	18.5	20.84	20.46
Ash	3.75	1.01	1.13
HHV (MJ/kg)	23.14	30.00	23.81
LHV (MJ/kg)	22.54	28.13	22.23

* = by difference

Table 4.29 shows that the by-product biochar obtained at 400°C has the carbon content around 60.12% and it has highest volatile matter of 72.85%. As pyrolysis temperature increases, to 500°C the carbon, oxygen and volatile matter contents were reduced. This is because a higher pyrolysis temperature enables higher volatilization of carbon and volatile matters in PS to form bio-oil instead of by-product biochar. Pyrolysis results at 500°C shows that by-product biochar produced has highest carbon content with significantly higher HHV 30 MJ/kg, since it can add the HHV [256]. These results are consistent with the results of Rafiq et al. for carbon stability of the by-product biochar attained at different temperatures [285]. Furthermore, FTIR analysis also confirmed the presence of more alkene, alkane and aromatics in the by-product biochar produced at 500°C. Thus, biomass pyrolysis temperature at 500°C produces maximum bio-oil as main product and by-product biochar that could be a promising approach of liquid and solid fuel production.

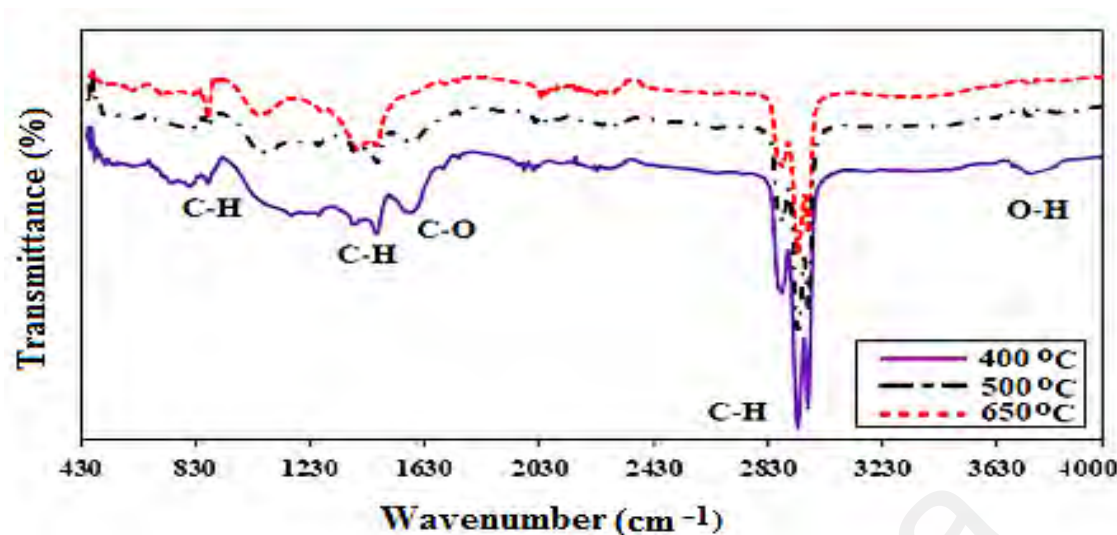


Figure 4. 14: FTIR spectra of the by-product biochar attained at different temperatures.

Table 4. 30: Functional group composition of the by-product biochar.

Group	Absorbance (cm ⁻¹)	Class of compounds
Alcohols/ Phenol	3640-3800	O-H Stretch
Alkanes	2924-2969	C-H Stretch
Carboxylic	1600-1630	C-O Stretch
Alkynes	~1500	C-H Stretch
Aromatics	~840	C-H Stretch

Figure 4.14 displays the FTIR spectra of by-product biochar derived from PS pyrolysis at 400, 500 and 650°C. FTIR spectrum of by-product biochar at 400°C showed significant O-H stretch intensity in the range of (3640-3800 cm⁻¹), while an increase in temperature caused a significant decrease in phenolics. Hamza et al. also reported similar trend and attributed it to the greater extent of hemicellulose and cellulose breakdown at higher pyrolysis temperature [286]. At higher pyrolysis temperature, the higher volatilization of PS biomass causes the carbon contents to be concentrated in the bio-oil instead of bio-char, causing a decrease in the carbon content of by-product biochar.

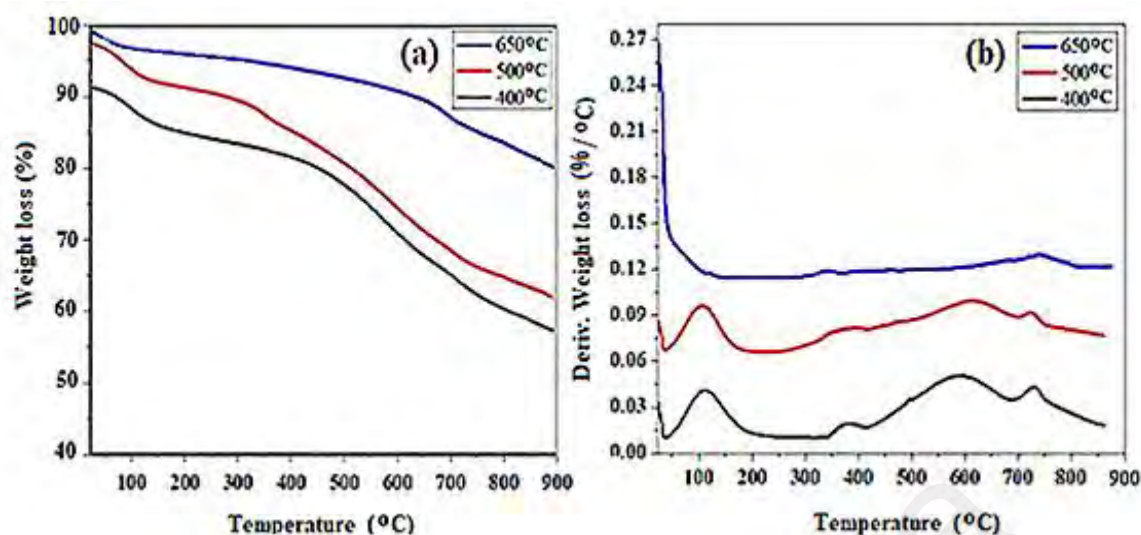


Figure 4. 15: (a) TGA analysis and (b) DTG analysis of by-product biochar obtained at 400, 500 and 650°C.

Table 4. 31: Detail of weight loss present of by-product biochar samples obtained at different temperatures.

Pyrolysis temperature (°C)	Weight loss (%)			Total weight loss (%)	Residue (%)
	1 (25-200 °C)	2 (200-700 °C)	3 (700-900 °C)		
400	12	25	10	36	64
500	7	10	3	20	80
650	5	2	2	9	91

Table 4. 32: DTG analysis of by-product biochar obtained at different temperatures.

Peak No.	Temperature (°C)			Temperature range (°C)	Content
	400	500	650		
Derivative weight loss (%)					
1	0.05	0.04	-	25-200	Moisture and volatile
2	0.02	0.02	0.003	200-430	Hemicellulose, cellulose and lignin
3	0.06	0.03	0.005	430-700	Hemicellulose, cellulose and lignin
4	0.05	0.01	-	700-750	Lignin

ND = Not Detected.

Based on Figure 4.15 and Table 4.31, the primary weight loss at temperature range of 25–200°C is attributed to the evaporation of moisture content. The second major weight loss at temperature range of 200–700°C corresponds to the decomposition of hemicellulose and lignin. The third major weight loss at temperature range of 700–900°C

corresponds to the further decomposition of lignin in by-product biochar. The second major weight loss shows the decomposition of hemicellulose, cellulose and lignin over a broad temperature range with smaller distinct DTG peaks which can be accounted for the respective decomposition of such components within this temperature range. Earlier studies also revealed the major weight loss of hemicellulose take place from 400–430°C [287, 288]. Biochar sample obtained at 650°C has the least weight loss since most of the biomass components have been converted to pyrolytic products within the bio-oil.

4.3.4.2 Effect of feed rate on physicochemical properties of by-product biochar

Table 4. 33: Ultimate and Proximate analysis of by-product biochar with different feed rates.

Characteristics	Byproduct char value		
	Feed rate (g/min)		
	5	15	25
Ultimate analysis (wt. %)			
C	60.98	57.45	54.64
H	8.73	8.21	6.57
N	0.42	1.28	1.97
S	0.03	0.67	0.02
O*	29.84	32.39	36.8
Proximate analysis (wt. %)			
Moisture content	10.20	10.94	11.90
Volatile matter*	67.45	67.21	65.85
Fixed carbon	20.46	19.51	19.50
Ash	1.89	2.34	2.75
HHV (MJ/kg)	27.83	25.43	21.32
LHV (MJ/kg)	25.92	23.64	19.88

* = by difference

Table 4.33 shows that the carbon, hydrogen contents and heating values were decreased when feed rate was increased. Higher feeding rate was indicated in the previous sections to improve volatilization of biomass components to form bio-oil which in turn reduces the available components within the biochar. The increase in oxygen content of by-product biochar at higher feed rate could also indicate the retention of oxygen during its catalytic cracking of oxygenates in bio-oil. Based on Figure 4.16, FTIR spectra shows

a decreasing trend in organics of biochar. A higher feed rate led to a higher volatiles thus increases bio-oil yield and reduces the by-product biochar and gas yield [289].

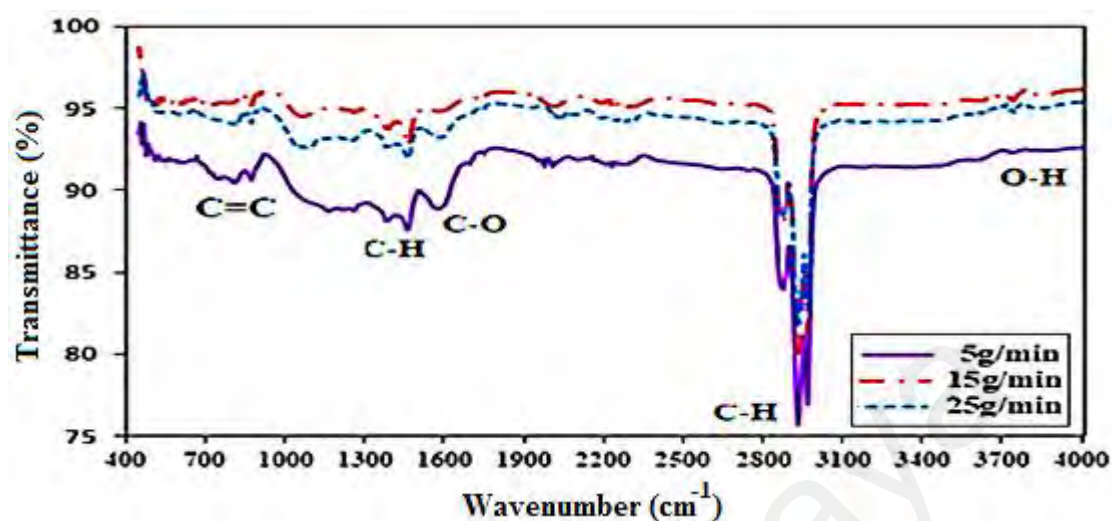


Figure 4. 16: FTIR spectra of the by-product biochar attained at different feed rate.

Table 4. 34: Functional group composition of the by-product biochar.

Group	Wavenumber (cm ⁻¹)	Class of compounds
Alcohols/ Phenol	3700-3800	O-H Stretch
Alkanes	2900-3000	C-H Stretch
Carboxylic	1600-1630	C-O Stretch
Alkynes	~1350	C-H Stretch
Alkenes	700-900	C=C Stretch

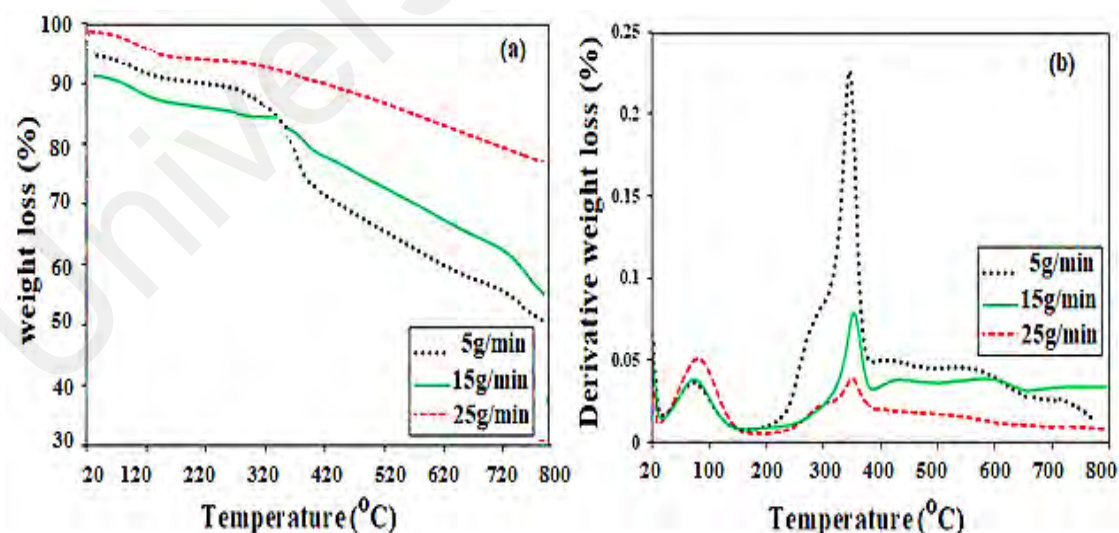


Figure 4. 17: (a) TGA analysis and (b) DTG analysis of by-product biochar attained with 5 g/min, 15 g/min and 25 g/min.

Table 4. 35: TGA analysis of by-product biochar samples obtained with different feed rates.

Feed rate (g/min)	Weight loss (%)				Total weight loss (%)	Residue (%)
	1 (20-150°C)	2 (200-390°C)	3 (390-550 °C)	4 (550-800 °C)		
5	3	10	10	2	25	75
15	2	4	3	-	9	91
25	1	1	2	-	4	96

Table 4. 36: DTG analysis of by-product biochar obtained with different feed rates.

Peak No.	Feed rate (g/min)			Temperature range (°C)	Content
	5	15	25		
Derivative weight loss (%)					
1	0.05	0.04	0.05	20-150	Moisture and volatile.
2	0.24	0.07	0.03	200-390	Hemicellulose, cellulose and lignin.
3	0.05	0.03	0.01	390-550	Hemicellulose, cellulose and lignin.
4	0.03	0.01	-	550-800	Lignin.

Based on Figure 4.17, Table 4.35 and Table 4.36, the primary weight loss at temperature range of 20–150°C is attributed to the evaporation of moisture content. The second and third major weight losses at temperature ranges of 200—390°C and 390—550°C corresponds to the decomposition of hemicellulose, cellulose and lignin. The fourth major weight loss at temperature range of 550—800°C corresponds to the further decomposition of lignin in biochar. Similar weight loss trends were also reported in Table 4.31 of section 4.4.4.1. When feed rate is increased, the greater extent of biomass causes most of the biomass components to be converted to pyrolytic products within the bio-oil instead of in by-product biochar.

4.4 Part 5: Palm shell pyrolysis in a novel helical screw fluidized bed reactor: Effect of particle size, pyrolysis time and vapor residence time on bio-oil yield and characteristic.

4.4.1 Effect of PS particle size

Figure 4.18 shows the phase separation process of liquid products obtained at different particle sizes from 0.25 to 10 mm. The bio-oil was initially dark brown, viscous and free-flowing liquid with strong smell. Phase separation process showed that, the liquid was divided into two and three layers with the top and bottom layers considered as the organic layers while the middle layer considered as the aqueous layer. The reason behind multilayers is due to the difference in density and presence of oxygenated compounds in the liquid product. Therefore, bio-oils have a polar affinity and formed redistribution of the different phases [221]. Similar trend was also reported by Lu et al. [222]. Furthermore, effect of particle size on product yields are shown in Table 4.36.

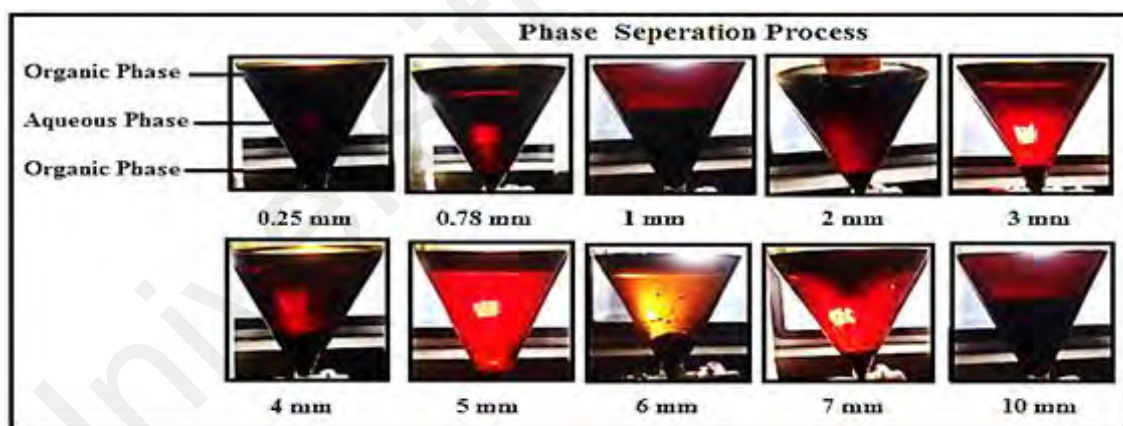


Figure 4. 18: Phase separation of bio-oil under the influence of polar affinity and gravity.

Table 4.37 shows the effect of particle size on product yields. Bio-oil yield slightly increased from 68.19 wt.% to 68.47wt.% when the particle size was increased from 0.25 mm to 0.78 mm whereas by-product biochar and gas yields decreased. Further increase in particle size from 1 mm to 2 mm resulted in the increase of bio-oil yield to 72.11 wt. %. These results are in line with the results reported by Chandrasekaran et al. who

reported that, the higher liquid yield of 38.3% was observed during continuing high heating rate and temperature. It is observed that with increase in particle size, the yield of char and gas decreases and bio-oil yield increases [290].

In addition, on further increasing particle size, slight reduction in bio-oil yield was observed due to heat transfer limitations at larger particle size. It is generally observed that as the particle size increases the heat transfer rate decreases. However, herein this HSFBR usage, the use of 6 mm to 10 mm particle size still resulted in good bio-oil yield (70.49—71.13 wt.%). These results shown the positive effect of helical screw which is still capable of providing good fluidization condition for larger particle size range (6—10 mm) as compared to the conventional fluidized pyrolyzer which requires an optimum 1—2 mm particle size range. Jalalifar et al. described that, gas fluidization reactors are restricted to 1-2 mm particle size for good hydrodynamics and bio-oil yield, However, increasing particle size causing decrease in bio-oil yield due to agglomeration of feed particles can cause reduction in temperature and pressure drop in the reactor [267, 291]. This feature of HSFBR offers the possibility for the saving of size reduction time and costs of biomass grinding.

Table 4.38 shows the characterization results of bio-oil obtained from different particle sizes of PS. The typical value of the density of bio-oil is from 1000 to 1240 kg/m³ at 15 to 40°C [233]. As the particle size increased from 0.25 mm to 0.78 mm, the density of organic phase improved from 1037 to 1043 kg/cm³ and as the bio-oil density increases, the content of energy also increases. However, viscosity and pH value remain similar. On further increase in particle size from 1 to 2 mm, minor increase in density of organic phase from 1041 to 1043 kg/m³ was reported while the density of aqueous phase noticeably decreased from 969 to 958 kg/m³, however viscosity and pH value remain in the range 21.22 to 24.36 cP for organic phase and 1.4 to 1.7 cP for aqueous phase. The pH values obtained at different particle size 2.5-2.8 does not differ much from each other. According

to Abdullahi et al. and Aziz et al. pH value of 2.7 using PS which is within the range of 2.7-3.3 is similar to the findings of current study [292, 293]. Gradually increase in particle size from 2 to 10 mm did not showed any noticeable change in the density, viscosity and pH value. The consistent results of density, viscosity and pH with different particle size from 0.25 to 10 mm is attributed to an adequate heat transfer rate due to high fluidization that was delivered by helical screw in the reactor hot zone.

Table 4. 37: Effect of particle size on product yields.

Particle size (mm)	Product distribution (wt. %)				
	Organic	Aqueous	Bio-oil* yield	Biochar	Gas
0.25	41.35	26.84	68.19	20.65	11.16
0.78	43.04	26.43	69.47	20.23	10.30
1	45.38	23.97	69.35	23.43	7.22
2	45.60	26.51	72.11	19.81	8.08
3	45.00	26.34	71.34	21.03	7.63
4	43.53	27.46	70.99	20.47	8.54
5	44.26	26.63	70.80	21.12	8.08
6	42.51	27.98	70.49	20.00	9.51
7	43.25	27.98	71.23	19.32	9.45
10	42.69	28.44	71.13	19.69	9.18

*Bio-oil = organic + aqueous

Table 4. 38: Effect of particle size on physico-chemical characteristics of bio-oil organic and aqueous phase*.

Particle size (mm)	Density (kg/m ³)		Viscosity (cP) 20 rpm		pH	
	Organic	Aqueous	Organic	Aqueous	Organic	Aqueous
0.25	1037	970	23.36	1.7	2.6	2.6
0.78	1041	972	24.36	1.6	2.6	2.6
1	1041	969	24.36	1.6	2.6	2.6
2	1043	959	22.23	1.4	2.7	2.6
3	1043	958	21.22	1.5	2.7	2.6
4	1043	978	23.12	1.7	2.8	2.7
5	1043	926	23.14	1.7	2.7	2.7
6	1043	974	24.34	1.5	2.7	2.7
7	1043	974	23.22	1.6	2.6	2.7
10	1043	978	23.24	1.7	2.6	2.5

*Bio-oil characterization at 25°C

The results of CHNS/O analysis with selected particle size of 0.25 mm, 4 mm and 10 mm are shown in Table 4.39. A minor change in bio-oil composition and HHV by increasing particle size from 0.25 to 10 mm was observed with CHNS/O analysis. The

carbon and oxygen contents were slightly increased from 76.4 % to 77.8 % and 0.3 % to 0.4 % respectively, which slightly affected the calorific value of bio-oil from 42.68 MJ/kg to 42.80 MJ/kg. This finding is supported by the results of Leng et al. who described that the bio-oil with decrease in O₂ can increase the heating value due to low percentage of oxygen content make it more appropriate as transportation fuel and improved the bio-oil heating value [223]. These findings are supported by the result of the physicochemical characteristics of bio-oil as shown in Table 4.38, where the density of bio-oil was increased from 1037 kg/m³ to 1043 kg/m³ with increasing particle size from 0.25 mm to 10 mm due to higher degree of cross-linking of high molecular weight components which is comparative with the HHV of diesel fuel (45 MJ/kg) [244]. A larger particle size is generally reported to reduce the quality of pyrolysis product due to greater mass and heat transfer limitations at larger particle size. However, herein this study, these minor increasing trends at larger particle size indicated the ability of HSFBR to reduce mass and heat transfer limitations through the mechanical mixing feature by the screw propeller system.

Table 4. 39: Ultimate analysis of bio-oil (organic phase) with selected particle size.

Particle size (mm)	Ultimate analysis of bio-oil (organic Phase)					
	C	H	N	S	O*	HHV (MJ/kg)
0.25	76.4	11.8	9.8	0.9	0.3	42.80
4	77.8	11.4	9.5	0.9	0.4	42.68
10	77.4	11.7	9.8	0.9	0.2	43.02

* = by difference.

Figure 4.19 shows the FTIR spectra of bio-oil organic phase attained with particle size of 0.25 mm, 4 mm, 10 mm at 500°C whereas Table 4.40 lists the identified functional groups of bio-oil. The results of FTIR indicated the major hydroxyl group (O-H stretching) was progressively decreased as the particle size gradually increased from 0.25 to 10 mm, indicating the quality of organic phase was significantly improved by having a lower oxygen content. A bio-oil of lower oxygen content is generally favored as high

oxygen content was known to cause thermal and chemical instability issues besides reducing its energy value [198, 252-254]. Here, one can observe the high intensity FTIR peaks of C—H functional group for HSFBR based pyrolysis involving large PS particle sizes, indicating high hydrocarbon content at these particle sizes.

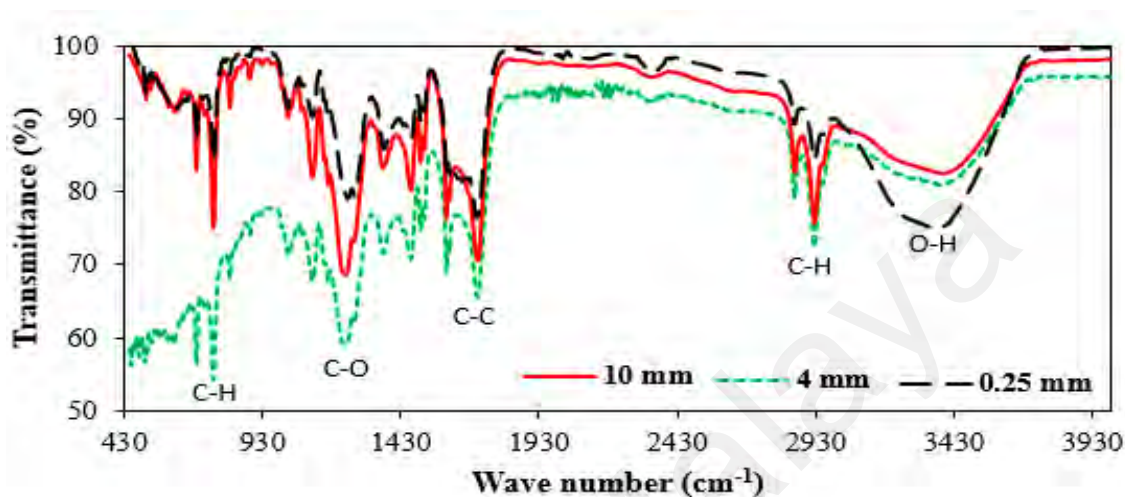


Figure 4. 19: FTIR spectra of the bio-oil (organic phase) obtained at selected particle sizes.

Table 4. 40: Functional group composition of the bio-oil (organic phase) 0.25 mm, 4 mm and 10 mm particle size.

Group	Wavenumber (cm ⁻¹)	Class of compounds
Alcohols and Phenol	3200 to 3550	O-H Stretch
Alkanes	2855- 3000	C-H Stretch
Alkenes and Aromatics	1750	C-C Stretch
Esters	~1236	C-O Stretch
Alkynes	~754	C–H Bending

Results of GC/MS analysis of bio-oil obtained with 0.25 mm, 4 mm and 10 mm particle size are shown in Table 4.41. The results of this analysis indicated the highest proportions of possible compounds were dodecanoic acid methyl ester, Dodecanoic acid, 1-(hydroxymethyl)-, cyclohexane, 1,2,4-Trimethoxybenzene, Phenol, 2,6-dimethoxy-based compounds with 14.19%, 6.145 %, 15.243 %, 5.866 %, 10.727 % and 20.194 %, respectively. The total concentration of carboxylic acids was the highest around 25.093

% in the bio-oil obtained at 4 mm particle size. The large percentage of carboxylic acids directly contributes to the lower pH value of the bio-oil as shown in Table 4.38. This is also consistent with a report by Oasmaa et. al. that the acidity of bio-oils is mainly derived from volatile acids [294]. However, concentration of carboxylic was reduced from 25.093 % to 17.969 % at 0.25 mm particle size as mesoporous by-product biochar served as catalyst which further caused cracking of oxygenated compounds such as carboxylic acid and phenols which increased the bio-oil yield [295, 296]. Furthermore, the second major group in bio-oil was clearly observed for aromatics and phenol with 22.962 % and 30.852 %, respectively. The fourth major group in bio-oil was esters with the highest percentage of 18.373 % at 0.25 mm particle size.

The fifth major group in bio-oil was alkenes and alkynes with high values of 12.33 % and 6.449 %, respectively. Among these chemical components, phenolics, alkenes and alkynes are advantageous for high-quality bio-oils due to their high carbon and hydrogen contents that bring the favorable effect in HHV improvement [212]. However, further upgrading process on phenolics such as hydrodeoxygenation is required to increase the deoxygenated hydrocarbons amount for better fuel stability and energy value. The presence of these groups indicating the suitability of the oil to be considered for value-added chemicals. In addition, it is possible to eliminate the oxygenates from bio-oil to obtain higher-quality liquid fuel [251].

Table 4. 41: GC/MS analysis of bio-oil produced at selected particle sizes of 0.25, 4 and 10 mm.

Identified compounds and group		Chemical formula	Relative content (%)		
			Particle size (mm)		
Esters			0.25	4	10
1	Octadecanoic acid, 2-propenyl ester	C ₂₁ H ₄₀ O ₂	3.378	2.151	1.651
2	9-Octadecenoic acid (Z)-, methyl ester	C ₁₉ H ₃₆ O ₂	2.199	1.813	1.442
3	Benzoic acid, perhydroquinolin-4-yl ester	C ₁₆ H ₂₁ NO ₂	1.688	-	1.773
4	Tetradecanoic acid, methyl ester	C ₁₅ H ₃₀ O ₂	1.148	2.412	1.216
5	Octanoic acid, 4-tridecyl ester	C ₂₁ H ₄₂ O ₂	1.122	-	1.673
6	2-Octynoic acid, methyl ester	C ₉ H ₁₄ O ₂	1.065	1.816	1.772
7	Octadecanoic acid, propyl ester	C ₂₁ H ₄₂ O ₂	1.628	1.656	1.771
8	Dodecanoic acid, methyl ester	C ₁₃ H ₂₆ O ₂	6.145	5.742	4.194
		Total	18.373	15.590	15.492
Carboxylic acid					
9	Dodecanoic acid	C ₁₂ H ₂₄ O ₂	7.191	15.243	12.143
10	Tetradecanoic acid	C ₁₄ H ₂₈ O ₂	2.152	1.46	3.443
11	n-Hexadecanoic acid	C ₁₆ H ₃₂ O ₂	1.441	1.015	1.77
12	2,4-Hexadienedioic acid, 3,4-diethyl-, dimethyl, (E,Z)-	C ₁₂ H ₁₈ O ₄	1.773	1.785	1.772
13	Octadecanoic acid	C ₁₈ H ₃₆ O ₂	1.212	1.098	1.321
14	cis-11-Eicosenoic acid	C ₂₀ H ₃₈ O ₂	1.771	1.206	1.543
15	3,5-Dimethoxy-4-hydroxyphenylacetic acid	C ₁₀ H ₁₂ O ₅	1.216	1.165	1.143
16	Allogibberic acid	C ₁₈ H ₂₀ O ₃	1.213	1.131	1.958
		Total	17.969	24.103	25.093
Alkenes					
17	Cyclohexene	C ₆ H ₁₀	5.866	3.304	2.015
18	trans-1,4-Hexadiene	C ₆ H ₁₀	4.304	2.463	1.235
19	2-Hexene, 4-methyl-, (E)-	C ₇ H ₁₄	2.166	2.075	2.098
		Total	12.336	7.842	5.348
Alkynes					
20	Cyclohexane, methyl-	C ₇ H ₁₄	3.231	2.231	2.851
21	Cyclobutane, ethenyl-	C ₆ H ₁₀	2.453	1.776	3.598
		Total	5.684	4.007	6.449
Aldehyde					
22	5-Hexenal	C ₆ H ₁₀ O	1.772	1.606	1.015
23	Cyclopentane acetaldehyde, 2-formyl-3-methyl- α -methylene	C ₁₀ H ₁₄ O ₂	1.457	1.793	1.275
24	3,4-Hexadienal, 2-butyl-2-ethyl-5-methyl-	C ₁₃ H ₂₂ O	1.963	1.631	1.231
25	Benzaldehyde, (2,4-dinitrophenyl) hydrazone	C ₁₃ H ₁₀ N ₄ O ₄	2.431	1.454	1.059
		Total	7.623	6.484	4.580
Aromatics					
26	1,2,4-Trimethoxybenzene	C ₉ H ₁₂ O ₃	10.727	10.433	7.252
27	Benzene, 1,2,3-trimethoxy-5-methyl-	C ₁₀ H ₁₄ O ₃	8.549	6.549	1.395
28	Cyclohexanol	C ₆ H ₁₂ O	3.686	5.654	3.539
		Total	22.962	22.636	12.186
Phenol					
29	Phenol, 2,6-dimethoxy-	C ₈ H ₁₀ O ₃	8.923	12.321	20.194
30	Phenol, 2,6-dimethoxy-4-(2-propenyl)-	C ₁₁ H ₁₄ O ₃	6.13	7.017	10.658
		Total	15.053	19.338	30.852
		Grand Total	100	100	100

Pyrolysis oil derived from thermal degradation of biomass must be tested for fuel properties before it is used as a source of energy in vehicles, boilers and turbines [213]. Focusing on these bio-oil applications, some of the fuel properties of bio-oil organic phase obtained at 0.25, 4 and 10 mm particle size was tested for fire point, flash point, dew point, pour point and HHV following ASTM standards. The fuel properties of bio-oils were altered between the liquids formed at different particle size. The values of fire, flash, dew point and pour points were higher in the liquid produced with 0.25 mm as compared with those produced with 10 mm particle size. The low fire point of 65°C was observed at 0.25 mm particle size which designates that the liquid holds adequate volatiles and offered high fuel ignition properties due to the low-density of 1040 kg/cm³ [214] as shown in Table 4.38. Table 4.41 depicted the flash point values at 4 mm and 10 mm particle size were at 64°C and 66°C, respectively. The high flashpoint for 10 mm particle size sample showed low fuel volatility and less energy content, which may cause more time during fuel ignition. The dew and pour points of the bio-oil obtained at 10 mm particle size were the highest with 69°C and 9°C, respectively. Furthermore, the HHV of the organic phase attained with 0.25, 4 mm and 10 mm particle size with 42.80, 42.68 and 43.02 MJ/kg, respectively. These values showed that the fuel properties of these bio-oil samples are consistent with the literature and comparable to those of diesel fuel oil [215].

Table 4. 42: Characterization of bio-oil (organic phase) for fuel properties at selected particle sizes.

Particle size (mm)	Fire point (°C)	Flash Point (°C)	Dew point (°C)	Pour point (°C)	HHV (MJ/kg)
0.25	65	60	63	6	42.80
4	67	64	66	8	42.68
10	72	66	69	9	43.02

4.4.2 Effect of pyrolysis time

Figure 4.20 shows the phase separation process of liquid product obtained at different pyrolysis time (20, 30, 40, 50 and 60 min). Phase separation process presented that, the liquid was separated into two and three layers with the top and bottom layers measured as the organic layers while the middle layer appeared as the aqueous layer. The reason behind multilayers is aforementioned in section 3.1. The bio-oil sample produced at pyrolysis time of 30 minutes is of the darkest color, indicating the highest concentration of organic phase as compared with other samples. Effect of pyrolysis time on product yields of PS using 10 mm particle size was investigated at different pyrolysis time from 20 min to 60 min with 50 rpm torque at 500°C. The results obtained from this study are summarized in Table 4.43.

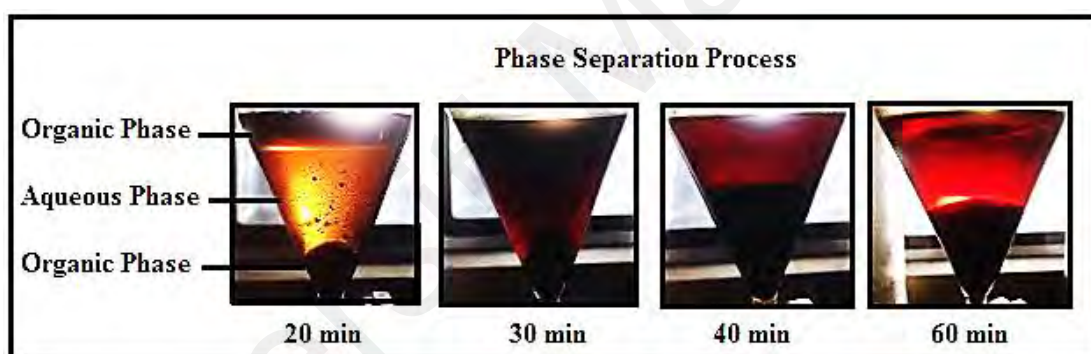


Figure 4. 20: Phase separation of bio-oil under the influence of polar affinity and gravity.

Table 4. 43: Effect of pyrolysis time on product yields.

Pyrolysis time (minutes)	Products distribution (wt.%)				
	Organic	Aqueous	Bio-oil*	Biochar	Gas
20	27.73	33.66	61.39	30.81	7.18
30	37.51	34.89	72.40	18.44	9.16
40	31.24	34.21	65.45	16.21	18.34
50	28.14	34.47	62.61	16.02	21.37
60	27.12	32.34	59.46	15.50	25.04

*Bio-oil = organic + aqueous

With 20 minutes of pyrolysis time, the yields of bio-oil, biochar and gas were 61.39, 30.81 and 7.18 wt.%, respectively. The reason behind the lesser bio-oil yield may be due to the insufficient pyrolysis time for the complete biomass decomposition. An

increase in pyrolysis time to 30 minutes resulted in an increase of bio-oil and gas yields. This high bio-oil yield depicted that the decomposition of PS was significant at this pyrolysis time. However, any further increase in pyrolysis time from 30 minutes onwards resulted in the higher formation of gas. This may be attributed to the extended secondary reactions over a long pyrolysis time which enabled a greater extent of lignin breakdown into smaller hydrocarbons [243]. The trend for gas product is consistent to the result reported by Sohaib et al. where slightly higher gas yield is achieved by increasing the pyrolysis time of corn stover due to the enhanced decomposition of biomass and secondary reaction [295]. Kim et al. also reported similar effects of extended pyrolysis time on bio-oil and gas yield [198].

Table 4.44 shows the relationship between pyrolysis time and physicochemical properties of bio-oil such as density, viscosity and pH. There is no direct trend observed between the pyrolysis time and physicochemical properties of bio-oil. However, one may observe that the bio-oil sample produced at 30 min pyrolysis time has the relatively better physicochemical properties as compared with samples obtained at other pyrolysis durations. In Table 4.49, the results of CHNS/O analysis also showed that bio-oil sample produced at pyrolysis time of 30 minutes has the highest carbon content and HHV. Its high carbon content by CHNS/O analysis was also verified by the high FTIR transmittance peak of C—H group is depicted in Figure 4.21. These observations corroborate with our postulate that a pyrolysis time of 30 minutes is the optimum pyrolysis duration in this study for maximum biomass conversion to bio-oil using HSFBR. At this pyrolysis time, sufficient duration was allowed for the biomass disintegration into liquid hydrocarbons and was insufficient for secondary cracking reactions to form C₁ to C₄ components. GC/MS analyses of bio-oil samples at different pyrolysis times also showed similar organic compounds as determined Table 4.52. However, a relatively lower phenol content and higher total hydrocarbon contents

(alkenes, alkynes and aromatics) at 30 min pyrolysis time indicate a higher stability and energy value of bio-oil produced at this condition.

Table 4. 44: Effect of pyrolysis time on physicochemical characteristics of bio-oil.

Pyrolysis time (min)	Density (kg/m ³)		Viscosity (cP)		pH	
	Organic	Aqueous	Organic	Aqueous	Organic	Aqueous
20	1038	926	21.50	1.50	3.0	3.0
30	1041	959	23.70	1.50	2.9	2.9
40	1039	978	22.40	1.50	3.0	2.9
50	1039	974	22.12	1.63	2.9	2.9
60	1038	926	21.22	1.35	2.9	3.0

Table 4. 45: CHNS/O analysis of bio-oil (organic phase) at selected pyrolysis time.

Pyrolysis time (min)	CHNS/O analysis of bio-oil (organic Phase)					
	C	H	N	S	O*	HHV (MJ/kg)
20	61.4	10.4	8.5	0.7	19.0	32.34
30	77.4	11.7	9.8	0.9	0.2	43.02
60	67.41	11.7	9.8	0.9	10.19	37.84

* = by difference.

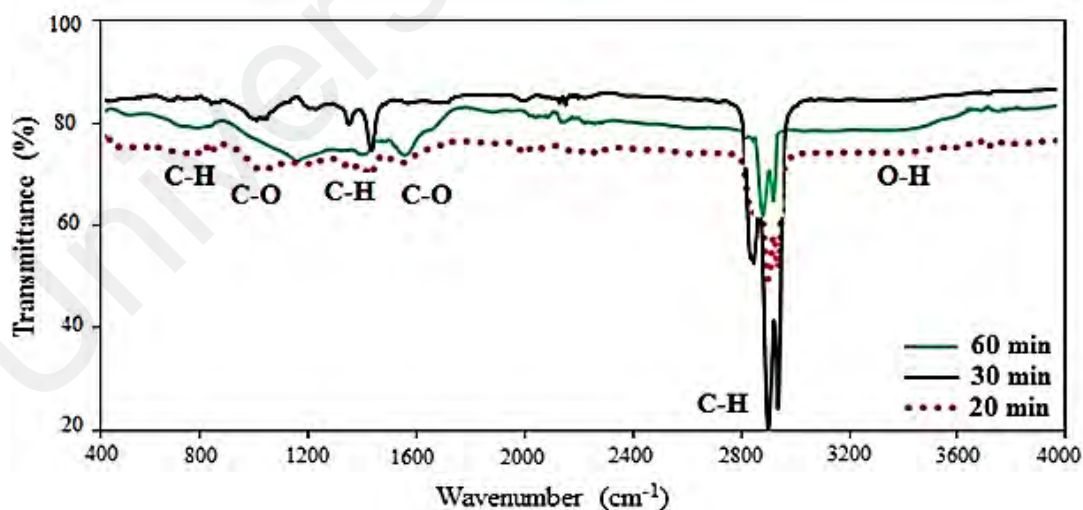


Figure 4. 21: FTIR spectra of bio-oil (organic phase) obtained at selected pyrolysis time.

Table 4. 46: GC/MS analysis of bio-oil achieved at selected pyrolysis time of 20, 30 and 60 min.

Identified compounds and group		Chemical formula	Relative content (%)		
			Pyrolysis time (min)		
Esters			20	30	60
1	Octadecanoic acid, 2-propenyl ester	C ₂₁ H ₄₀ O ₂	1.211	2.151	3.378
2	9-Octadecenoic acid (Z)-, methyl ester	C ₁₉ H ₃₆ O ₂	1.442	1.813	2.199
3	Benzoic acid, perhydroquinolin-4-yl ester	C ₁₆ H ₂₁ NO ₂	1.253	1.501	1.688
4	Tetradecanoic acid, methyl ester	C ₁₅ H ₃₀ O ₂	1.216	3.412	1.148
5	Octanoic acid, 4-tridecyl ester	C ₂₁ H ₄₂ O ₂	2.173	1.125	1.122
6	2-Octynoic acid, methyl ester	C ₉ H ₁₄ O ₂	1.242	1.816	1.065
7	Octadecanoic acid, propyl ester	C ₂₁ H ₄₂ O ₂	1.211	1.656	1.628
8	Dodecanoic acid, methyl ester	C ₁₃ H ₂₆ O ₂	3.194	3.863	6.145
Total			12.942	17.337	18.373
Carboxylic acid					
9	Dodecanoic acid	C ₁₂ H ₂₄ O ₂	5.243	3.191	5.143
10	Tetradecanoic acid	C ₁₄ H ₂₈ O ₂	3.46	1.152	2.443
11	n-Hexadecanoic acid	C ₁₆ H ₃₂ O ₂	1.015	1.441	1.721
12	2,4-Hexadienedioic acid, 3,4-diethyl-, dimethyl, (E,Z)-	C ₁₂ H ₁₈ O ₄	1.785	1.773	1.28
13	Octadecanoic acid	C ₁₈ H ₃₆ O ₂	1.098	1.212	1.321
15	3,5-Dimethoxy-4-hydroxyphenylacetic acid	C ₁₀ H ₁₂ O ₂	1.368	2.426	3.101
Total			13.969	11.195	15.009
Alkenes					
16	Cyclohexene	C ₆ H ₁₀	3.132	3.015	4.432
17	Hexadecane	C ₁₆ H ₃₄	6.230	5.635	2.102
18	trans-1,4-Hexadiene	C ₆ H ₁₀	3.549	5.545	3.304
19	2-Hexene, 4-methyl-, (E)-	C ₇ H ₁₄	3.075	2.098	1.164
Total			15.986	16.293	11.002
Alkynes					
20	Cyclohexane, methyl-	C ₇ H ₁₄	4.362	5.231	3.904
21	Norbornane	C ₇ H ₁₂	5.598	3.453	2.532
Total			9.96	8.684	6.436
Aldehyde					
22	1-Cyclohexene-1-carboxaldehyde	C ₇ H ₁₀ O	1.015	1.606	2.772
23	Cyclopentane acetaldehyde, 2-formyl-3-methyl- α -methylene	C ₁₀ H ₁₂ O ₃	1.275	1.793	1.457
24	3,4-Hexadienal, 2-butyl-2-ethyl-5-methyl-	C ₁₃ H ₂₂ O	1.131	1.631	2.056
25	Hexanal	C ₆ H ₁₂ O	1.159	1.454	2.431
Total			4.58	6.484	8.716
Aromatics					
26	1,2,4-Trimethoxybenzene	C ₉ H ₁₂ O ₃	11.325	14.867	11.755
27	Benzene, 1,2,3-trimethoxy-5-methyl-	C ₁₀ H ₁₄ O ₃	5.471	6.549	5.549
28	Cyclopentane acetaldehyde	C ₇ H ₁₄ O	6.466	5.654	2.654
Total			23.262	27.07	19.958
Phenol					
29	Phenol, 2,6-dimethoxy-	C ₈ H ₁₀ O ₃	7.744	4.923	6.321
30	Creosol	C ₈ H ₁₀ O ₂	7.899	3.649	6.664
31	Phenol, 2,6-dimethoxy-4-(2-propenyl)-	C ₁₁ H ₁₄ O ₃	3.658	4.365	7.521
Total			19.301	12.937	20.506
Grand Total			100	100	100

Table 4. 47: Characterization of bio-oil (organic phase) for fuel properties at selected pyrolysis time of 20, 30 and 60 min.

Pyrolysis Time (min)	Fire point (°C)	Flash Point (°C)	Dew point (°C)	Pour point (°C)	HHV (MJ/kg)
20	70	66	61	7	32.34
30	63	60	63	8	43.02
60	67	64	66	9	37.84

Some of the fuel properties of bio-oil organic phase were investigated fire point, flash point, dew point, pour point and HHV obtained at 20, 30 and 60 min pyrolysis time are summarized in Table 4.49. The high fire point of 70°C for sample obtained at 20 min pyrolysis time indicates inadequate volatiles as confirmed from the physicochemical properties of bio-oil. The values for flash point at 30 min and 60 min pyrolysis time were observed as 60°C and 64°C, respectively. The low flashpoint for sample of 30 min pyrolysis time showed high fuel volatility which could increase the fuel ignition property.

4.4.3 Effect of vapor residence time

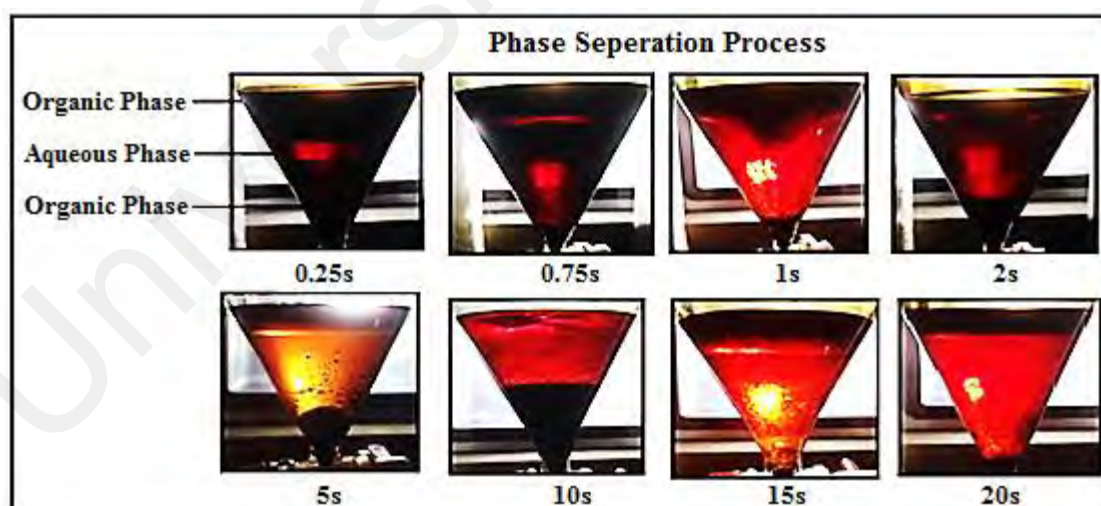


Figure 4. 22: Phase separation of bio-oil under the influence of polar affinity and gravity.

Similar phase separation process was reported for pyrolysis done at different vapor residence times. Based on Figure 4.22, the bio-oil becomes lighter in color as vapor residence time increases, indicating the decreasing amount of organic phase. The effect

of vapor residence time on products yield of PS is presented in Table 4.48. The vapor residence time was measured by controlling the vapor outlet flow rate valve provided between the pyrolysis reactor and condenser. The total bio-oil yield decreased significantly (73.86 wt.% to 57.06 wt.%) when vapor residence time increased from 0.25 s to 20 s. As for the maximum organic phase distribution (45.63 wt.%), a 2 second of vapor residence time was noted to be the appropriate condition for pyrolysis in HSFBR. The opposite trend was noted for biochar and gas yields. The extended vapor residence time resulted in greater extent of secondary vapor cracking and re-polymerization reaction which led to more formation of gas and less bio-oil [243]. Other researchers also reported of these similar effects of vapor residence time on pyrolysis product yields [243, 297].

Table 4. 48: Effect of vapor residence time on product yields.

Vapor residence time (s)	Product distribution (wt. %)				
	Organic	Aqueous	Bio-Oil*	Biochar	Gas
0.25	40.28	33.58	73.86	16.81	9.33
0.78	40.21	33.12	73.33	15.98	10.69
1	41.21	32.02	73.23	15.95	10.82
2	45.63	25.98	71.61	15.52	12.87
5	43.53	26.56	70.09	16.66	13.25
10	37.66	23.20	60.86	19.57	19.57
15	34.36	25.23	59.59	20.00	20.41
20	33.36	23.70	57.06	20.00	22.94

*Bio-oil = organic + aqueous

Table 4. 49: Effect of vapor residence time on physicochemical characteristics of bio-oil organic and aqueous phase*.

Vapor residence time (s)	Density (kg/m ³)		Viscosity (cP)		pH	
	Organi	Aqueou	Organi	Aqueou	Organi	Aqueou
	c	s	c	s	c	s
0.25	1042	970	24.6	1.5	2.9	2.6
0.78	1042	972	24.3	1.7	2.9	2.8
1	1041	969	23.2	1.7	3.2	2.8
2	1040	955	20.7	1.6	2.8	2.7
5	1040	959	20.4	1.8	2.7	2.7
10	1039	974	18.7	1.7	2.7	2.6
15	1039	978	16.2	1.8	2.8	2.6
20	1037	975	18.3	2.1	2.8	2.7

*Bio-oil characterization at 25°C

Table 4. 50: CHNS/O analysis of bio-oil (organic phase) at selected vapor residence time.

Vapor residence time (s)	CHNS/O analysis of bio-oil (organic Phase)					HHV (MJ/kg)
	C	H	N	S	O*	
0.25	78.4	11.7	7.8	0.7	1.4	43.14
10	75.3	11.7	9.8	0.7	2.5	41.89
20	72.5	11.9	10.5	0.8	4.3	40.91

* = by difference.

The extended vapor residence time had also caused the density and viscosity of bio-oil sample to decrease can be seen in Table 4.48. CHNS/O analysis also indicated the decrease in carbon content and HHV and the increase in oxygen content at extended vapor residence time. In addition, the decrease in carbon content is also confirmed via the decreasing FTIR transmittance peak intensity of C—H group and the decrease in total hydrocarbon contents (alkenes, alkynes, aromatics) via GC/MS analysis (Figure 4.23 and Table 4.52). The GC/MS analysis also reported of the overall increase in the proportion of oxygenated compounds (esters, acids, aldehydes and phenols) at extended vapor residence time which corroborates with results on oxygen content by CHNS/O analysis (Table 4.50). This indicates that bio-oil produced at longer vapor residence time has poorer stability due to its high oxygen content.

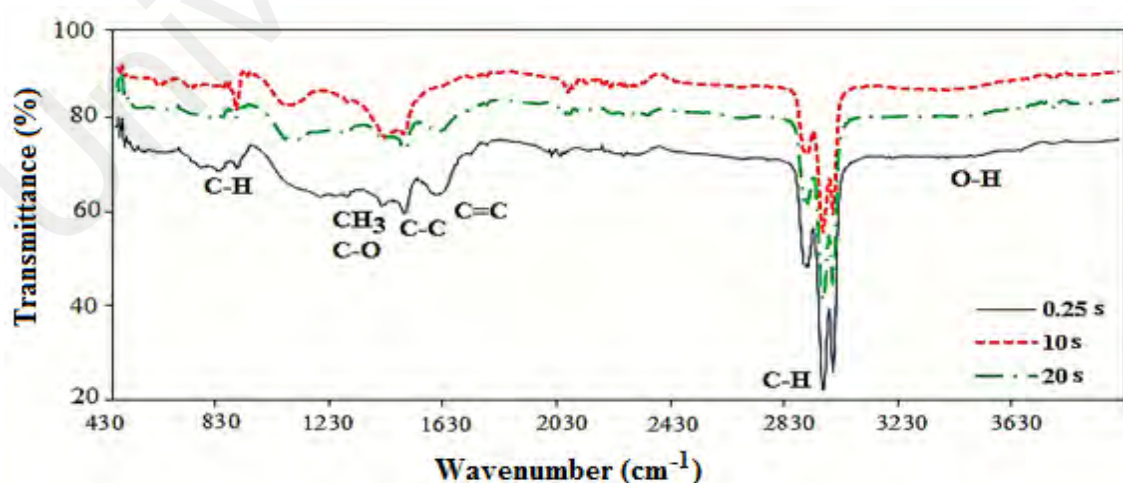


Figure 4. 23: FTIR spectra of bio-oil (organic phase) obtained at selected vapor residence time.

One of the reported main reasons for these deteriorations of bio-oil is the char-vapor interaction at extended vapor residence time [235]. The char functioned as the catalyst for secondary vapor cracking, thus reducing the formation of C₅-C₁₅ components for bio-oil. From here, it can be noted that PS pyrolysis involving extended vapor residence time is unfavorable as it produces bio-oil in lesser quantity and quality. Therefore, a rapid removal of vapors from the hot reactor to low temperature condenser is an important mitigating step for this issue. [298]. Table 4.51 visibly shows the low fire point of 65°C was observed at 0.25 s vapor residence time indicated that the bio-oil (organic phase) has adequate volatiles for sustained combustion at lower temperature [214]. The low flash point of bio-oil sample produced at 0.25 s vapor residence time showed high fuel volatility which could increase the ignition property.

Table 4. 51: Characterization of bio-oil (organic phase) for fuel properties at selected vapor residence time at 0.25, 10 and 20 s.

Vapor residence time (s)	Fire point (°C)	Flash Point (°C)	Dew point (°C)	Pour point (°C)	HHV (MJ/kg)
0.25	65	62	63	8	43.14
10	67	64	66	9	41.89
20	70	65	66	9	40.91

Table 4. 52: GC/MS analysis of bio-oil achieved at selected vapor residence time of 0.25, 10 and 20 s.

Identified compounds and groups		Chemical formula	Relative content (%)		
			Vapor residence time (s)		
	Esters		0.25	10	20
1	9-Octadecenoic acid (Z)-, methyl ester	C ₁₉ H ₃₆ O ₂	3.093	3.964	3.577
2	Benzoic acid, perhydroquinolin-4-yl ester	C ₁₆ H ₂₁ NO ₂	1.773	1.501	1.688
3	Tetradecanoic acid, methyl ester	C ₁₅ H ₃₀ O ₂	2.216	1.412	1.148
4	Octanoic acid, 4-tridecyl ester	C ₂₁ H ₄₂ O ₂	1.673	1.125	1.122
5	2-Octynoic acid, methyl ester	C ₉ H ₁₄ O ₂	1.772	1.816	1.065
6	Octadecanoic acid, propyl ester	C ₂₁ H ₄₂ O ₂	1.771	1.656	1.628
7	Dodecanoic acid, methyl ester	C ₁₃ H ₂₆ O ₂	4.194	2.863	6.145
Total			16.492	14.337	16.373
Carboxylic acid					
8	Dodecanoic acid	C ₁₂ H ₂₄ O ₂	4.243	4.191	5.143
9	Tetradecanoic acid	C ₁₄ H ₂₈ O ₂	3.46	2.152	2.443
10	2,4-Hexadienedioic acid, 3,4-diethyl-, dimethyl, (E,Z)-	C ₁₂ H ₁₈ O ₄	1.015	1.654	2.77
11	Octadecanoic acid	C ₁₈ H ₃₆ O ₂	1.785	1.773	1.772
12	3,5-Dimethoxy-4-hydroxyphenylacetic acid	C ₁₀ H ₁₂ O ₅	1.098	1.212	3.277
13	Allogibberic acid	C ₁₈ H ₂₀ O ₃	2.368	1.216	1.143
Total			13.969	12.198	16.548
Alkenes					
14	Cyclohexene	C ₆ H ₁₀	4.132	3.015	3.432
15	2-Hexene, 4-methyl-, (E)-	C ₇ H ₁₄	4.23	4.068	2.154
16	trans-1,4-Hexadiene	C ₆ H ₁₀	4.549	4.542	4.304
17	Trans-4-Methyl-2-Hexene	C ₇ H ₁₄	2.075	2.098	1.166
Total			14.986	13.723	11.056
Alkynes					
18	Cyclohexane, methyl-	C ₇ H ₁₄	2.876	2.206	2.298
19	Tridecane, 7-cyclohexyl-	C ₁₉ H ₃₈	3.047	1.453	2.581
20	Norbornane	C ₇ H ₁₂	1.451	1.025	1.889
21	Cyclopentane, 1,2-dimethyl-, cis-	C ₇ H ₁₄	1.551	1.567	1.987
Total			8.925	6.251	8.755
Aldehyde					
22	Benzaldehyde, (2,4-dinitrophenyl) hydrazone	C ₁₃ H ₁₀ N ₄ O ₄	1.015	2.606	1.958
23	Cyclopentane acetaldehyde, 2-formyl-3-methyl- α -methylene	C ₁₀ H ₁₄ O ₂	1.275	2.793	1.457
24	3,4-Hexadienal, 2-butyl-2-ethyl-5-methyl-	C ₁₃ H ₂₂ O	1.131	1.631	1.963
25	Hexanal	C ₆ H ₁₂ O	1.159	3.454	1.431
Total			4.58	10.484	6.809
Aromatics					
26	Cyclopentane acetaldehyde	C ₇ H ₁₄ O	13.252	5.433	4.723
27	1,2,4-Trimethoxybenzene	C ₉ H ₁₂ O ₃	2.471	3.549	3.549
28	Benzene, 1,2,3-trimethoxy-5-methyl-	C ₁₀ H ₁₄ O ₃	2.466	3.654	4.654
29	1,2,3-Trimethoxybenzene	C ₉ H ₁₂ O ₃	2.073	3.434	4.032
Total			20.262	16.070	16.958
Phenol					
30	Creosol	C ₈ H ₁₀ O ₂	8.614	9.923	8.321
31	Phenol, 4-ethyl-2-methoxy-	C ₉ H ₁₂ O ₂	7.899	8.649	7.659
32	Phenol, 2,6-dimethoxy-4-(2-propenyl)-	C ₁₁ H ₁₄ O ₃	4.273	8.365	7.521
Total			20.786	26.937	23.501
Grand Total			100	100	100

4.4.4 Optimized conditions of HSFBR

Based on the parametric study on the effects of PS particle size, pyrolysis time and vapor residence time, the PS pyrolysis in HSFBR is best suited to be done at 2 mm particle size, 30 minutes of pyrolysis total time and 0.25 s vapor residence time. This set of conditions was noted to produce bio-oil of the highest quality and quantity. Previous reports have also reported the similar range of condition in other reactors to maximize bio-oil yield [267, 290, 299]. At this condition, sufficient mass and heat transfer and time was allowed for the biomass disintegration into C₅-C₁₅ components while minimizing the over disintegration of biomass into condensable hydrocarbon gases at extended duration. One of the main important findings in this study is the ability of HSFBR setup to sustain good pyrolysis performance over a large particle size range up to 10 mm. A particle size of 2 mm is the limit as reported by many researchers because any further increase will increase secondary pyrolysis reaction to reduce bio-oil yield. However, even with a fivefold of increase in particle size (10 mm), the HSFBR pyrolysis only showed less than 1% and 3% decrease in bio-oil yield and energy value respectively. This is because, in the previous work, the screw propeller system of HSFBR was noted to provide sufficient mechanical energy to biomass mixing and in-situ size reduction [300]. With this finding, the HSFBR pyrolysis processes could be done in the absence of size reduction process for biomass such as milling, crushing or grinding, which in turn reduces the overall process complexity and cost.

CHAPTER 5: CONCLUSION AND RECOMMENBATIONS FOR FUTURE

WORK

5.1 Conclusions

The conclusion drawn on the basis of this study are stated below:

5.1.1 Part 1: A technical review on semi-continuous and continuous pyrolysis process of biomass to bio-oil.

Present study has provided comprehensive knowledge on existing semi-continuous and continuous pyrolysis reactor technologies, feed treatment methods, feeding systems and effect of operating parameters on product recovery. Thermal treatment of biomass through drying has significantly showed a decrease in the moisture content, increase in the grinding ability and improved the liquid product properties. On the other hand, physical treatment was shown to increase the interfacial surface area of biomass in order to avoid coagulation and increase the heat and mass transfer rate during pyrolysis. It has been found that screw/auger feeding system is more suitable in terms of efficiency and good feed control over the other feeding equipment. The roles of operating parameters for instance heating rate, temperature, feeding rate, gas flow rate, and reaction/residence time were studied in which temperature was found to be the most significant parameter in improving liquid yield. Furthermore, it was found that different reactors have different maximum liquid yield: BFB (67%–70 wt.%), CFB (70–75 wt.%), CSBR (70 wt.%), RC reactor (65 wt.%), ablative reactor (70 wt.%) and screw/auger reactor (30–59 wt.%). However, due to high carbon conservation, extended solid residence time, low ash transfer, difficulties in char removal, small particle sizes and high gas fluidizing velocity, BFB and CFB are expensive processes and further require liquid refining which makes them even more expensive. On the other hand, CSBR has been proven as substitute for BFB and CFB. In addition, due to its complex design, high gas fluidization requirement and difficult operation has restricted this technology for

upgradation on large scale bio-oil production. Additionally, RCR technology is mostly dependent on centrifugal force for circulation of heated sand along biomass continuously without any sweeping or carrier gas. However, ablative reactor can handle much large biomass particle size with no carrier gas. Nevertheless, it is also a complex mechanical design which posed as a challenge for its scale up. In addition, higher reactor cost, elevated pressure and higher heat losses restricted this technology for industrialization. Screw/auger reactor operates at 400°C on continuous mode but its upgradation is difficult as the moving parts of reactor are in contact of hot zone, so high heat transfer rate on large scale liquid production is not possible. Thus, it is not being proven yet for large scale commercialization. Therefore, by considering all types of the reactors, design aspects, facilities, advantages and disadvantages, the designing of a more efficient semi-continuous or continuous pyrolysis reactor would certainly be of great need and advantage in the field of pyrolysis process.

5.1.2 Part 2: Novel helical screw-fluidized bed reactor for bio-oil production in slow pyrolysis mode: A preliminary study.

This research was the first attempt on the use of HSFBR for bio-oil production by using slow pyrolysis mode under the pyrolysis temperature of 500°C. The results showed that the performance of helical screw reactor at 50 rpm successfully improved the heat transfer rate, saved the pyrolysis time, improved the quantity and quality of liquid product. Although the process was operated at the heating rate of 10°C/min, the liquid product was successfully obtained higher than 50 wt.%. In addition, the significant finding of this reactor also can be clearly observed from the obtained quality of liquid which contained high organic phase, low water content, and high energy density. Based on the results, HSFBR can be proposed as an alternative reactor to cover the weakness of slow heating rate condition in producing the high liquid yield product.

5.1.3 Part 3: Pyrolysis of Palm Shell using Helical Screw-Fluidized Bed Reactor: Effect of Heating Rate.

Pyrolysis experiments were performed at different heating rates ranging from 50 to 275°C/min with constant torque 50 rpm of helical screw at 500°C. The following results were drawn from this study. Bio-oil and gas yields increased with the increase in heating rate. A maximum bio-oil yield of 72.86 wt.% was achieved at heating rate of 275°C/min. The density of the oil was improved from 1040 to 1053kg/m³ and water content was reduced from 4.71 to 2.44 wt.% and viscosity was progressively increased from 21.5 to 29.9 Cp when the heating rate was increased from 50 to 275°C/min. Fuel properties analysis showed HHV of about 44.41 MJ/kg which is compatible with the diesel fuel HHV (45 MJ/kg). The FTIR analysis showed that the bio-oil was dominated by carboxylic acid and alkenes. The high content of carboxylic acid 39.47%, alkenes 20.9% and alkyl group with 14.68 % were identified by GCMS analysis are highly suitable for extraction from the bio-oil as value-added chemicals. Ultimate analysis of by-product biochar showed a decrease in the carbon content on increasing heating rate and FTIR analysis showed high concentration of OH groups with greater intensity of the band in the range of 2750-3000 cm⁻¹. The TGA analysis depicted higher decomposition profile of by-product biochar sample with 50°C/min heating rate, while the DTG profile illustrated the high degradation rate followed with 0.04, 0.06, 0.10 and 0.53 wt.%/min, respectively of by-product char was observed with four sharp peaks.

5.1.4 Part 4: Effect of temperature and feed rate on pyrolysis oil produced via helical screw fluidized bed reactor

Parametric study on the effects of pyrolysis temperature and biomass feeding rate on the production of PS-derived bio-oil by helical screw fluidized bed reactor was done in this work. The results showed that the temperature and the feed rate had significant effects on the physicochemical properties of pyrolytic products. When pyrolysis temperature or feed rate was increased, the yields of bio-oil and gas were increased while biochar yield was decreased. The increase in these parameters enabled better heat transfer rate and reactant mixing to promote biomass volatilization. FTIR and GC/MS analyses indicated the presence of aromatics, alkanes, alkenes, alcohols, phenols, ketones, aldehydes, acids and esters within the bio-oil and the biochar. The enhanced biomass volatilization at higher feed rate and pyrolysis temperature also resulted in greater extent in oxygenates cracking to produce bio-oil of higher heating values, carbon, hydrogen contents and lower oxygen contents. With the production of bio-oil at higher quantity and quality at these settings, the biochar was noted to decrease in its yield and quality as most of the pyrolytic products were volatilized and concentrated in the liquid product. The presence of oxygenate residue within bio-oil also indicates the necessity of subsequent oxygen removal process such as hydrodeoxygenation to further reduce the oxygen content and increase the heating value of bio oil so as to be comparative with the properties of conventional liquid fuel.

5.1.5 Part 5: Palm shell pyrolysis in a novel helical screw fluidized bed reactor: Effect of particle size, pyrolysis time and vapor residence time on bio-oil yield and characteristics

Herein this study, the pyrolysis of palm shell was investigated in a locally designed and fabricated helical screw fluidized bed reactor. The effects of PS particle size, pyrolysis time and vapor residence time on the production quantity and quality of bio-oil were investigated. The following conclusions have been drawn in the light of these experimental results. The optimum condition for PS pyrolysis in HSFBR is at 2 mm particle size, 30 min pyrolysis time and 0.25s vapor residence time to produce PS derived bio-oil of the highest yield (73.86 wt.%) and HHV (43.14 MJ/kg). This condition provided the optimum heat and mass transfer and reaction time for the biomass conversion to C₅-C₁₅ components while reducing the tendency of secondary cracking reactions which further convert these components into condensable hydrocarbon gases at extended duration. While the optimized conditions reported here may alter depending on the scale, type of reactor and type of feedstock, herein this study, we have also shown one of distinct features of HSFBR in handling large biomass particle size ranging up to 10 mm with good production of bio-oil in terms of quantity and quality. While previous studies have recommended a particle size of 2 mm for optimum mass and heat transfers for maximum bio-oil yield, the HSFBR pyrolysis only showed a slight deterioration in bio-oil yield and HHV by less than 1% and 3% respectively. This insight would offer the possibility of reducing the need for size reduction process, thereby minimizing pyrolysis process complexity and cost. The data obtained by this research can establish a useful benchmark to optimize biomass pyrolysis process via HSFBRs of different scales in future studies.

5.2 Recommendations for future work

This project work has demonstrated the performance of novel helical screw fluidized bed reactor. Furthermore, this is entirely a different method of biomass fluidization without using any inert gas and particulate separation device for bio-oil production at slow, medium and fast pyrolysis mode. The following recommendations are suggested for future research on pyrolysis reactor to enhance the product quality.

- Considering all types of the reactors, design aspects, facilities, advantages and disadvantages, the designing of a more efficient semi-continuous or continuous pyrolysis reactor would certainly be of great need and advantage in the field of pyrolysis process.
- The presence of oxygenate residue within the bio-oil also indicates the necessity of subsequent oxygen removal process such as hydrodeoxygenation to further reduce the oxygen content and increase the heating value of bio oil so as to be comparative with the properties of conventional liquid fuel.
- The new reactor technology and operating parameters is a topic to be explored further which seems to be the main effecting factors on bio-oil composition and quality in obtaining HHV.
- Upgrading of bio-oils is currently confined to expensive catalysts such as Pt, Pd, Co etc. Therefore, byproduct biochar can be tested with different loading after activation for bio-oil upgradation.
- Electrical furnaces increase the process cost to achieve high temperatures during the pyrolysis. While, pyrolysis process produces by-product biochar and syn gas, which might be considered as one of the potential energy source to cut the pyrolysis cost.

REFERENCES

- [1] M. Jahirul, M. G. Rasul, A. A. Chowdhury, and N. Ashwath, "Biofuels production through biomass pyrolysis-A technological review," *Energies*, vol. 5, pp. 4952-5001, 2012.
- [2] F. Abnisa, W. M. A. Wan Daud, and J. N. Sahu, "Optimization and characterization studies on bio-oil production from palm shell by pyrolysis using response surface methodology," *Biomass and Bioenergy*, vol. 35, pp. 3604-3616, 2011.
- [3] F. Abnisa, A. Arami Niya, W. M. A. Wan Daud, J. N. Sahu, and I. M. Noor, "Utilization of oil palm tree residues to produce bio-oil and bio-char via pyrolysis," *Energy Conversion and Management*, vol. 76, pp. 1073-1082, 2013.
- [4] O. P. Gupta, "Elements of Fuels, Furnaces and Refractories," *Khanna Publishers.*, vol. 6th ed.
- [5] N. Gomez, J. G. Rosas, J. Cara, O. Martinez, J. A. Albuquerque, and M. E. Sanchez, "Slow pyrolysis of relevant biomasses in the Mediterranean basin. Part 1. Effect of temperature on process performance on a pilot scale," *Journal of Cleaner Production*, vol. 1, pp. 1-10, 2014.
- [6] W. M. Koo, S. H. Jung, and J. S. Kim, "Production of bio-oil with low contents of copper and chlorine by fast pyrolysis of alkaline copper quaternary-treated wood in a fluidized bed reactor," *Energy*, vol. 68, pp. 555-561, 2014.
- [7] Ioannis D. Manariotis, K. N. Fotopoulou., and H. K. Karapanagioti, "Preparation and characterization of biochar sorbents produced from malt spent rootlets," *Industrial & Engineering Chemistry Research*, vol. 54, pp. 9577-9584, 2015.
- [8] T. M. Huggins, A. Haeger, J. C. Biffinger, and Z. J. Ren, "Granular biochar compared with activated carbon for wastewater treatment and resource recovery," *Water Research*, vol. 94, pp. 225-232, 2016.
- [9] F. Abnisa and W. M. A. Wan Daud, "A review on co-pyrolysis of biomass: An optional technique to obtain a high-grade pyrolysis oil," *Energy Conversion and Management*, vol. 87, pp. 71-85, 2014.
- [10] S. S. Lam, R. K. Liew, A. Jusoh, C. T. Chong, F. N. Ani, and H. A. Chase, "Progress in waste oil to sustainable energy, with emphasis on pyrolysis techniques," *Renewable and Sustainable Energy Reviews*, vol. 53, pp. 741-753, 2016.
- [11] S. D. Anuar Sharuddin, F. Abnisa, W. M. A. Wan Daud, and M. K. Aroua, "A review on pyrolysis of plastic wastes," *Energy Conversion and Management*, vol. 115, pp. 308-326, 2016.
- [12] A. M. C. W. M. Ronald, A. S. Bradly, , "Introduction to Chemical Reaction Engineering & Kinetics," *John Wiley & Sons, Inc.*, vol. 1, 1999.

- [13] W. Green. Don and H. Perry. Robert, *Perrys Chemical Engineering Hand Book*, 8th ed. vol. 1: McGraw-Hill, 2008.
- [14] T. Kan, V. Strezov, and T. Evans, "Lignocellulosic biomass pyrolysis: A review of product properties and effects of pyrolysis parameters," *Renewable and Sustainable Energy Reviews*, vol. 57, pp. 1126-1140, 2016.
- [15] J. Ngoh and E. W. C. Lim, "Effects of particle size and bubbling behavior on heat transfer in gas fluidized beds," *Applied Thermal Engineering*, vol. 105, pp. 225-242, 2016.
- [16] A. Burton and H. Wu, "Influence of biomass particle size on bed agglomeration during biomass pyrolysis in fluidised bed," *Proceedings of the Combustion Institute*, pp. 1-7, 2016.
- [17] J. Gan, Z. Zhou, and A. Yu, "Particle scale study of heat transfer in packed and fluidized beds of ellipsoidal particles," *Chemical Engineering Science*, vol. 144, pp. 201-215, 2016.
- [18] F. Gao, "Pyrolysis of waste plastics into fuels," Doctor of Philosophy, Chemical and Process Engineering, University of canterbury new zealand, New Zealand, 2010.
- [19] W. N. R. W. Isahak, M. W. M. Hisham, M. A. Yarmo, and T. y. Yun Hin, "A review on bio-oil production from biomass by using pyrolysis method," *Renewable and Sustainable Energy Reviews*, vol. 16, pp. 5910-5923, 2012.
- [20] P. V and S. J, "Large-Scale Pyrolysis Oil Production," *A national laboratory of the U.S. Department of Energy Office of Energy Efficiency & Renewable Energy*, U.S., 2006.
- [21] A. V. Bridgwater, "Principles and practice of biomass fast pyrolysis processes for liquids," *Journal of Analytical and Applied Pyrolysis*, vol. 51, pp. 3-22, 1999.
- [22] D. L. Klass, "Biomass for Renewable Energy," in *Fuels and Chemicals*, Academic Press: San Diego, USA1998.
- [23] J. Shen, X.-S. Wang, M. Garcia-Perez, D. Mourant, M. J. Rhodes, and C.-Z. Li, "Effects of particle size on the fast pyrolysis of oil mallee woody biomass," *Fuel*, vol. 88, pp. 1810-1817, 2009.
- [24] R. Azargohar, K. L. Jacobson, E. E. Powell, and A. K. Dalai, "Evaluation of properties of fast pyrolysis products obtained, from Canadian waste biomass," *Journal of Analytical and Applied Pyrolysis*, vol. 104, pp. 330-340, 2013.
- [25] N. Puy, R. Murillo, M. V. Navarro, J. M. Lopez, J. Rieradevall, G. Fowler, *et al.*, "Valorisation of forestry waste by pyrolysis in an auger reactor," *Waste Management*, vol. 31, pp. 1339-1349, 2011.

- [26] M. Milhe, L. van de Steene, M. Haube, J. M. Commandre, W. F. Fassinou, and G. Flamant, "Autothermal and allothermal pyrolysis in a continuous fixed bed reactor," *Journal of Analytical and Applied Pyrolysis*, vol. 103, pp. 102-111, 2013.
- [27] A. Tumbalam Gooty, D. Li, F. Berruti, and C. Briens, "Kraft lignin pyrolysis and fractional condensation of its bio-oil vapors," *Journal of Analytical and Applied Pyrolysis*, vol. 106, pp. 33-40, 2014.
- [28] D. D. Hsu, "Life cycle assessment of gasoline and diesel produced via fast pyrolysis and hydroprocessing," *Biomass and Bioenergy*, vol. 45, pp. 41-47, 2012.
- [29] J. Susanne, M. Pimphan, S. Lesley, and P. Asanga, "Process design and economics for the conversion of lignocellulosic biomass to hydrocarbon fuels," National renewable energy laboratory 2013.
- [30] L. Paul and K. Masaomi, "Biomass for Heat and Power," 2015.
- [31] A. V. Bridgwater, "Review of fast pyrolysis of biomass and product upgrading," *Biomass and Bioenergy*, vol. 38, pp. 68-94, 2012.
- [32] J. Alvarez, G. Lopez, M. Amutio, J. Bilbao, and M. Olazar, "Bio-oil production from rice husk fast pyrolysis in a conical spouted bed reactor," *Fuel*, vol. 128, pp. 162-169, 2014.
- [33] J. N. Brown, "Development of a lab-scale auger reactor for biomass fast pyrolysis and process optimization using response surface methodology," Master of Science, Mechanical Engineering; Biorenewable Resources and Technology, Iowa State University, USA, 2009.
- [34] J. Lede, "Comparison of contact and radiant ablative pyrolysis of biomass," *Journal of Analytical and Applied Pyrolysis*, vol. 70, pp. 601-618, 2003.
- [35] B. Robert C and H. Jennifer, "Fast pyrolysis and bio-oil upgrading," Iowa state university USA.
- [36] D. Radlein and A. Quignard, "A short historical review of fast pyrolysis of biomass," *Oil & Gas Science and Technology*, vol. 68, pp. 765-783, 2013.
- [37] A. V. Bridgwater, "Renewable fuels and chemicals by thermal processing of biomass," *Chemical Engineering Journal*, vol. 91, pp. 87-102, 2003.
- [38] S. Nanda, "Reactors and fundamentals of reactors design for chemical reaction," Ph.D Dept.of pharmaceutical sciences M.D. university, Haryana, 2008.
- [39] O. Anja, S. Yrjo, A. Vesa, K. Eeva, and S. Kai, "Fast Pyrolysis Bio-Oils from Wood and Agricultural Residues," *Energy & Fuels*, vol. 24 pp. 1380-1388, 2010.
- [40] E. Butler, G. Devlin, D. Meier, and K. McDonnell, "A review of recent laboratory research and commercial developments in fast pyrolysis and upgrading," *Renewable and Sustainable Energy Reviews*, vol. 15, pp. 4171-4186, 2011.

- [41] E. Hoekstra, K. J. Hogendoorn, X. Wang, R. Westerhof, S. Kersten, W. Swaaij, *et al.*, "Fast Pyrolysis of Biomass in a Fluidized Bed Reactor: In Situ Filtering of the Vapors," *Ind. Eng. Chem. Res.*, vol. 48, pp. 4744-4756, 2009.
- [42] P. Basu, "Biomass gasification and pyrolysis : practical design and theory," Elsevier 2010.
- [43] S. Yorgun and D. Yıldız, "Slow pyrolysis of paulownia wood: Effects of pyrolysis parameters on product yields and bio-oil characterization," *Journal of Analytical and Applied Pyrolysis*, vol. 114, pp. 68-78, 2015.
- [44] T. Aysu and M. M. Kucuk, "Biomass pyrolysis in a fixed-bed reactor: Effects of pyrolysis parameters on product yields and characterization of products," *Energy*, vol. 64, pp. 1002-1025, 2014.
- [45] J. D. Martinez, N. Puy, R. Murillo, T. Garcia, M. V. Navarro, and A. M. Mastral, "Waste tyre pyrolysis-A review," *Renewable and Sustainable Energy Reviews*, vol. 23, pp. 179-213, 2013.
- [46] R. M, P. V, and S. J, "Large-Scale Pyrolysis Oil Production," 2006.
- [47] A. V. Bridgwater, "Review of fast pyrolysis of biomass and product upgrading," *Biomass and Bioenergy*, vol. 38, pp. 68-94, 2012.
- [48] J. Dai and J. R. Grace, "Biomass granular screw feeding: An experimental investigation," *Biomass and Bioenergy*, vol. 35, pp. 942-955, 2011.
- [49] C. Liu, H. Wang, A. M. Karim, J. Sun, and Y. Wang, "Catalytic Fast Pyrolysis of Lignocellulosic Biomass," *Chemical Society Reviews*, vol. 1, pp. 1-53, 2014
- [50] J. F. Peters, F. Petrakopoulou, and J. Dufour, "Exergetic analysis of a fast pyrolysis process for bio-oil production," *Fuel Processing Technology*, vol. 119, pp. 245-255, 2014.
- [51] J. Ward, M. G. Rasul, and M. M. K. Bhuiya, "Energy recovery from biomass by fast pyrolysis," *Procedia Engineering*, vol. 90, pp. 669-674, 2014.
- [52] R. Zhang, H. M. El Mashad, K. Hartman, F. Wang, G. Liu, C. Choate, *et al.*, "Characterization of food waste as feedstock for anaerobic digestion," *Bioresource Technology*, vol. 98, pp. 929-935, 2007.
- [53] T. Kandaramath Hari, Z. Yaakob, and N. N. Binitha, "Aviation biofuel from renewable resources: Routes, opportunities and challenges," *Renewable and Sustainable Energy Reviews*, vol. 42, pp. 1234-1244, 2015.
- [54] X. Peng, X. Ma, Y. Lin, Z. Guo, S. Hu, X. Ning, *et al.*, "Co-pyrolysis between microalgae and textile dyeing sludge by TG-FTIR: Kinetics and products," *Energy Conversion and Management*, vol. 100, pp. 391-402, 2015.

- [55] C. Sethuraman, K. Srinivas, and G. Sekaran, "Pyrolysis coupled pulse oxygen incineration for disposal of hazardous chromium impregnated fine particulate solid waste generated from leather industry," *Journal of Environmental Chemical Engineering*, vol. 2, pp. 516-524, 2014.
- [56] F. Alireza, B. Farzaneh, J. Leila, A. C. Nor, and A. E. Bayat, "Malaysia's stand on municipal solid waste conversion to energy: A review," *Renewable and Sustainable Energy Reviews*, vol. 58, pp. 1007-1016, 2016.
- [57] P. McKendry, "Energy production from biomass (part 1): overview of biomass," *Bioresource Technology*, vol. 83, pp. 37-46, 2002.
- [58] S. N. Duric, Z. L. Kaluderovic, T. R. Kosanic, M. B. Ceranic, M. M. Milotic, and S. D. Brankov, "Experimental investigation of pyrolysis process of agricultural biomass mixture," *Periodica Polytechnica Chemical Engineering*, vol. 58, pp. 141-147, 2014.
- [59] V. P. M. Ringer, and J. Scahill "Large scale pyrolysis oil production," A national laboratory of the U.S. department of energy office of energy efficiency and renewable energy, U.S.2006.
- [60] H. Li, Q. Chen, X. Zhang, K. N. Finney, V. N. Sharifi, and J. Swithenbank, "Evaluation of a biomass drying process using waste heat from process industries: A case study," *Applied Thermal Engineering*, vol. 35, pp. 71-80, 2012.
- [61] S. Megha and S. Sanjay, "Solar Drying Technologies: A review," *International Refereed Journal of Engineering and Science*, pp. 29-35, 2015.
- [62] M. Kumar, S. K. Sansaniwal, and P. Khatak, "Progress in solar dryers for drying various commodities," *Renewable and Sustainable Energy Reviews*, vol. 55, pp. 346-360, 2016.
- [63] X. Wang, H. Chen, S. Zhang, B. Zhu, and H. Yang, "Microwave drying of biomass and its effect on pyrolysis characteristics," *Journal of Fuel Chemistry and Technology*, 2011.
- [64] S. Sachidananda, M. Din, R. Chandrika, G. Sahoo, and S. D. Roy., "Performance evaluation of biomass fired dryer for copra drying: A comparison with traditional drying in subtropical climate," *Journal of Food Process Technology*, vol. 5, pp. 1-5, 2014.
- [65] R. Patil and R. Gawande, "A review on solar tunnel greenhouse drying system," *Renewable and Sustainable Energy Reviews*, vol. 56, pp. 196-214, 2016.
- [66] G. Pirasteh, R. Saidur, A. Rahman, and A. Rahim, "A review on development of solar drying applications," *Renewable and Sustainable Energy Reviews*, vol. 31, pp. 133-148, 2014.
- [67] M. Asadullah, "Barriers of commercial power generation using biomass gasification gas: A review," *Renewable and Sustainable Energy Reviews*, vol. 29, pp. 201-215, 2014.

- [68] P. A. Puschner, "Microwave vacuum drying for advanced process technology," ed, 2015.
- [69] L. Fagernas, J. Brammer, C. Wilén, M. Lauer, and F. Verhoeff, "Drying of biomass for second generation synfuel production," *Biomass and Bioenergy*, vol. 34, pp. 1267-1277, 2010.
- [70] Z. Miao, T. E. Grift, A. C. Hansen, and K. C. Ting, "Energy requirement for comminution of biomass in relation to particle physical properties," *Industrial Crops and Products*, vol. 33, pp. 504-513, 2011.
- [71] Manlu. Yu, Alvin R. Womac, and L. O. Pordesimo, "Review of biomass size reduction technology," presented at the presented at the annual international meeting american society of agricultural engineers , riviera hotel and convention center las vegas, nevada,USA, 2003.
- [72] S. Mani, L. G. Tabil, and S. Sokhansanj, "Grinding performance and physical properties of wheat and barley straws, corn stover and switchgrass," *Biomass and Bioenergy*, vol. 27, pp. 339-352, 2004.
- [73] J. Akhtar and N. Saidina Amin, "A review on operating parameters for optimum liquid oil yield in biomass pyrolysis," *Renewable and Sustainable Energy Reviews*, vol. 16, pp. 5101-5109, 2012.
- [74] E. Ortega-Rivas, *Unit Operations of Particulate Solids: Theory and Practice* vol. 2. U.S: Taylor and Francis Group, 2011.
- [75] J. S. Tumuluru, L. G. Tabil, Y. Song, K. L. Iroba, and V. Meda, "Grinding energy and physical properties of chopped and hammer-milled barley, wheat, oat, and canola straws," *biomass and bioenergy*, vol. 60, pp. 58-67, 2014.
- [76] B. Liu, H. Wang, T. Hu, P. Zhang, Z. Zhang, S. Pan, *et al.*, "Ball-milling changed the physicochemical properties of SPI and its cold-set gels," *Journal of Food Engineering*, vol. 195, pp. 158-165, 2017.
- [77] C. Gong, J. Huang, C. Feng, G. Wang, L. Tabil, and D. Wang, "Effects and mechanism of ball milling on torrefaction of pine sawdust," *Bioresource Technology*, vol. 214, pp. 242-247, 2016.
- [78] D. W. Fuerstenau and A. Z. M. Abouzeid, "The energy efficiency of ball milling in comminution," *International Journal of Mineral Processing*, vol. 67, pp. 161-185, 2002.
- [79] M. D. Dilts, "Application of the rollermill and hammermill for biomass fractionation," MASTER OF SCIENCE, Iowa State University, 2007.
- [80] S. Romuli, S. Karaj, and J. Müller, "Influence of physical properties of *Jatropha curcas* L. seeds on shelling performance using a modified disc mill," *Industrial Crops and Products*, vol. 77, pp. 1053-1062, 2015.

- [81] J. Dai, H. Cui, and J. R. Grace, "Biomass feeding for thermochemical reactors," *Progress in Energy and Combustion Science*, vol. 38, pp. 716-736, 2012.
- [82] K. H. Kim, X. Bai, M. Rover, and R. C. Brown, "The effect of low concentration oxygen in sweep gas during pyrolysis of red oak using a fluidized bed reactor," *Fuel*, vol. 124, pp. 49-56, 2014.
- [83] R. Michael, K. Deepak, S. Karthick, and B. Abirami, "Improvements in Existing Controls and Silo Capacity," *IJESC*, vol. 6, pp. 3544-3549, 2016.
- [84] G. Velmurugan, E. Palaniswamy, M. Sambathkumar, R. Vijayakumar, and T. M. Sakthimuruga, "Conveyor Belt Troubles (Bulk Material Handling)," *IJEERT*, vol. 2, pp. 21-30, 2014.
- [85] A. U. Ltd. Operating Manual (Original) for Air operated Pinch Valves [Online]. Available: <https://ako-knc1tkgpuqdk3k2d.netdna-ssl.com/wp-content/uploads/2016/10/Operating-Manual-for-AKO-Pinch-Valves.pdf>
- [86] G. G. Chase, *Solids notes 10, The University of Akron United States*, 2004
- [87] R. Deepak, K. Deepak, S. Karthick, and B. Abirami, "Improvements in existing controls and silo capacity," *International Journal of Engineering Science and Computing*, vol. 6, pp. 3544-3549, 2016.
- [88] J. R. Couper, W. R. Penney, and J. R. Fair, *Chemical Process Equipment-Selection and Design revised 2nd edition*, 2nd ed. vol. 1. UK: Butterworth-Heinemann, 2010.
- [89] D. Lathouwers and J. Bellan, "Yield Optimization and Scaling of Fluidized Beds for Tar Production from Biomass," *Energy & Fuels*, vol. 15, pp. 1247-1262, 2001.
- [90] D. Czajczynska, L. Anguilano, H. Ghazal, R. Krzyżyńska, A. J. Reynolds, N. Spencer, *et al.*, "Potential of pyrolysis processes in the waste management sector," *Thermal Science and Engineering Progress*, vol. 3, pp. 171-197, 2017/09/01/2017.
- [91] C. C. M. w. Ltd., Ed., ed. Canada: www.continentalconveyor.ca, 1986.
- [92] S. A. Simon and M. A. L. Nicoletis. (2002). *Methods in Chemosensory Research*. Available: <https://books.google.com.my/books?id=rA3OBQAAQBAJ&pg=PA37&lpg=PA37&dq=research+on+Pinch+valve+problems&sour>.
- [93] M. G. Rasul and M. I. Jahirul, "Recent developments in biomass pyrolysis for bio-fuel production: Its potential for commercial applications," in *Recent Researches in Environmental and Geological Sciences*, ed, 2012, pp. 256-265.
- [94] V. Kachrimanidou, N. Kopsahelis, C. Webb, and A. A. Koutinas, "Chapter 24- Bioenergy technology and food industry waste valorization for integrated production of polyhydroxyalkanoates," in *Bioenergy Research: Advances and Applications*, V. K. Gupta, M. G. T. P. Kubicek, and J. S. Xu, Eds., ed Amsterdam: Elsevier, 2014, pp. 419-433.

- [95] B. Valle, A. Remiro, B. Aramburu, J. Bilbao, and A. G. Gayubo, "Strategies for maximizing the bio-oil valorization by catalytic transformation," *Journal of Cleaner Production*, vol. 88, pp. 345-348, 2015.
- [96] G. S. Miguel, J. Makibar, and A. R. F. Akarreg, "New advances in the fast pyrolysis of biomass," *Journal of Biobased Materials and Bioenergy*, vol. 6, pp. 1-11, 2012.
- [97] M. Verma, S. Godbout, S. K. Brar, O. Solomatnikova, S. P. Lemay, and J. P. Larouche, "Biofuels Production from Biomass by Thermochemical Conversion Technologies," *International Journal of Chemical Engineering*, vol. 1, pp. 1-18, 2012.
- [98] M. Carrier, J.-E. Joubert, S. Danje, T. Hugo, J. Görgens, and J. Knoetze, "Impact of the lignocellulosic material on fast pyrolysis yields and product quality," *Bioresource Technology*, vol. 150, pp. 129-138, 2013.
- [99] N. Jendoubi, F. Broust, J. M. Commandre, G. Mauviel, M. Sardin, and J. Lédé, "Inorganics distribution in bio oils and char produced by biomass fast pyrolysis: The key role of aerosols," *Journal of Analytical and Applied Pyrolysis*, vol. 92, pp. 59-67, 2011.
- [100] L. Dongbing, B. Cedric, and B. Franco, "Improved lignin pyrolysis for phenolics production in a bubbling bed reactor – Effect of bed materials," *Bioresource Technology*, vol. 189, pp. 7-14, 2015.
- [101] S. Li, A. Sanna, and J. M. Andresen, "Influence of temperature on pyrolysis of recycled organic matter from municipal solid waste using an activated olivine fluidized bed," *Fuel Processing Technology*, vol. 92, pp. 1776-1782, 2011.
- [102] D. Li, F. Berruti, and C. Briens, "Autothermal fast pyrolysis of birch bark with partial oxidation in a fluidized bed reactor," *Fuel*, vol. 121, pp. 27-38, 2014.
- [103] C. S. Lira, F. M. Berruti, P. Palmisano, F. Berruti, C. Briens, and A. A. B. Pecora, "Fast pyrolysis of Amazon tucuma (*Astrocaryum aculeatum*) seeds in a bubbling fluidized bed reactor," *Journal of Analytical and Applied Pyrolysis*, vol. 99, pp. 23-31, 2013.
- [104] E. Butler, G. Devlin, D. Meier, and K. McDonnell, "Fluidised bed pyrolysis of lignocellulosic biomasses and comparison of bio-oil and micropyrolyser pyrolysate by GC/MS-FID," *Journal of Analytical and Applied Pyrolysis*, vol. 103, pp. 96-101, 2013.
- [105] A. J. S. Marshall, "Overview of Pyrolysis and Chemical Conversion Technologies," *Commercial Application of Pyrolysis Technology in Agriculture*, vol. 1, pp. 1-66, 2013.
- [106] B. Franco, B. Cedric, B. Federico, and F. Lorenzo. A Mobile Pyrolyzer for Converting Agricultural and Forestry Residues into Liquid Bio-Oil and Bio-Char [Online]. Available: http://dc.engconfintl.org/cgi/viewcontent.cgi?article=1017&context=co2_summit

- [107] P. C. Badger and P. Fransham, "Use of mobile fast pyrolysis plants to densify biomass and reduce biomass handling costs—A preliminary assessment," *Biomass and Bioenergy*, vol. 30, pp. 321-325, 2006.
- [108] K. C. Sembiring, N. Rinaldi, and S. P. Simanungkalit, "Bio-oil from Fast Pyrolysis of Empty Fruit Bunch at Various Temperature," *Energy Procedia*, vol. 65, pp. 162-169, 2015.
- [109] M. Jussi, "Cooperation is key in developing new technologies," in *ENERGY TECHNOLOGY IN FOCUS*, ed. Finland, 2015.
- [110] V. d. V. Manon, F. Xianfeng, I. Andy, and B. Jan, "Fast Pyrolysis of Biomass in a Circulating Fluidised Bed," in *The 12th International Conference on Fluidization - New Horizons in Fluidization Engineering*, 2007, pp. 897-904.
- [111] J.-P. Cao, X.-B. Xiao, S.-Y. Zhang, X.-Y. Zhao, K. Sato, Y. Ogawa, *et al.*, "Preparation and characterization of bio-oils from internally circulating fluidized-bed pyrolyses of municipal, livestock, and wood waste," *Bioresource Technology*, vol. 102, pp. 2009-2015, 2011.
- [112] W. C. Dai Xianwen, Li Haibin, and Chen Yong, "The Fast Pyrolysis of Biomass in CFB Reactor," *Energy & Fuels*, vol. 14, pp. 552-557, 2000.
- [113] D. Tongli, L. Songgeng, X. Jianjun, S. Wenli, Y. Jianzhong, and L. Weigang, "Rapid Pyrolysis of Wheat Straw in a Bench-Scale Circulating Fluidized-Bed Downer Reactor," *Chem. Eng. Technol.*, vol. 35, pp. 2170-2176, 2012.
- [114] K. Duanguppama, N. Suwapaet, and A. Pattiya, "Fast pyrolysis of contaminated sawdust in a circulating fluidised bed reactor," *Journal of Analytical and Applied Pyrolysis*, vol. 118, pp. 63-74, 2016.
- [115] L. Gartzen, A. Maider, E. Gorika, A. Maite, A. Haritz, and M. Olazar, "A conical spouted bed reactor for the valorization of waste tires" in *The 13th International Conference on Fluidization - New Paradigm in Fluidization Engineering*, ed. Spain, 2010, pp. 1-9.
- [116] M. Amutio, G. Lopez, M. Artetxe, G. Elordi, M. Olazar, and J. Bilbao, "Influence of temperature on biomass pyrolysis in a conical spouted bed reactor," *Resources, Conservation and Recycling*, vol. 59, pp. 23-31, 2012.
- [117] A. G. Haritz, Lopez. Javier, Bilbao. Martin, Olazar., "Minimum Spouting Velocity of Conical Spouted Beds Equipped with Draft Tubes of Different Configuration," *Ind. Eng. Chem. Res.*, vol. 52, pp. 2995-3006, 2013.
- [118] Z. Zhang, T. P. Hills, S. A. Scott, and P. S. Fennell, "Spouted bed reactor for kinetic measurements of reduction of Fe₂O₃ in a CO₂/CO atmosphere Part I: Atmospheric pressure measurements and equipment commissioning," *Chemical Engineering Research and Design*, vol. 114, pp. 307-320, 2016.

- [119] A. Fernandez, J. Makibar, G. Lopez, M. Amutio, and M. Olazar, "Design and operation of a conical spouted bed reactor pilot plant (25kg/h) for biomass fast pyrolysis," *Fuel Processing Technology*, vol. 112, pp. 48-56, 2013.
- [120] J. Makibar, A. R. Fernandez-Akarregi, M. Amutio, G. Lopez, and M. Olazar, "Performance of a conical spouted bed pilot plant for bio-oil production by poplar flash pyrolysis," *Fuel Processing Technology*, vol. 371, pp. 283-289, 2015.
- [121] A. Fernandez-Akarreguia, J. Makibara, I. Alavaa, L. Diaza, F. Cuevaa, R. Aguadob, *et al.*, "Sand attrition in conical spouted beds," *Particuology*, vol. 10, pp. 592- 599, 2012.
- [122] J. Alvarez, M. Amutio, G. Lopez, I. Barbarias, J. Bilbao, and M. Olazar, "Sewage sludge valorization by flash pyrolysis in a conical spouted bed reactor," *Chemical Engineering Journal*, vol. 273, pp. 173-183, 2015.
- [123] L. Gartzzen, A. Maider, E. Gorika, A. Maite, E. Aitziber, B. Astrid, *et al.*, "Waste tyre pyrolysis in a conical spouted bed reactor under vacuum conditions," *Int. Conf. Energy Dev., Environ. Biomed., 4th*, vol. 1, pp. 91-96, 2010.
- [124] EMPYRO Project – New commercial scale fast pyrolysis plant [Online]. Available: <https://biorrefineria.blogspot.my/2015/06/empyro-project-commercial-scale-fast-pyrolysis-plant.html>
- [125] R. W. J. Westerhout, J. Waanders, J. A. M. Kuipers, and W. P. M. van Swaaij, "Development of a continuous rotating cone reactor pilot plant for the pyrolysis of polyethene and polypropene," *Industrial & Engineering Chemistry Research*, vol. 37, pp. 2316-2322, 1998.
- [126] B. M. Wagenaar, R. H. Venderbosch, J. Carrasco, R. Strenziok, and B. J. van der Aa, "Rotating Cone Bio-Oil Production and Applications," in *Progress in Thermochemical Biomass Conversion*, ed: Blackwell Science Ltd, 2008, pp. 1268-1280.
- [127] B. M. Wagenaar, W. Prins, and W. P. M. van Swaaij, "Pyrolysis of biomass in the rotating cone reactor: modelling and experimental justification," *Chemical Engineering Science*, vol. 49, pp. 5109-5126, 1994/12/01 1994.
- [128] J. Li, "The Optimal of Pyrolysis Process in the Rotating Cone Reactor and Pyrolysis Product Analysis," presented at the International Conference on Challenges in Environmental Science and Computer Engineering, Harbin,China, 2010.
- [129] H. Guoxin, G. Xiwu, H. Hao, F. Haojie, and W. Zheng, "Experimental studies on flow and pyrolysis of coal with solid heat carrier in a modified rotating cone reactor," *Chemical Engineering and Processing: Process Intensification*, vol. 47, pp. 1777-1785, 2008.

- [130] G. V. C. Peacocke, C. M. Dick, R. A. Hague, L. A. Cooke, and A. V. Bridgwater, "Comparison of ablative and fluid bed fast pyrolysis products: yields and analyses," in *Biomass for Energy and the Environment*, ed Oxford: Pergamon, 1996, pp. 1632-1637.
- [131] V. Barkha, S. Abhijit, S. Pooja, K. S. Parbhat, S. Chanda, and P. S. Rajeev, *Recycling of Solid waste for biofuels and bio-chemicals*: Springer Singapore, 2016.
- [132] D. S. Scott, P. Majerski, J. Piskorz, and D. Radlein, "A second look at fast pyrolysis of biomass-the RTI process," *Journal of Analytical and Applied Pyrolysis*, vol. 51, pp. 23-37, 1999.
- [133] A. V. Bridgwater, D. Meier, and D. Radlein, "An overview of fast pyrolysis of biomass," *Organic Geochemistry*, vol. 30, pp. 1479-1493, 1999.
- [134] J. Lede, P. Janis, Z. L. Huai, and V. Jacques, "Fast pyrolysis of wood: direct measurement and study of ablation rate," *FUEL*, vol. 64, pp. 1-7, 1985.
- [135] G. Luo, D. S. Chandler, L. C. A. Anjos, R. J. Eng, P. Jia, and F. L. P. Resende, "Pyrolysis of whole wood chips and rods in a novel ablative reactor," *Fuel*, vol. 194, pp. 229-238, 2017.
- [136] G. V. C. Peacocke and A. V. Bridgwater, "Ablative plate pyrolysis of biomass for liquids," *Biomass and Bioenergy*, vol. 7, pp. 147-154, 1994.
- [137] N. Bech, P. A. Jensen, and K. Dam-Johansen, "Ablative flash pyrolysis of straw and wood bench scale results," ed, 2007.
- [138] A. Veses, M. Aznar, J. M. Lopez, M. S. Callen, R. Murillo, and T. García, "Production of upgraded bio-oils by biomass catalytic pyrolysis in an auger reactor using low cost materials," *Fuel*, vol. 141, pp. 17-22, 2015.
- [139] J. E. Joubert, M. Carrier, N. Dahmen, R. Stahl, and J. H. Knoetze, "Inherent process variations between fast pyrolysis technologies: A case study on Eucalyptus grandis," *Fuel Processing Technology*, vol. 131, pp. 389-395, 2015.
- [140] H. Raclavska, A. Corsaro, D. Juchelkova, V. Sassmanova, and J. Frantík, "Effect of temperature on the enrichment and volatility of 18 elements during pyrolysis of biomass, coal, and tires," *Fuel Processing Technology*, vol. 131, pp. 330-337, 2015.
- [141] D. Mohan., U. P. Charles, and H. S. Philip, "Pyrolysis of Wood/Biomass for Bio-oil: A Critical Review," *Energy & Fuels*, vol. 20, pp. 848-889, 2006.
- [142] I. Agirre, T. Griessacher, G. Rosler, and J. Antrekowitsch, "Production of charcoal as an alternative reducing agent from agricultural residues using a semi-continuous semi-pilot scale pyrolysis screw reactor," *Fuel Processing Technology*, vol. 106, pp. 114-121, 2013.

- [143] A. Veses, M. Aznar, I. Martínez, J. D. Martínez, J. M. López, M. V. Navarro, *et al.*, "Catalytic pyrolysis of wood biomass in an auger reactor using calcium-based catalysts," *Bioresource Technology*, vol. 162, pp. 250-258, 2014.
- [144] R. Aguado, M. Olazar, M. J. San José, G. Aguirre, and J. Bilbao, "Pyrolysis of Sawdust in a Conical Spouted Bed Reactor. Yields and Product Composition," *Industrial & Engineering Chemistry Research*, vol. 39, pp. 1925-1933, 2000.
- [145] I. Estiati, H. Altzibar, M. Tellabide, and M. Olazar, "A new method to measure fine particle circulation rates in draft tube conical spouted beds," *Powder Technology*, vol. 316, pp. 87-91, 2017.
- [146] H. Altzibar, I. Estiati, G. Lopez, J. F. Saldarriaga, R. Aguado, J. Bilbao, *et al.*, "Fountain confined conical spouted beds," *Powder Technology*, vol. 312, pp. 334-346, 2017.
- [147] S. Aramideh, "Numerical simulation of biomass fast pyrolysis in fluidized bed and auger reactors," Master of Science, Mechanical Engineering, Iowa State University USA, 2014.
- [148] A. Sharma, V. Pareek, and D. Zhang, "Biomass pyrolysis—A review of modelling, process parameters and catalytic studies," *Renewable and Sustainable Energy Reviews*, vol. 50, pp. 1081-1096, 2015.
- [149] A. V. Bridgwater, "Review of fast pyrolysis of biomass and product upgrading," *Biomass and Bioenergy*, vol. 38, pp. 68-94, 2012.
- [150] G. Yildiza, M. Pronkb, M. Djokicc, K. M. Geemc, F. Ronssea, R. V. Durenb, *et al.*, "Validation of a new set up for continuous catalytic fast pyrolysis of biomass coupled with vapour phase upgrading," *Journal of Analytical and Applied Pyrolysis*, vol. 103, pp. 343-351, 2013.
- [151] S. Sensoz, D. Angn, and S. Yorgun, "Influence of particle size on the pyrolysis of rapeseed (*Brassica napus* L.) fuel properties of bio-oil," *Biomass and Bioenergy International Refereed Journal of Engineering and Science*, vol. 19, pp. 271-279, 2000.
- [152] X. Qingang, A. Soroush, and K. Song-Charng, "Modeling Effects of Operating Conditions on Biomass Fast Pyrolysis in Bubbling Fluidized Bed Reactors," *Energy Fuels* vol. 27, p. 5948–5956, 2013.
- [153] H. Aghdas, S. Ralph, Y. Habibollah, R. Alimorad, T. Nicole, and G. Ali Asghar, "Effect of process conditions on product yield and composition of fast pyrolysis of *Eucalyptus grandis* in fluidized bed reactor," *Journal of Industrial and Engineering Chemistry*, vol. 20, pp. 2594-2602, 2014.
- [154] S. Dijan, K. Eny, and Y. Haisa, "Yield and Composition of Bio-oil from Co-Pyrolysis of Corn Cobs and Plastic Waste of HDPE in a Fixed Bed Reactor," *Journal of the Japan Institute of Energy*, vol. 95, pp. 621-628, 2016.

- [155] Y. Le Brech, L. Jia, S. Cissé, G. Mauviel, N. Brosse, and A. Dufour, "Mechanisms of biomass pyrolysis studied by combining a fixed bed reactor with advanced gas analysis," *Journal of Analytical and Applied Pyrolysis*, vol. 117, pp. 334-346, 2016.
- [156] N. Ozbay, A. Putun, and E. Putun, "Bio-oil production from rapid pyrolysis of cottonseed cake: product yields and compositions," *International Journal of Energy Research*, vol. 30, pp. 501-510, 2006.
- [157] Z. Zhezi, Y. Setyawati, Z. Mingming, L. Jianbo, and Z. Dongke, "Effect of Temperature and Heating Rate in Pyrolysis on the Yield, Structure and Oxidation Reactivity of Pine Sawdust Biochar " presented at the Challenging Tomorrow, Australia, 2013.
- [158] A. Najaf, S. Mahmood, S. Khurram, H. Sadiq, and C. Arshad, "Effect of operating parameters on production of bio-oil from fast pyrolysis of maize stalk in bubbling fluidized bed reactor," *Pol. J. Chem. Tech.*, vol. 18, pp. 88-96, 2016.
- [159] A. Heidari, R. Stahl, H. Younesi, A. Rashidi, N. Troeger, and A. A. Ghoreyshi, "Effect of process conditions on product yield and composition of fast pyrolysis of *Eucalyptus grandis* in fluidized bed reactor," *Journal of Industrial and Engineering Chemistry*, vol. 20, pp. 2594-2602, 2014.
- [160] R. Miandad, A. S. Nizami, M. Rehan, M. A. Barakat, M. I. Khan, A. Mustafa, *et al.*, "Influence of temperature and reaction time on the conversion of polystyrene waste to pyrolysis liquid oil," *Waste Management*, vol. 58, pp. 250-259, 2016.
- [161] K. Smets, P. Adriaensens, G. Reggers, S. Schreurs, R. Carleer, and J. Yperman, "Flash pyrolysis of rapeseed cake: Influence of temperature on the yield and the characteristics of the pyrolysis liquid," *Journal of Analytical and Applied Pyrolysis*, vol. 90, pp. 118-125, 2011.
- [162] L. Gartzen, A. Maider, E. Gorika, A. Maite, E. Aitziber, B. Astrid, *et al.*, "Waste tyre pyrolysis in a conical spouted bed reactor under vacuum conditions," *Fuel*, vol. 89, pp. 1946-1952, 2010.
- [163] H. Wang, D. C. Elliott, R. J. French, S. Deutch, and K. Iisa, "Biomass Conversion to Produce Hydrocarbon Liquid Fuel Via Hot-vapor Filtered Fast Pyrolysis and Catalytic Hydrotreating," *J Vis Exp*, vol. 118, pp. 1-25, 2016.
- [164] G. V. C. Peacocke, "Ablative pyrolysis of biomass," PHD thesis, Chemical Engineering and Applied Chemistry, Aston University, Birmingham, UK, 1994.
- [165] A. Pattiya, S. Sukkasi, and V. Goodwin, "Fast pyrolysis of sugarcane and cassava residues in a free-fall reactor," *Energy*, vol. 44, pp. 1067-1077, 2012.
- [166] S. Benhadid-Dib and A. Benzaoui, "Refrigerants and their Environmental Impact Substitution of Hydro Chlorofluorocarbon HCFC and HFC Hydro Fluorocarbon. Search for an Adequate Refrigerant," *Energy Procedia*, vol. 18, pp. 807-816, 2012.

- [167] M. M. Shah, "Prediction of heat transfer during condensation in inclined plain tubes," *Applied Thermal Engineering*, vol. 94, pp. 82-89, 2016.
- [168] T. Schulzke, S. Conrad, and J. Westermeyer, "Fractionation of flash pyrolysis condensates by staged condensation," *Biomass and Bioenergy*, vol. 95, pp. 287-295, 2016.
- [169] H. Jae. Gyu, C. Hang. Seok, and P. Hoon. Chae, "Condensation performance of two different heat exchangers for collecting pyrolyzed oil," presented at the The 26th Annual Conference of JSMCWM Republic of Korea, 2015
- [170] A. Tumbalam Gooty, D. Li, C. Briens, and F. Berruti, "Fractional condensation of bio-oil vapors produced from birch bark pyrolysis," *Separation and Purification Technology*, vol. 124, pp. 81-88, 2014.
- [171] D. Chen, L. Yin, H. Wang, and P. He, "Reprint of: Pyrolysis technologies for municipal solid waste: A review," *Waste Management*, vol. 37, pp. 116-136, 2015.
- [172] R. Singh and A. Shukla, "A review on methods of flue gas cleaning from combustion of biomass," *Renewable and Sustainable Energy Reviews*, vol. 29, pp. 854-864, 2014.
- [173] P. J. Woolcock and R. C. Brown, "A review of cleaning technologies for biomass-derived syngas," *Biomass and Bioenergy*, vol. 52, pp. 54-84, 2013.
- [174] K. Elsayed, "Analysis and Optimization of Cyclone Separators Geometry Using RANS and LES Methodologies," PhD, Department of Mechanical Engineering, Brussels, Belgium, 2011.
- [175] A. A. Lappas, M. C. Samolada, D. K. Iatridis, S. S. Voutetakis, and I. A. Vasalos, "Biomass pyrolysis in a circulating fluid bed reactor for the production of fuels and chemicals," *Fuel*, vol. 81, pp. 2087-2095, 2002.
- [176] M. A, "Electrostatic Precipitation," presented at the IEEE Transactions on Dielectrics and Electrical Insulation 2000
- [177] E. B. F. Alkateb, S. Nath, and A. K. Nema, "Methods & Executions of Electrostatic Precipitator and Its Fundamental Plan," *Journal of Environmental Science, Computer Science and Engineering & Technology*, vol. 5, pp. 92-103, 2016.
- [178] D. Meier and O. Faix, "State of the art of applied fast pyrolysis of lignocellulosic materials-a review," *Bioresource Technology*, vol. 68, pp. 71-77, 1999.
- [179] C. Paenpong, S. Inthidech, and A. Pattiya, "Effect of filter media size, mass flow rate and filtration stage number in a moving-bed granular filter on the yield and properties of bio-oil from fast pyrolysis of biomass," *Bioresource Technology*, vol. 139, pp. 34-42, 2013.

- [180] T. Chen, C. Wu, R. Liu, W. Fei, and S. Liu, "Effect of hot vapor filtration on the characterization of bio-oil from rice husks with fast pyrolysis in a fluidized-bed reactor," *Bioresource Technology*, vol. 102, pp. 6178-6185, 2011.
- [181] D. Chen, L. Yin, H. Wang, and P. He, "Pyrolysis technologies for municipal solid waste: A review," *Waste Management*, vol. 34, pp. 2466-2486, 2014.
- [182] A. Oasmaa and C. Peacocke, *A guide to physical property characterisation of biomass-derived fast pyrolysis liquids* 2001.
- [183] F. Abnisa, W. M. A. W. Daud, W. N. W. Husin, and J. N. Sahu, "Utilization possibilities of palm shell as a source of biomass energy in Malaysia by producing bio-oil in pyrolysis process," *Biomass and Bioenergy*, vol. 35, pp. 1863-1872, 2011.
- [184] M. Dinesh, U. P. Charles, and S. H. Philip, "Pyrolysis of Wood/Biomass for Bio-oil: A Critical Review," *Energy & Fuels*, vol. 20, pp. 848-889, 2006.
- [185] C. J. Mulligan, L. Strezov, and V. Strezov, "Technological advances of industrial biomass pyrolysis," in *Pyrolysis: Types, Processes, and Industrial Sources and Products*, ed, 2009, pp. 237-266.
- [186] M. Jorge. Ivan, C. J. Farid, and G. P. Manuel, "Fast pyrolysis of biomass: A review of relevant aspects. Part I: Parametric study " *DYNA*, vol. 82, pp. 239-248, 2015.
- [187] A. V. Bridgwater, "Bimass fast pyrolysis," *Thermal Science*, vol. 8, pp. 21-49, 2004.
- [188] F. Visscher, J. van der Schaaf, T. A. Nijhuis, and J. C. Schouten, "Rotating reactors – A review," *Chemical Engineering Research and Design*, vol. 91, pp. 1923-1940, 2013.
- [189] Z. Ma, D. Chen, J. Gu, B. Bao, and Q. Zhang, "Determination of pyrolysis characteristics and kinetics of palm kernel shell using TGA–FTIR and model-free integral methods," *Energy Conversion and Management*, vol. 89, pp. 251-259, 2015.
- [190] Z. Ma, J. Wang, Y. Yang, Y. Zhang, C. Zhao, Y. Yu, *et al.*, "Comparison of the thermal degradation behaviors and kinetics of palm oil waste under nitrogen and air atmosphere in TGA-FTIR with a complementary use of model-free and model-fitting approaches," *Journal of Analytical and Applied Pyrolysis*, 2018.
- [191] McCabe, L. Warren, and J. Smith, *Unit Operations of Chemical Engineering*, 5 ed. vol. 1. New York: McGraw-Hill, Inc, 1993.
- [192] G. Kabir, A. T. M. Din, and B. H. Hameed, "Pyrolysis of oil palm mesocarp fiber and palm frond in a slow-heating fixed-bed reactor: A comparative study," *Bioresource Technology*, vol. 241, pp. 563-572, 2017.

- [193] A. Aho, N. Kumar, K. Eranen, B. Holmbom, M. Hupa, T. Salmi, *et al.*, "Pyrolysis of Softwood Carbohydrates in a Fluidized Bed Reactor," *International Journal of Molecular Sciences*, vol. 9, pp. 1665-1675, 2008.
- [194] D. K. Z. L. Shen, "Low Temperature Pyrolysis of an Australian Brown Coal in a Fluidised Bed Reactor," *Dev. Chem. Ens. Mineral Process*, vol. 8, pp. 293-309, 2000.
- [195] J. Bridgwater, "Mixing of particles and powders: Where next?," *Particuology*, vol. 8, pp. 563-567, 2010.
- [196] L. Valentina, G. Charles, B. Cedric, and B. Franco, "Mixing and operability characteristics of mechanically fluidized reactors for the pyrolysis of biomass," *Powder Technology*, vol. 274, pp. 205-212, 2015.
- [197] M. N. Islam, R. Zailani, and F. N. Ani, "Pyrolytic oil from fluidised bed pyrolysis of oil palm shell and its characterisation," *Renewable Energy*, vol. 17, pp. 73-84, 1999.
- [198] S. W. Kim, B. S. Koo, J. W. Ryu, J. S. Lee, C. J. Kim, D. H. Lee, *et al.*, "Bio-oil from the pyrolysis of palm and Jatropha wastes in a fluidized bed," *Fuel Processing Technology*, vol. 108, pp. 118-124, 2013.
- [199] A. Heidari, R. Stahl, H. Younesi, A. Rashidi, N. Troeger, and A. S. Ghoreyshi, "Effect of process conditions on product yield and composition of fast pyrolysis of *Eucalyptus grandis* in fluidized bed reactor," *Journal of Industrial and Engineering Chemistry*, vol. 20, pp. 2594-2602, 2014.
- [200] W. S. Ralph J. Tyler Ian, H. Edwards "Flash Pyrolysis Of Agglomerating Coal " Australia Patent 4,309,270 1982
- [201] D. Czajczyńska, L. Anguilano, H. Ghazal, R. Krzyżyńska, A. J. Reynolds, N. Spencer, *et al.*, "Potential of pyrolysis processes in the waste management sector," *Thermal Science and Engineering Progress*, vol. 3, pp. 171-197, 2017.
- [202] F. Abnisa, A. N. Arash, W. M. A. W. Daud, and J. N. Sahu, "Characterization of Bio-oil and Bio-char from Pyrolysis of Palm Oil Wastes," *Bioenerg. Res.*, vol. 6, pp. 830-840, 2013.
- [203] M. Hongting, D. Na, L. Xueyin, L. Chen, L. Junwen, and L. Zihao, "Experimental study on the heat transfer characteristics of waste printed circuit boards pyrolysis," *Science of The Total Environment*, vol. 633, pp. 264-270, 2018.
- [204] C. P. A. Oasmaa. A Guide to Physical Property Characterization of Biomass-Derived Fast Pyrolysis Liquids [Online]. Available: <https://www.vtt.fi/Documents/P450.pdf>
- [205] Y. Yang, J. G. Brammer, A. S. N. Mahmood, and A. Hornung, "Intermediate pyrolysis of biomass energy pellets for producing sustainable liquid, gaseous and solid fuels," *Bioresource Technology*, vol. 169, pp. 794-799, 2014.

- [206] R. Peerapon, T. Harakhun, and V. Tharapong, "Bio-Oil Production by Pyrolysis of Oil Palm Empty Fruit Bunch in Nitrogen and Steam Atmospheres " *Journal of Sustainable Bioenergy Systems*, vol. 2, pp. 75-85 2012.
- [207] C. Hu, H. Zhang, and R. Xiao, "Effects of nascent char on ex-situ catalytic fast pyrolysis of wheat straw," *Energy Conversion and Management*, vol. 177, pp. 765-772, 2018.
- [208] C. Wang, A. Thygesen, Y. Liu, Q. Li, M. Yang, D. Dang, *et al.*, "Bio-oil based biorefinery strategy for the production of succinic acid," *Biotechnology for Biofuels*, vol. 6, pp. 74-74, 2013.
- [209] W. Danyan, X. Shanzhi, L. Biao, C. Yingquan, Y. Haiping, W. Xianhua, *et al.*, "Influence of lignin content on pyrolysis characteristics of biomass based on part of lignin removal " *Chinese Society of Agricultural Engineering*, vol. 34, pp. 193-197, 2018.
- [210] M. V. Kumar, A. V. Babu, and P. R. Kumar, "Experimental investigation on the effects of diesel and mahua biodiesel blended fuel in direct injection diesel engine modified by nozzle orifice diameters," *Renewable Energy*, vol. 119, pp. 388-399, 2018.
- [211] A. Kumar, D. D. Jones, and M. A. Hanna, "Thermochemical Biomass Gasification: A Review of the Current Status of the Technology " *Energies* vol. 2, pp. 556-581, 2009.
- [212] S. H. Chang, "Bio-oil derived from palm empty fruit bunches: Fast pyrolysis, liquefaction and future prospects," *Biomass and Bioenergy*, vol. 119, pp. 263-276, 2018.
- [213] S. Czernik and A. V. Bridgwater, "Overview of Applications of Biomass Fast Pyrolysis Oil," *Energy & Fuels*, vol. 18, pp. 590-598, 2004.
- [214] P. Das, M. Dinda, N. Gosai, and S. Maiti, "High Energy Density Bio-oil via Slow Pyrolysis of *Jatropha curcas* Shells," *Energy & Fuels*, vol. 29, pp. 4311-4320, 2015.
- [215] S. Frigo, M. Seggiani, M. Puccini, and S. Vitolo, "Liquid fuel production from waste tyre pyrolysis and its utilisation in a Diesel engine," *Fuel*, vol. 116, pp. 399-408, 2014.
- [216] A. Funke, A. Niebel, D. Richter, M. M. Abbas, A. K. Muller, S. Radloff, *et al.*, "Fast pyrolysis char – Assessment of alternative uses within the bioliq® concept," *Bioresource Technology*, vol. 200, pp. 905-913, 2016.
- [217] J. Waluyo, I. G. B. N. Makertihartha, and H. Susanto, "Pyrolysis with intermediate heating rate of palm kernel shells: Effect temperature and catalyst on product distribution," *AIP Conference Proceedings*, vol. 1977, p. 020026, 2018.

- [218] F. Abnisa and W. M. A. Wan Daud, "Optimization of fuel recovery through the stepwise co-pyrolysis of palm shell and scrap tire," *Energy Conversion and Management*, vol. 99, pp. 334-345, 2015.
- [219] O. J. Seung, G.-G. Choi, and J.-S. Kim, "Characteristics of bio-oil from the pyrolysis of palm kernel shell in a newly developed two-stage pyrolyzer," *Energy*, vol. 113, pp. 108-115, 2016.
- [220] S. Xiaoyin, S. Ruifeng, L. Xuhui, P. Jihua, L. Xing, D. Ruonan, *et al.*, "Characterization of 60 types of Chinese biomass wasteland resultant biochars in terms of their candidacy for soil application," *GCB Bioenergy Volume* vol. 9, pp. 1423-1435.
- [221] D. T. Maria Silvana A. Moraes, Juliana M. da Silva, Maria Elisabete Machado, Laíza C. Krause, Claudia A. Zini, Rosangela A. Jacques and Elina B. Caramao, "Chromatographic Methods Applied to the Characterization of Bio-Oil from the Pyrolysis of Agro-Industrial Biomasses," ed, 2017, pp. 70-116.
- [222] Y. Lu, G.-S. Li, Y.-C. Lu, X. Fan, and X.-Y. Wei, "Analytical Strategies Involved in the Detailed Componential Characterization of Biooil Produced from Lignocellulosic Biomass," *International journal of analytical chemistry*, vol. 2017, pp. 9298523-9298523, 2017.
- [223] L. Leng, H. Li, X. Yuan, W. Zhou, and H. Huang, "Bio-oil upgrading by emulsification/microemulsification: A review," *Energy*, vol. 161, pp. 214-232, 2018/10/15/ 2018.
- [224] C. Wang, A. Thygesen, Y. Liu, Q. Li, M. Yang, D. Dang, *et al.*, "Bio-oil based biorefinery strategy for the production of succinic acid," *Biotechnology for Biofuels*, vol. 6, p. 74, 2013.
- [225] F. Abnisa, "Study on pyrolysis of oil palm solid wastes and co-pyrolysis of palm shell with plastic and tyre waste," PhD, Chemical Engineering, Malaya, Malaysia, 2015.
- [226] J. L. Klinger, T. L. Westover, R. M. Emerson, C. L. Williams, S. Hernandez, G. D. Monson, *et al.*, "Effect of biomass type, heating rate, and sample size on microwave-enhanced fast pyrolysis product yields and qualities," *Applied Energy*, vol. 228, pp. 535-545, 2018.
- [227] A. V. Bridgwater, "Biomass for Energy and Industry," presented at the Fifth EC Conference, London:, 1990.
- [228] L. Qiuxing, F. Xing, L. Jindong, Y. Wang, L. Xiaoyan, and H. Changwei, "Effect of Heating Rate on Yields and Distribution of Oil Products from the Pyrolysis of Pubescen," *Energy Technology*, vol. 6, pp. 1-15, 2017.
- [229] J. Akhtar and N. S. Amin, "A review on operating parameters for optimum liquid oil yield in biomass pyrolysis," *Renewable and Sustainable Energy Reviews*, vol. 16, pp. 5101-5109, 2012.

- [230] J. Li, B.-g. Fan, B. Li, Y.-X. Yao, R.-P. Huo, R. Zhao, *et al.*, "Effects of Pyrolysis Mode and Particle size on the Microscopic Characteristics and Mercury Adsorption Characteristics of Biomass Char," *Bio Resources*, vol. 13, pp. 5450-5471, 2018.
- [231] A. V. Bridgwater, "Review of fast pyrolysis of biomass and product upgrading," *Biomass Bioenergy*, vol. 38, pp. 68-94, 2012.
- [232] C. Karunanithy and K. Muthukumarappan, *Rheological Characterization of Bio-Oils from Pilot Scale Microwave Assisted Pyrolysis*, 2011.
- [233] M. Bardalai and D. K. Mahanta, "A Review of Physical Properties of Biomass Pyrolysis Oil," *International Journal of Renewable Energy Research*, vol. 5, pp. 277-286, 2015.
- [234] L. J. Klinger, T. L. Westover, R. M. Emerson, C. L. Williams, S. Hernandez, G. D. Monson, *et al.*, "Effect of biomass type, heating rate, and sample size on microwave-enhanced fast pyrolysis product yields and qualities," *Applied Energy*, vol. 228, pp. 535-545, 2018.
- [235] Y. Zixu, K. Ajay, and L. H. Raymond, "Review of recent developments to improve storage and transportation stability of bio-oil," *Renewable and Sustainable Energy Reviews*, vol. 50, pp. 859-870, 2015.
- [236] O. Anja, E. Douglas, Douglas, and K. Jaana, "Acidity of Biomass Fast Pyrolysis Bio-oils," *Energy & Fuels*, vol. 24, pp. 6548-6554 2010.
- [237] R. Lodeng and H. Bergem, "7 - Stabilisation of pyrolysis oils," in *Direct Thermochemical Liquefaction for Energy Applications*, L. Rosendahl, Ed., ed: Woodhead Publishing, 2018, pp. 193-247.
- [238] O. Anja, E. C. Douglas, and K. Jaana, "Acidity of Biomass Fast Pyrolysis Bio-oils," *Energy & Fuels*, vol. 24, pp. 6548-6554, 2010.
- [239] M. I. Jahirul, M. G. Rasul, A. A. Chowdhury, and N. Ashwath, "Biofuels Production through Biomass Pyrolysis-A Technological Review," *Energies*, vol. 5, pp. 4952-5001, 2012.
- [240] S. Wang, "High-Efficiency Separation of Bio-Oil," in *Biomass Now - Sustainable Growth and Use*, M. D. Matovic, Ed., ed, 2013.
- [241] Y. Yu, Y. W. Chua, and H. Wu, "Characterization of Pyrolytic Sugars in Bio-Oil Produced from Biomass Fast Pyrolysis," *Energy & Fuels*, vol. 30, pp. 4145-4149, 2016.
- [242] S. Nanda, P. Mohanty, J. A. Kozinski, and A. K. Dalai, "Physico-Chemical Properties of Bio-Oils from Pyrolysis of Lignocellulosic Biomass with High and Slow Heating Rate " *Energy and Environment Research*, vol. 4, pp. 21-32, 2014.
- [243] K. M. Qureshi, A. N. K. Lup, S. Khan, F. Abnisa, and W. M. A. W. Daud, "A technical review on semi-continuous and continuous pyrolysis process of biomass to bio-oil," *Journal of Analytical and Applied Pyrolysis*, vol. 131, pp. 52-75, 2018.

- [244] S. Jain, "17 - The production of biodiesel using Karanja (*Pongamia pinnata*) and Jatropha (*Jatropha curcas*) Oil," in *Biomass, Biopolymer-Based Materials, and Bioenergy*, D. Verma, E. Fortunati, S. Jain, and X. Zhang, Eds., ed: Woodhead Publishing, 2019, pp. 397-408.
- [245] S. Khana, A. N. K. Lup, K. M. Qureshi, F. Abnisad, W. M. Ashri, and M. Fazly, "A review on deoxygenation of triglycerides for jet fuel range hydrocarbons," *Journal of Analytical and Applied Pyrolysis* vol. 140, pp. 1-24, 2019.
- [246] A. N. Kay Lup, F. Abnisa, W. M. A. W. Daud, and M. K. Aroua, "Synergistic interaction of metal–acid sites for phenol hydrodeoxygenation over bifunctional Ag/TiO₂ nanocatalyst," *Chinese Journal of Chemical Engineering*, vol. 27, pp. 349-361, 2019.
- [247] A. N. K. Lup, F. Abnisa, W. M. A. W. Daud, and M. K. Aroua, "Atmospheric hydrodeoxygenation of phenol as pyrolytic-oil model compound for hydrocarbon production using Ag/TiO₂ catalyst," *Asia-Pacific Journal of Chemical Engineering*, vol. 14, p. e2293, 2019.
- [248] A. N. K. Lup, F. Abnisa, W. M. A. W. Daud, and M. K. Aroua, "Acidity, oxophilicity and hydrogen sticking probability of supported metal catalysts for hydrodeoxygenation process," *IOP Conference Series: Materials Science and Engineering*, vol. 334, p. 012074, 2018.
- [249] A. N. K. Lup, F. Abnisa, W. M. A. W. Daud, and M. K. Aroua, "Temperature-programmed reduction of silver(I) oxide using a titania-supported silver catalyst under a H₂ atmosphere," *J Chin Chem Soc.*, vol. 66, pp. 1-13, 2019.
- [250] M. K. Lam and K. T. Lee, *Scale-up and commercialization of algal cultivation and biofuels production*, Second Edition ed., 2019.
- [251] J. O. Ogunkanmi, D. M. Kulla, N. O. Omisanya, M. Sumaila, D. O. Obada, and D. Dodoo-Arhin, "Extraction of bio-oil during pyrolysis of locally sourced palm kernel shells: Effect of process parameters," *Case Studies in Thermal Engineering*, vol. 12, pp. 711-716, 2018.
- [252] S. Khan, A. N. Kay Lup, K. M. Qureshi, F. Abnisa, W. M. A. Wan Daud, and M. F. A. Patah, "A review on deoxygenation of triglycerides for jet fuel range hydrocarbons," *Journal of Analytical and Applied Pyrolysis*, vol. 140, pp. 1-24, 2019.
- [253] A. N. Kay Lup, F. Abnisa, W. M. A. Wan Daud, and M. K. Aroua, "A review on reactivity and stability of heterogeneous metal catalysts for deoxygenation of bio-oil model compounds," *Journal of Industrial and Engineering Chemistry*, vol. 56, pp. 1-34, 2017.
- [254] A. N. Kay Lup, F. Abnisa, W. M. A. W. Daud, and M. K. Aroua, "A review on reaction mechanisms of metal-catalyzed deoxygenation process in bio-oil model compounds," *Applied Catalysis A: General*, vol. 541, pp. 87-106, 2017.

- [255] K. Qian, A. Kumar, K. Patil, D. Bellmer, D. Wang, W. Yuan, *et al.*, "Effects of Biomass Feedstocks and Gasification Conditions on the Physiochemical Properties of Char " *Energies* vol. 6, pp. 3972-3986, 2013.
- [256] T. Miranda, I. Montero, F. Sepúlveda Justo, J. Arranz, C. Victoria Rojas, and S. Nogales, *A Review of Pellets from Different Sources* vol. 8, 2015.
- [257] A. K. James, R. W. Thring, S. Helle, and H. S. Ghuman, "Ash Management Review—Applications of Biomass Bottom Ash," *Energies*, vol. 5, pp. 3856-3873, 2012.
- [258] F. Abnisa, A. Arami-Niya, W. M. A. Wan Daud, J. N. Sahu, and I. M. Noor, "Utilization of oil palm tree residues to produce bio-oil and bio-char via pyrolysis," *Energy Conversion and Management*, vol. 76, pp. 1073-1082, 2013.
- [259] K. M. Qureshi, F. Abnisa, and W. M. A. Wan Daud, "Novel helical screw-fluidized bed reactor for bio-oil production in slow-pyrolysis mode: A preliminary study," *Journal of Analytical and Applied Pyrolysis*, 2019.
- [260] J. I. Montoya, F. Chejne-Janna, and M. Garcia-Perez, "Fast pyrolysis of biomass: A review of relevant aspects.: Part I: Parametric study," *DYNA*, vol. 82, pp. 239-248, 2015.
- [261] C. Z. Zaman, K. Pal, W. A. Yehye, S. Sagadevan, S. T. Shah, G. A. Adebisi, *et al.*, "Pyrolysis: A Sustainable Way to Generate Energy from Waste," in *Pyrolysis*, ed, 2017.
- [262] E. Ranzi, A. Cuoci, T. Faravelli, A. Frassoldati, G. Migliavacca, S. Pierucci, *et al.*, "Chemical Kinetics of Biomass Pyrolysis," *Energy & Fuels*, vol. 22, pp. 4292-4300, 2008.
- [263] C. Branca and C. Di Blasi, "Multistep Mechanism for the Devolatilization of Biomass Fast Pyrolysis Oils," *Industrial & Engineering Chemistry Research*, vol. 45, pp. 5891-5899, 2006.
- [264] R. Powar and S. Gangil, *Study of effect of temperature on yield of bio-oil, bio-char and NCG from soybean stalk in continuous feed bio-oil reactor* vol. 3, 2013.
- [265] P. T. Williams and E. A. Williams, "Fluidised bed pyrolysis of low density polyethylene to produce petrochemical feedstock," *Journal of Analytical and Applied Pyrolysis*, vol. 51 pp. 107-126, 1999.
- [266] M. G.-P. Shuai. Zhou, Brennan. Pecha, Armando. G. McDonald, Sascha. R. A. Kersten, Roel. J. M. Westerhof, "Secondary Vapor Phase Reactions of Lignin-Derived Oligomers Obtained by Fast Pyrolysis of Pine Wood," *Energy Fuels* vol. 27, p. 1428–1438, 2013.
- [267] S. Jalalifar, R. Abbassi, V. Garaniya, K. Hawboldt, and M. Ghiji, "Parametric analysis of pyrolysis process on the product yields in a bubbling fluidized bed reactor," *Fuel*, vol. 234, pp. 616-625, 2018.

- [268] R. E. Guedes, Aderval. S.Luna, and A. R. Torres, "Operating parameters for bio-oil production in biomass pyrolysis: A review," *Journal of Analytical and Applied Pyrolysis*, vol. 129, pp. 134-149, 2018.
- [269] W. Treedet and R. Suntivarakorn, "Design and operation of a low cost bio-oil fast pyrolysis from sugarcane bagasse on circulating fluidized bed reactor in a pilot plant," *Fuel Processing Technology*, vol. 179, pp. 17-31, 2018.
- [270] H. Heo, H. Park, Y.-K. Park, C. Ryu, D. Suh, Y.-W. Suh, *et al.*, "Bio-Oil Production From Fast Pyrolysis of Waste Furniture Sawdust in a Fluidised Bed," *Bioresource technology*, vol. 101, pp. S91-6, 2009.
- [271] P. S.Tanvidkar, "Catalytic up-gradation of bio-oil by pyrolysis of biomass," Master, Chemical Engineering, National Institute of Technology Rourkela Odisha, India, 2015.
- [272] M. Bertero, H. A. Gorostegui, C. J. Orrabalís, C. A. Guzmán, E. L. Calandri, and U. Sedran, "Characterization of the liquid products in the pyrolysis of residual chañar and palm fruit biomasses," *Fuel*, vol. 116, pp. 409-414, 2014.
- [273] Q. Lu, W.-Z. Li, and X.-F. Zhu, "Overview of fuel properties of biomass fast pyrolysis oils," *Energy Conversion and Management*, vol. 50, pp. 1376-1383, 2009.
- [274] M. Ringer, V. Putsche, and J. Scahill, "Large-scale pyrolysis oil production: a technology assessment and economic analysis," National Renewable Energy Lab.(NREL), Golden, CO (United States)2006.
- [275] C. L. Yiin, S. Yusup, P. Udomsap, B. Yoosuk, and S. Sukkasi, "Stabilization of Empty Fruit Bunch (EFB) derived Bio-oil using Antioxidants," in *Computer Aided Chemical Engineering*. vol. 33, J. J. Klemeš, P. S. Varbanov, and P. Y. Liew, Eds., ed: Elsevier, 2014, pp. 223-228.
- [276] T. Kan, V. Strezov, and T. J. Evans, "Lignocellulosic biomass pyrolysis: A review of product properties and effects of pyrolysis parameters," *Renewable and Sustainable Energy Reviews*, vol. 57, pp. 1126-1140, 2016.
- [277] K. Kundu, A. Chatterjee, T. Bhattacharyya, M. Roy, and A. Kaur, "Thermochemical Conversion of Biomass to Bioenergy: A Review," ed, 2018, pp. 235-268.
- [278] F. M. Hossain, J. Kosinkova, R. J. Brown, Z. Ristovski, B. Hankamer, E. Stephens, *et al.*, "Experimental Investigations of Physical and Chemical Properties for Microalgae HTL Bio-Crude Using a Large Batch Reactor," *Energies*, vol. 10, p. 467, 2017.
- [279] A. N. Kay Lup, F. Abnisa, W. M. A. W. Daud, and M. K. Aroua, "Atmospheric hydrodeoxygenation of phenol as pyrolytic-oil model compound for hydrocarbon production using Ag/TiO₂ catalyst," *Asia-Pacific Journal of Chemical Engineering*, vol. 14, p. e2293, 2019.

- [280] G. Lyu, S. Wu, and H. Zhang, "Estimation and Comparison of Bio-Oil Components from Different Pyrolysis Conditions," *Frontiers in Energy Research*, vol. 3, 2015.
- [281] P. Fu, S. Hu, J. Xiang, P. Li, D. Huang, L. Jiang, *et al.*, "FTIR study of pyrolysis products evolving from typical agricultural residues," *Journal of Analytical and Applied Pyrolysis*, vol. 88, pp. 117-123, 2010.
- [282] R. Kaur, P. Gera, and M. Kumar Jha, *Study on Effects of Different Operating Parameters on the Pyrolysis of Biomass: A Review* vol. 1, 2015.
- [283] A. N. K. Lup, F. Abnisa, W. M. A. W. Daud, and M. K. Aroua, "Acidity, oxophilicity and hydrogen sticking probability of supported metal catalysts for hydrodeoxygenation process," presented at the 3rd ICChESA 2017: Materials Science and Engineering, 2018.
- [284] L. Fan, Y. Zhang, S. Liu, N. Zhou, P. Chen, Y. Cheng, *et al.*, "Bio-oil from fast pyrolysis of lignin: Effects of process and upgrading parameters," *Bioresource Technology*, vol. 241, pp. 1118-1126, 2017.
- [285] M. K. Rafiq, R. T. Bachmann, M. T. Rafiq, Z. Shang, S. Joseph, and R. Long, "Influence of Pyrolysis Temperature on Physico-Chemical Properties of Corn Stover (*Zea mays* L.) Biochar and Feasibility for Carbon Capture and Energy Balance," *PloS one*, vol. 11, pp. e0156894-e0156894, 2016.
- [286] U. Hamza, N. Nasri, N. A. Saidina Amin, J. Mohammed, and H. Zain, *Characteristics of oil palm shell biochar and activated carbon prepared at different carbonization times* vol. 57, 2015.
- [287] H. Yang, R. Yan, H. Chen, D. H. Lee, and C. Zheng, "Characteristics of hemicellulose, cellulose and lignin pyrolysis," *Fuel*, vol. 86, pp. 1781-1788, 2007.
- [288] Y. Lu, Y.-C. Lu, H.-Q. Hu, F.-J. Xie, X.-Y. Wei, and X. Fan, "Structural Characterization of Lignin and Its Degradation Products with Spectroscopic Methods," *Journal of Spectroscopy*, vol. 2017, pp. 1-15, 2017.
- [289] S.-J. Kim, S.-H. Jung, and J.-S. Kim, "Fast pyrolysis of palm kernel shells: Influence of operation parameters on the bio-oil yield and the yield of phenol and phenolic compounds," *Bioresource Technology*, vol. 101, pp. 9294-9300, 2010.
- [290] A. Chandrasekaran, S. Ramachandran, and S. Subbiah, "Modeling, experimental validation and optimization of *Prosopis juliflora* fuelwood pyrolysis in fixed-bed tubular reactor," *Bioresource Technology*, vol. 264, pp. 66-77, 2018.
- [291] W. S. Ralaph, J. Tylerlan, and H. Edwards, "Flash Pyrolysis of agglomerating coal in, commonwelth scientific and Industrial research organization, Australia," vol. 5, 1982.
- [292] N. Abdullahi, F. Sulaiman, and A. A. Safana, "Bio-Oil and Biochar Derived from the Pyrolysis of Palm Kernel Shell for Briquette," *Sains Malaysiana*, vol. 46, pp. 2441-2445, 2017.

- [293] S. M. Abdul Aziz, R. Wahi, Z. Ngaini, and S. Hamdan, "Bio-oils from microwave pyrolysis of agricultural wastes," *Fuel Processing Technology*, vol. 106, pp. 744-750, 2013/02/01/ 2013.
- [294] A. Oasmaa, D. Elliott, Douglas, and J. Korhonen, *Acidity of Biomass Fast Pyrolysis Bio-oils* vol. 24, 2010.
- [295] Q. Sohaib, M. Habib, S. Fawad Ali Shah, U. Habib, and S. Ullah, "Fast pyrolysis of locally available green waste at different residence time and temperatures," *Energy Sources, Part A: Recovery, Utilization, and Environmental Effects*, vol. 39, pp. 1639-1646, 2017/08/03 2017.
- [296] R. E. Guedes, A. S. Luna, and A. R. Torres, "Operating parameters for bio-oil production in biomass pyrolysis: A review," *Journal of Analytical and Applied Pyrolysis*, vol. 129, pp. 134-149, 2018.
- [297] A. Najaf, S. Mahmood, S. Khurram, R. Mujahid, and C. Arshad, *Effect of Temperature on the Bio Oil Yield from Pyrolysis of Maize Stalks in Fluidized Bed Reactor*, 2014.
- [298] J. Dong, Y. Chi, Y. Tang, N. Mingjiang, AngeNzihou, E. Weiss-Hortala, *et al.*, "Effect of Operating Parameters and Moisture Content on Municipal Solid Waste Pyrolysis and Gasification," *Energy & Fuels*, vol. 30, pp. 3994-4001, 2016.
- [299] J. Dong, Y. Chi, Y. Tang, M. Ni, A. Nzihou, E. Weiss-Hortala, *et al.*, "Effect of Operating Parameters and Moisture Content on Municipal Solid Waste Pyrolysis and Gasification," *Energy & Fuels*, vol. 30, pp. 3994-4001, 2016.
- [300] K. M. Qureshi, F. Abnisa, and W. M. A. Wan Daud, "Novel helical screw-fluidized bed reactor for bio-oil production in slow-pyrolysis mode: A preliminary study," *Journal of Analytical and Applied Pyrolysis*, vol. 142, p. 104605, 2019.